Addis Ababa University

Africa Center of Excellence for Water Management

M.Sc Research Thesis

On

Analysis of Temporal and Spatial Trends of Hydro-Climatic Indices in the Lake Kyoga Basin

Submitted to Africa center of Excellence for Water Resources Management

By

Josephine Mendela

Email: josephine.mendela@aau.edu.et

Supervisor

Hadush Kidane Meresa (PhD)

Senior researcher in hydrology and hydrodynamics

Email: kidane.hadush@gmail.com

Addis Ababa, June 2020

ADDIS ABABA UNIVERSITY

AFRICA CENTER OF EXCELLENCE FOR WATER MANAGEMENT

Thesis Approval form

APPROVED BY BOARD OF EXAMINERS

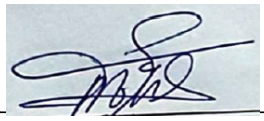
This is to certify that we the undersigned, have examined this MSc Thesis titled **"ANALYSIS OF TEMPORAL AND SPATIAL TRENDS OF HYDRO-CLIMATIC INDICES IN THE LAKE KYOGA BASIN"** and that in our opinion; it is fully adequate, in scope and quality, as an MSc research thesis for the Degree of Master of Science in Water Management (Hydrology and Water Resources Management).

Advisor: Hadush Kidane Meresa (PhD)

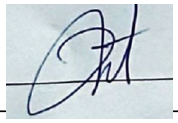
Signature

Date_____21/08/20_____

External Examiner: Tenalem Ayenew (Professor)

Signature Date_____28/08/20_____

Internal Examiner: Dessie Nedaw (PhD)

Signature Date_____25/08/20_____

Chairperson: Beteley Tekola (PhD)

Signature Date_____25/08/20_____

DECLARATION

I declare that this thesis is a presentation of my original research work and that it has not been submitted, in whole or in part, in any previous application for a degree. Wherever contributions of others are involved, every effort is made to indicate this clearly, with due reference to the literature, and acknowledgement of collaborative research and discussions.

Name: Josephine Mendela Signature:  Date: 04/Aug/2020

Acknowledgment

I would like to extend my sincere gratitude towards Africa Center of Excellence for Water Management (ACEWM), the main proprietor of my master's education hence this study. Am very grateful for the opportunity and financial support that has facilitated this study.

I would like in a special way to also thank Dr. Hadush Kidane Meresa my supervisor for his guidance and counsel towards compiling this thesis. The timely responses to inquiries, reading materials provided and corrections made toward helping me understand and come up with a better write up. Thank you for being patient with me, may God bless him.

My appreciation also goes to Makerere University, college of agricultural and environmental sciences for hosting me during the data collection period. Am grateful for the guidance and supervision of Mr. Charles Juuko during this period.

I would also like to thank my friends who have supported me along the course of coming up with this thesis. Am very grateful to my guardians for all the love, support, care, prayers made and encouragement they have given me. Most of all, I thank the Almighty God for his grace and for helping me make this exercise a successful one. Thank you Lord.

Acronyms

AMO:	Atlantic Multidecadal Oscillation
CRD:	Cumulative Rand Difference
CRU:	Climatic Research Unit
DWT:	Discrete Wavelet Transformation
EOFs:	Empirical Orthogonal Functions
IOD:	Indian ocean Dipole
IPCC:	Intergovernmental Panel on Climate Change
LKB:	Lake Kyoga Basin
m.s.l:	mean sea level
MK:	Mann Kendall
MWE:	Ministry of Water and Environment
NAO:	Northern Atlantic Oscillation
NCAR:	National Center for Atmospheric Research
NCEP:	National Centers for Environmental Prediction
NMC:	National Metrological Center
NRMSE:	Normalized Root Mean Square Efficiency
PC:	Principal Component
PCA:	Principal component analysis
PMM:	Predictive Mean Matching
Prec:	Precipitation
QPM:	Quantile Perturbation Method
RFE:	Rainfall Estimate
SLP:	Sea Level Pressure
SOI:	Southern Oscillation Index
SPI:	Standardized Precipitation Index
SSI:	Standardized Streamflow Index
SST:	Sea Surface Temperature
TAMSAT:	Tropical Application of Meteorology Using Satellite Data
UNMA:	Uganda National Meteorological Authority
WTC:	Wavelet Transformation Coherent

TABLE OF CONTENTS

Acknowledgment i

Acronyms ii

TABLE OF CONTENTS iii

List of Figures vi

List of Tables viii

Abstract ix

1. INTRODUCTION 1

1.1 Backgrounds 1

1.2 Statement of the problem 3

1.3 Objective of the study 4

1.4 Significance of the study 5

1.5 Novelty/contribution of the study 5

1.6 Scope of study 6

1.7 Study area description 6

2. LITERATURE REVIEW 9

2.1 Climate variability 9

2.2 Hydro-climatic Indices 10

2.3 Hydrological variability 11

2.4 Interrelationship between climatic and hydrological extremes 12

2.5 Implication of hydro-climate variability on agriculture, reservoir operation, water storage, drought, flood 13

2.6 General methods to detect the hydro-climate variability 14

2.7 Previous similar studies in the basin 15

3. MATERIALS AND METHODS 17

3.1 Data Sets 17

3.1.1 Hydrological and meteorological datasets 17

3.1.2 Climate Indices (NAO and ENSO indices) 20
3.2 Methods 21
3.2.1 Estimation of potential evapotranspiration (PET) 21
3.2.2 Standardised Precipitation Indices (SPI) 21
3.2.3 Standardised Streamflow index (SSI) 23
3.2.4 Aridity index (AI) 23
3.2.5 Hydro-climatic Indices 24
3.2.6 Persistence of Hydroclimatic Indices (Hurst exponent) 25
3.2.7 Trend of Hydroclimatic Indices (Modified Mann-Kendell Test) 26
3.2.8 Change point Detection (Pettit Test) 28
3.2.9 Wavelet transformation coherent 30
4. RESULTS AND DISCUSSION 31
4.1 Data consistency 31
4.2 Extracted indices from precipitation, temperature and streamflow 34
4.2.1 Standardised Precipitation Index (SPI) and Standardised Streamflow Index (SSI) 34
4.2.2 The maximum 5-day precipitation during a year (Rx5day), the 95th percentile of precipitation on wet days (R95) and the 5-percentile flow (Q95) 37
4.2.3 Aridity Index 38
4.3 Homogeneity and Persistence of indices 39
4.3.1 Homogeneity Analysis of the Indices (break point analysis) 39
4.3.2 Persistence Analysis of the Indices 40
4.4 Trend Analysis of the Indices (p-value, Z, H) 42
4.5 Climate teleconnections 47
4.6 Interaction among the indices 48
4.6.1 Interaction between SPI-3 and SSI-3 49
4.5.2 Interaction between R95 and AI 50
4.6.2 Interaction between NAO and Hydro-climatic indices 51

4.5.3 Interaction between Niño 3.4 and Hydro-climatic indices 57
4.5.4 Interaction between Niño 3 and Hydro-climatic indices 63
5. CONCLUSION AND RECOMMENDATION 70
5.1 Conclusion.....70
5.2 Recommendation.....71
REFERENCES 72

List of Figures

Figure 1.1: Location of Lake Kyoga Basin (LKB) 8
Figure 3.1: Streamflow hydrograph and precipitation hyetograph of Kelim and Mpologoma sub-catchments. 18
Figure 3.2: Streamflow hydrograph and precipitation hyetograph of Ssezibwa and Victoria Nile sub-catchments. 19
Figure 4.1: Double mass curve for precipitation data of the selected stations in LKB 31
Figure 4.2: Thiessen polygon showing the weighting factor for each selected station in the Kyoga basin, Okere and Mpologoma sub-catchments 33
Figure 4.3: SPI and SSI of the Kelim, Mpologoma and Ssezibwa sub-catchments in LKB ... 34
Figure 4.4: The Rx5, R95 and Q95 of the selected sub-catchments in LKB 38
Figure 4.5: The AI of the selected sub-catchments in LKB 39
Figure 4.6: Trend of indices in the Kelim sub-catchment 43
Figure 4.7:Trend of indices in the Mpologoma sub-catchment 44
Figure 4.8:Trend of indices in the Ssezibwa sub-catchment 45
Figure 4.9: Trend of indices in the Victoria Nile sub-catchment 46
Figure 4.10: Trends of indices in the Okere sub-catchment 47
Figure 4.11: Monthly and annual variation of climate teleconnections 48
Figure 4.12: Three months moving average of the climate teleconnections 48
Figure 4.13: Wavelet coherence between SPI and SSI for the different sub-catchments 50
Figure 4.14: Wavelet coherence between R95 and AI 51
Figure 4.15: Wavelet coherence between NOA and SPI 53
Figure 4.16: Wavelet coherence between NAO and Rx5 53
Figure 4.17: Wavelet coherence between NAO and Rx95 54
Figure 4.18: Wavelet coherence between NAO and AI 55
Figure 4.19: Wavelet coherence between NAO and Q95 56
Figure 4.20: Wavelet coherence between NAO and SSI 57
Figure 4.21: Wavelet coherence between Niño 3.4 and SPI 58
Figure 4.22: Wavelet coherence between Niño3.4 and Rx5 of selected stations in LKB 59
Figure 4.23: Wavelet coherence between Niño3.4 and R95 of selected stations in LKB 60
Figure 4.24: Wavelet coherence between Niño 3.4 and AI of selected stations in LKB 61
Figure 4.25: Wavelet coherence between Niño 3.4 and SSI 62
Figure 4.26: Wavelet coherence between Niño 3.4 and Q95 63

Figure 4.27: Wavelet coherence between Niño 3 and SPI of the selected stations in LKB 64
Figure 4.28: Wavelet coherence between Niño 3 and Rx5 of selected stations in LKB 65
Figure 4.29: Wavelet coherence between Niño3 and R95 for selected stations in LKB.....66
Figure 4.30: Wavelet coherence between Niño 3 and AI for selected station in LKB.....67
Figure 4.31: Wavelet coherence between Niño3 and SSI of the gauged sub-catchments in LKB.....68
Figure 4.32: Wavelet coherence between Niño 3 and Q95 of the gauged sub-catchments in LKB.....69

List of Tables

Table 1.1: Sub-catchments in LKB and the corresponding selected weather stations 7
Table 3.1: Selected river gaging stations in Kyoga Basin 17
Table 3.2 Drought intensities as per SPI values Adopted from Agnew & Chappell (1999) ...23
Table 3.3: The list of hydro-climatic indices used in this study 25
Table 4.1 : Break point analysis results for all indices 40
Table 4.2: Persistence analysis results for all indices 41
Table 4.3: The number of droughts and categories in the different years per sub-catchment .35

Abstract

Understanding of hydro-climatic variability is very crucial in water resource management, predictive planning, agricultural water management and flood risk management. In water scarce regions, hydro-climatic variability has huge impact on the available water quality and quantity. Both hydrological and climate extremes have become more problematic due to changes in anthropogenic activities and climate variability. Long-term variability in the hydro-climatic variables can affect the overall spatial, and temporal distribution of surface water. Thus, it is important to comprehend the variation in observed hydro-climatic variables on seasonal and annual time scales plus the associated effect on the hydrology and water resources. This research aimed to understand the spatial-temporal variability of hydro-climatic variables (precipitation, temperature, and streamflow) and its implication on the water resource management in the Lake Kyoga Basin (LKB), Uganda. Different hydro-climatic indices (SPI-3, Rx5, Rx95, AI, Q95 and SSI-3) were selected from the main variables (precipitation, temperature, and streamflow). A combination of different statistical techniques (Hurst, Modified Mann-Kendell and wavelet coherence) were employed to assess the trend, variability, and their interaction among the selected hydro-climatic indices. The interaction of the different variables plus their effect on water resource management were evaluated using wavelet coherent statistical approach. The results obtained from this study are an indication of climate variability in the LKB, exhibiting extremes events of both drought and floods. Both extremes have an impact on the river flows as floods can be associated with soil erosion, land slides among others and prolonged droughts with water and food scarcity. In most parts of the LKB precipitation is decreasing while aridity is increasing. The decreasing precipitation in LKB has been attributed to the climatic teleconnection which might imply that the teleconnections have a cause in the variations of the hydro-climatic indices

Keywords: hydro-climatic indices, trend, Modified Mann-Kendall, wavelet, extremes, Uganda

1. INTRODUCTION

1.1 Backgrounds

Water is extremely important to both society and nature, the availability of water resources is among the major concerns about the consequences of climate change (Bawden et al., 2014) . Global warming has increased by about 1ºC since the pre-industrial times due to various human activities increasing the atmospheric concentration of greenhouse gases(IPCC, 2013). The rising trend in temperature has increased evapotranspiration rates and the variability of precipitation, leading to changes worldwide in the hydrological cycle in the form of stream flow volume as well as its distribution throughout the year and temporally causing significant water stress (Bawden et al., 2014; Khalid et al., 2013; Nashwan & Shahid, 2019). In addition, hydrological systems are anticipated to experience not only the changes in the average availability of water but also changes in the extremes such as droughts and floods (Husain & Hamid, 2012).

Precipitation is the hydro-climatic element with the highest spatial and temporal variability (Basalirwa, 1995), with its hydro-climate indices more frequent and intense (Meresa & Gatachew, 2019). Variations in precipitation over different time scales namely; daily, monthly, seasonal, annual, and decadal have an impact on water balances (De Lima et al., 2010) . Thus, it is important to understand the variation in precipitation patterns and other hydroclimatic variables as part of the long-term behavior of the hydrological process (De Lima et al., 2010). In recent years, detection of the hydro-climatic variability and modeling has attracted widespread research interest. This is not only because of the concerns about the global warming, but the rising demand for water (Palizdan et al., 2016), the availability of water resources, as well as their management and use within a drainage basin. The study of the spatial-temporal variability of precipitation, temperature, and discharge is essential in analyzing its impacts on water resources planning and management (Gedefaw et al., 2018; Meresa et al., 2017). Additionally, the interaction and causality of hydro-climatic indices time series analyses are very vital for regional development and predictive planning, financial management, weather forecasting, hydrological forecasting, environmental pollution control, astronomy, and oceanography (Mahmood et al., 2019).

Long-term variability in the hydro-climatic variables can affect the overall availability, spatial, and temporal distribution of surface water in a basin (Nourani et al., 2018). Streamflow is affected by changes in evapotranspiration, which is dependent upon air temperature, as well as precipitation (Bawden et al., 2014; Onyutha, 2016a). The change in climate (especially precipitation) alters the hydrological systems, affecting water resources in both quantity and quality. The discharge of many rivers in the world has been changing due to climate change and intensive human activities (Gedefaw et al., 2018). Large-scale ocean-atmosphere conditions, regional and local factors also play a role in the variation of water resources (Onyutha et al., 2020). The 1997–1998 ENSO event is linked with catastrophic disruption of socio-economic infrastructure and loss of life in East Africa (Indeje et al., 2000).

Several methods both parametric and nonparametric statistical tests have been used to explore the presence of trend in hydro-climatic time series. The parametric methods include; T-test, F-test, bootstrap and linear regression and nonparametric methods Mann-Kendall MK (Mann 1945; Kendall 1955) and the Spearman's rho tests (Burn et al., 2010). Recently, graphical methods of trend detection have also been explored (Onyutha, 2016a; Şen, 2012) . The corresponding results from precipitation, temperature and streamflow trends are essential for an assessment of the impacts of climate change and variability and hydrological change on both regional and catchment scales (Meresa et al., 2017). Notably, detection and attribution of past trends, changes and variability in climatic variables is essential for the understanding of potential future changes resulting from anthropogenic activities (Zhang et al., 2001).

There are several indices (climate and hydrology) used to express the variability in precipitation, temperature and streamflow. These are based on several influencing factors. They include those based on extreme climate events, drought, sea level pressure (SLP) and sea surface temperature (SST). Among these, the most relevant hydro-climatic indices that are highly related to water resource management and planning were used in this study.

Developing countries like Uganda are adversely affected by climate variability mainly because majority of the population relies on rain-fed agriculture as the main source of livelihood (Tumusiime & Ageet, 2018). In addition, they do not have the ability to adapt to extreme events coupled with low resilience(Tumusiime & Ageet, 2018) .

In Uganda, climate variability together with population growth pose a great threat to the surrounding water resources. Particularly, spatial and temporal variability in precipitation often results into floods, landslides and droughts. Several sub-basins in Uganda indicated negative

trends in annual rainfall, these; Albert Nile, River Aswa, Lake Albert, Lake Edward & George, Lake Kyoga and Lake Victoria(Nsubuga et al., 2014). In Lake Kyoga Basin, the decreasing trends are reflected in decrease of water resources, Tumusiime & Ageet, (2018) which depicted a 6% decrease in the water levels of Lake Kyoga.

1.2 Statement of the problem

Climate variability appears to have a very marked effect on many hydrological series. Among all the atmospheric variables, variability in precipitation is a critical factor in determining the spatial-temporal influence of the climate system on hydrology and related water management applications (Onyutha & Willems, 2015). Disasters such as landslides, floods, drought that are related to the scarcity or surplus of water are directly based on the occurrences of extreme precipitation events, which in turn tend to be influenced by climate variability (Onyutha & Willems, 2017).

In Uganda, climate variability has had significant socio-economic impacts in the past decades leaving a wide spread of infrastructure damage, displacement and loss of livelihood (Tumusiime & Ageet, 2018) . The effects of varied precipitation are especially noticeable in the eastern part of Uganda (which covers a large portion of the Lake Kyoga Basin), where drought has been reported to be frequent in the last decades and has drastically altered the landscape as portrayed in the Bududa landslides of 2010 (Nsubuga et al., 2014). Thus, it is important to comprehend the variation in historical hydro-climatic variables at seasonal and annual time scales together with the associated effect on the hydrology and water resources of the Lake Kyoga Basin (Nsubuga et al., 2014; Onyutha & Willems, 2017).

The Lake Kyoga basin also commonly referred to as the upper Nile basin is the second largest basin in Uganda (Nsubuga et al., 2014; Kigobe et al., 2014). The basin is rich in water resources especially in the south including rivers, lakes and swamps. The major rivers in this basin include Mpologoma, Ssezibwa and the Victoria Nile. The Victoria Nile has two major dams, i.e. Nalubale dam and Bujagali dam that produce about 430 MW of power both for domestic market and export to neighboring Nations. The water resources in the Lake Kyoga basin are also used for agriculture, fisheries and industrial production.

Further studies to address the issue of trend attribution and to establish a linkage between climatic variability and hydrological trends in Uganda were recommended by Nsubuga et al (2014). Trend detection and variability of hydro-climatic factors in the Lake Kyoga basin have

been explored using different methods namely; Trend Testing Tool, quantile perturbation method (QPM), Cumulative Rand Difference (CRD) and Sen's T test. Upward (increasing) trends were detected for both precipitation and temperature and decreasing trend in discharge (Nyenje & Batelaan , 2009; Nsubuga et al., 2014; Onyutha & Willems, 2015; Onyutha, 2016a; Onyutha, 2016b; Onyutha, 2016c).

It is noticeable that some of the previous studies focused on the trends and the probable causes of the trend in the climatic variable. The effect of the trends and its implication on the water resource management in the basin was not explored. These studies include; Onyutha & Willems (2015) that found an increasing trend in the precipitation which is suspected to be influenced by the North Atlantic Ocean, Niño 3, Niño 3.4, and the Indian Ocean. Kansiime et al (2013) also found an increasing trend in rainfall and noted that there was higher variability in the rainfall in highlands as compared to the low lands.

This study therefore, attempted to explore the spatial-temporal variability of hydro-climate of the Lake Kyoga Basin (Upper Nile) using a combination of the Modified Mann-Kendell and wavelet coherence method, the interaction of the different hydro-climatic variables and the effect of the variation on the water resources in the Lake Kyoga Basin. Most of the indices that were used in this study have not deeply been explored by the previous studies in this study area.

1.3 Objective of the study

The main objective of this research is to analyze the spatial-temporal variability indices of hydro-climatic variables (precipitation, temperature, and streamflow) and its effect and implications on water resources in the Kyoga Basin (Upper Nile). These indices serve as good indicators of how the hydro-climate variability has evolved with the changing water resource availability. Studies on climate variables in the Nile Basin (which covers the Kyoga Basin) indicate an increase in temperature, and patterns of precipitation have experienced changes(Onyutha, 2016c). Streamflow tends to reflect how a catchment area as a whole has been responding to the variability in climate. Spatial-temporal characteristics of hydro-climatic variables like precipitation, streamflow and temperature are vital in understanding the effects on local scale water resources quantity (Zhang et al., 2001).

The specific objectives of this study are:

- To derive indices from the main hydro-climatic variables that can reflect the water resource status in the Lake Kyoga Basin.
- To assess the seasonal and annual variability of hydro-climatic indices.
- To understand and evaluate the spatial-temporal interaction of hydro-climatic indices using wavelet transformation coherent (WTC).
- To identify the implication of hydro-climatic indices variability on agriculture water management and ecological re-storage.

1.4 Significance of the study

The information generated in this could be vital to the water resources managers while investigating the effect of hydrological and climate variability on water resources management and planning.

Trend detection and analysis in the hydro-climatic variables can also bring out issues which need to be considered as part of adaptation and mitigation efforts associated with extreme variability. It can also be useful for agriculture (e.g. growing seasons, irrigation schemes, and crop productions) production management and planning, including food security and sustainability.

Moreover, the results of this research could be used for the current and future water resources planning and management efforts in Uganda, as it involves making extensive reasonable assessment on the dynamic interaction of hydro-climatic indices. This study provides significant contribute to the scientific community of hydro-climatic modeling and agriculture field.

1.5 Novelty/contribution of the study

Some trend detection on hydro-climate variability studies have been conducted in Uganda and the Upper Nile using statistical and deterministic approach. However, it is important and novel to add the WTC approach to fully understand the interaction and causality of the selected hydro-climate indices. Selection of the WTC method is premised in its being simple and new approach in hydrology to understand temporal variability. The method is also important in considering the seasonality and oscillation of the hydro-climatic variables. This research contributes to generating knowledge on understanding of the hydro-climatic indices and its interaction in intera and inter annual time scale using statistical approach.

1.6 Scope of study

The study entirely focuses on hydro-climate indices variability and detection of their temporal trend. Similarly, the temporal analysis is mainly based on two-time scales (seasonal and annual).

1.7 Study area description

Lake Kyoga Basin (hereinafter referred as to as "LKB") occupying 25% of the Uganda area is approximately 58,000 km^2, and is the second largest catchment among eight basins in the entire country. Figure 1.1 shows the location of the Basin. The basin covers the central and extends to the eastern and north-eastern part of Uganda. It lies within latitudes 0.15^0 – 3.8^0 N and longitudes 32^0 – 35^0 E. The elevation ranges from about 890 m above sea level (m.a.s.l) in the floodplains near Lake Kyoga to around 4318 m.a.s.l in the areas of Mountain Elgon in at the border of Uganda with Kenya. There are several sub-catchments within the Lake Kyoga basin, some of these are shown in the figure 1.1 and the selected stations for each sub-catchment are shown in the table 1.1.

The Basin is considerably blessed with water resources, namely rivers (e.g. Victoria Nile, Mpologoma, Manafwa, Namatala, Malaba, and Ssezibwa, Okere, Ngalatapolon), lakes (Kyoga, Bisina), extensive wetlands and groundwater. The climate experienced in the basin is the modified equatorial with an annual precipitation of more than 1,200mm and average temperature of 22°C. The main land uses in the Basin are agriculture (mainly subsistence), growing crops such as maize, cassava, rice, cotton, coffee, tea, beans, sorghum, potato, banana, and sugarcane among others (JICA, 2011). The Manafwa and Malaba wetlands have large-scale rice irrigation schemes, but small-scale rice farms were also started immediately downstream of the large irrigation schemes. Upstream areas of Namatala and Naigombwa wetlands have also been converted for small-scale rice farming(Kayendeke & French, 2019). Fishing is also another economic activity especially along the shores of Lake Kyoga (JICA, 2011).

Table 1.1: Sub-catchments in LKB and the corresponding selected weather stations

Sub-catchment	Catchment Area (km^2)	Weather stations	Lat (N)	Long (E)	H(m)	Average Annual rainfall (mm)	Average Annual temperature(^0C)
Okere	13,704	-Kotido -Morulem -Kangole -Magoro -Soroti	3.02 2.62 2.47 1.73 1.72	34.10 33.77 34.45 34.10 33.62	1200 1440 1200 1080 1132	721 1159 699 909 1413	21 23 24 25 25
Kelim	1,931	-Buginyanya	1.28	34.37	1845	2108	20
Mpologoma	7,519	-Tororo -Kibale VTC	0.68 1.20	34.17 33.78	1170 1080	1495 999	24 21
Victoria Nile	2,321	-Mutai Forest	0.57	33.23	1128	1289	23
Ssezibwa	1,509	-Mukono Agric	0.45	32.75	1200	1332	23

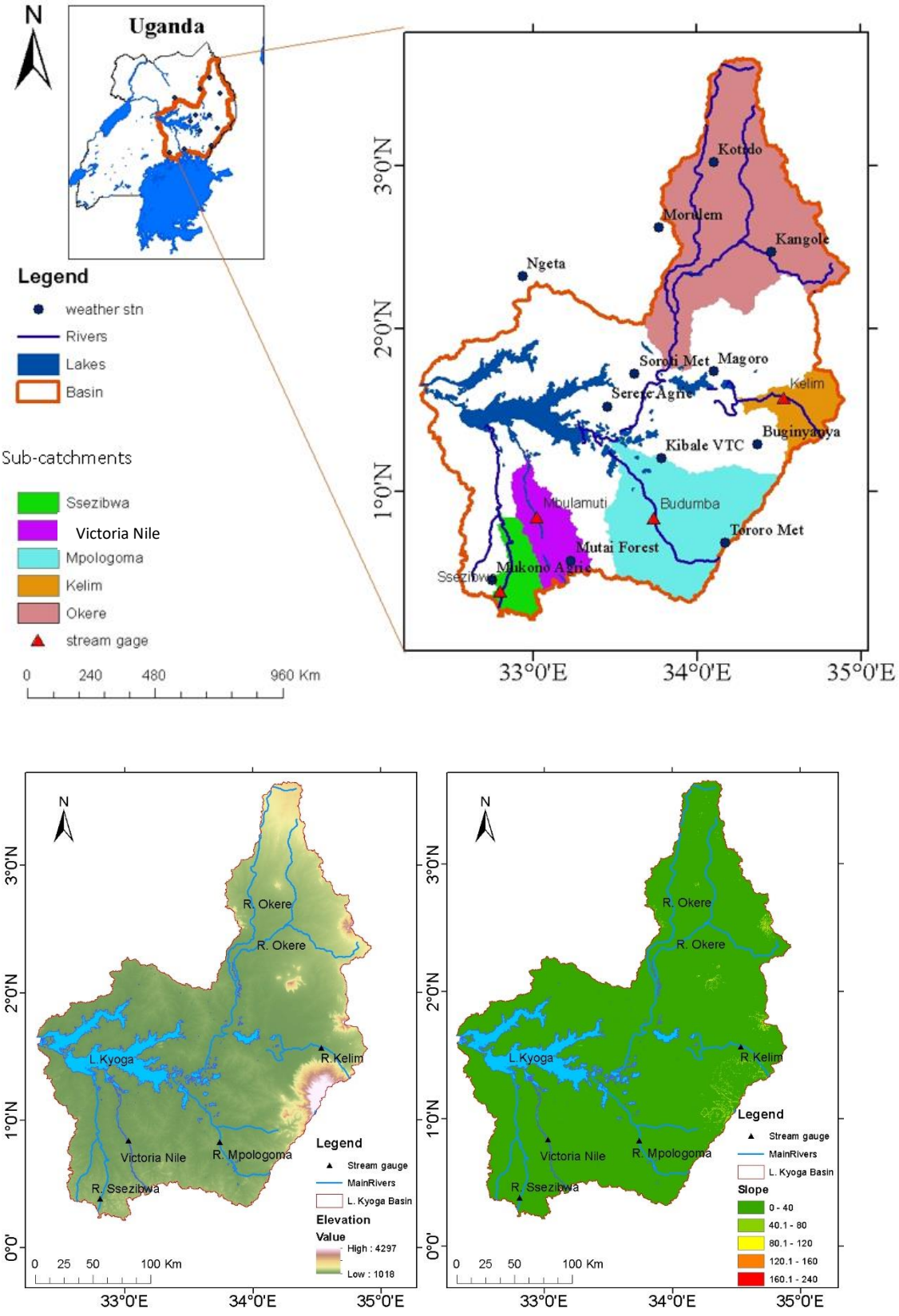


Figure 1.1: Location of Lake Kyoga Basin (LKB)

2. LITERATURE REVIEW

2.1 Climate variability

It is very important to understand the difference between climate variability and change, where climate variability is the natural variation in the climate from one period to the next. Climate variability appears to have a very marked effect on many hydrological series. This has two important consequences: Climate variability can easily give rise to apparent trend when records are short-these are trends that would be expected to disappear once more data had been collected (Kundzewicz & Robson, 2004).

Climate variability can be triggered by large scale atmospheric-ocean circulations and/or by anthropogenic activities (Nyeko-ogiramoi et al., 2013). Atmosphere-ocean circulations cause climate to vary in season-to-season or year-to-year time periods. The issue on climate variability relies heavily on the detection of trends in instrumental records of hydro-climatic variables such as air temperature, precipitation and streamflow (Nyeko-ogiramoi et al., 2013).

Uganda experiences a tropical climate with quite high rainfall (annual average rainfall >1000 mm) and strong seasonal patterns. The primary influence on seasonality is the Inter Tropical Convergence Zone (ITCZ), which drives southeasterly and northeasterly moist air currents from the Indian Ocean (Basalirwa, 1995; Kigobe et al., 2011). This causes two rainy seasons—the southeast and northeast Monsoons-each of which lags the migration of the Sun around the Equator by approximately one month. In Uganda, these two monsoon seasons are called the "long rains" in March, April and May (MAM) and the "short rains" in October, November and December (OND) (Basalirwa, 1995; Indeje et al., 2000; Kigobe et al., 2011; Onyutha, 2016c). This bimodality is strong around the Equator, becoming less strong in the northern and southern regions of the country. Other influences on rainfall variability include tropical storms, continental low-level troughs, extra-tropical weather systems and the moist westerlies from Zaire, locally termed Congo air mass (Basalirwa, 1995; Indeje et al., 2000). Local patterns are also influenced by the presence of water bodies, in particular, Lake Victoria and Lake Kyoga, and topography and vegetation cover influences. These features introduce significant modifications in the general wind- flow patterns over the region (Basalirwa, 1995; Indeje et al., 2000).

Temperature is associated with several extremes weather events such as heat waves and cold spells which impacts human health, the physical environment, ecosystems, and energy consumption (Filahi et al., 2016). The IPCC report indicates the Europe and Asia are likely to experience temperature extremes. This is consistent with the forecast study done by Kigobe et al., (2014) indicating that there will be an increase in temperature in the Kyoga Basin. Similarly, there is a strong association between precipitation and droughts or floods (Filahi et al., 2016). According to IPCC report of 2013, future increase in precipitation extremes related to the monsoon is very likely in South America, Africa, East Asia, South Asia, Southeast Asia and Australia.

2.2 Hydro-climatic Indices

The ENSO phenomenon is known to be a fundamental and quasi-periodic feature of the ocean atmosphere system, with periodicities ranging from seasonal to about 8 years (Indeje et al., 2000). There are several indices used to express this phenomenon with the Southern Oscillation index being the oldest and several others. These indices are based mainly on the sea surface temperature (Trenbeth et al., 2002). Dry and wet conditions across the East Africa can be linked to the increase or decrease in the Sea Surface Temperature (SST) or atmospheric pressure at the sea level across the various oceans (Onyutha et al., 2020).

Drought indices or models are used for assessment of occurrence and severity of droughts (Wambua et al., 2014). Drought Indices (DIs) were developed for specific regions using specific structures and forms of data input. These indices provide quantities for determining the onset and end of a drought event, in addition to the level of drought severity (Bernard et al., 2013). Drought indices are often derived from massive amounts of hydroclimatic data and are used for making decisions on water resource management and water allocation for mitigating the impact of drought. Many drought indices exist; e.g., the Palmer Drought Severity Index (PDSI), Streamflow Drought Index, Standardized streamflow Index (SSI), Bhalme-Mooley Index, Standardized Precipitation Index (SPI), Normalized Difference Water Index, Crop Moisture Index, Surface Water Supply Index, Precipitation Anomaly Classification, Reclamation Drought Index, National Rainfall Index and Soil Moisture Drought Index (Bernard et al., 2013). The SPI seems to be more suitable for monitoring droughts in Easter Africa than the other indices, because it is easily adapted to the local climate (Ntale & Gan, 2003) . Streamflow time-series indices that are designed to facilitate the analysis of (i) changes

in the regional water balance, (ii) changes in the seasonal cycle, (iii) floods, and (iv) low flows (Gudmundsson et al., 2018).

The Aridity Index (defined as the ratio of potential evaporation to precipitation), summarizes the aridity concept into a single number (Greve et al., 2017) . The term aridity refers to the lack of moisture which usually results from the rate of evapotranspiration being higher than the precipitation in a drainage basin (Greve et al., 2019) Regions where aridity index is less than 1.0 are classified as wet areas; the regions where aridity index is more than 1 are classified as dry areas since the evaporative demand cannot be met by precipitation (Huang et al., 2016; Ponce et al., 2000). Unlike drought, aridity refers to a more or less permanent climatic condition (Tabari & Aghajanloo, 2013).

Extreme events can be classified by means of percentile-, threshold- or duration-based indices, or by analyzing the statistical behavior of the tail of a weather element's probability distribution (Sillmann & Roeckner, 2008). Indices for climate extremes based on daily temperature and precipitation data were defined by the Expert Team on Climate Change Detection Monitoring and Indices (ETCCDMI).

2.3 Hydrological variability

Hydrological variability is the change in hydrological quantity when comparing one spatial location with another or one time with another. Variability occurs naturally, and also because of anthropogenic activity (e.g. land cultivation, urbanization, and forest management)

(Conway et al., 2009; Woods, 2005). We can see evidence of this variability in measurements of rainfall, air temperature, soil moisture, snow cover, groundwater level, and streamflow, or any other hydrological quantity(Woods, 2005).

An important and dramatic practical expression of temporal variability is the occurrence of extreme hydrological events – most obviously floods, very high lake and groundwater levels, also droughts along with very low levels in lakes, rivers, and groundwater. The temporal distribution of floods depends greatly on the physical setting, with some regions having floods that occur at consistent times of the year because of the seasonal weather cycle and its interaction with the landscape and with water resource management, while others can have floods at any time of year, or in fact have years without any significant floods, or even any streamflow at all. Temporal variability can be done at a wide range of timescales, both the

relatively regular diurnal and annual fluctuations, as well as irregular fluctuations (Woods, 2005).

Spatial phenomena in hydrology are mainly driven externally by spatial patterns in climate, soils, vegetation, topography, and geology. However, at very long timescales, complex spatial organization develops which is created by the internal dynamics of the hydrological system. In surface hydrology, this self-organization appears to manifest itself in (i) consistent upslope-to-downslope structure of soils and hillslope geomorphology; (ii) regularities in channel network geomorphology; and (iii) braided river networks. However, our knowledge of how and why such regularities emerge remains very limited, and as a result, they (and other emergent features) have yet to find a place in a coherent theory of hydrology(Woods, 2005).

In Africa both precipitation and river flows display high levels of variability across a range of spatial and temporal scales, with important consequences for the management of water resource systems. Examples of variability include prolonged periods of high flows for rivers draining large parts of East and central Africa (Conway et al., 2009).

The main driver of much of the observed variability in river flows precipitation, particularly at the scale of large river basins(Conway et al., 2009) In East Africa some extreme tends to be associated with periodic circulation dipole events in the Indian Ocean and complex interaction with the El Nino–Southern Oscillation (ENSO), particularly during the short October–December rains(Conway et al., 2009; Onyutha, 2018)

2.4 Interrelationship between climatic and hydrological extremes

Weather and climate are the most common direct cause of observed temporal variation in hydrological phenomena such as soil moisture, river flow, or groundwater levels (Cahill, 2002; Woods, 2005). However, the effect of climate change/variability on the hydrological cycle is highly nonlinear, extremely complex, and less certain, and it furthermore differs substantially within and among different hydrometeorological region(Fan & He, 2015). Hydrological systems modulate the meteorological variations, damping some of them and amplifying others, but the ultimate cause of temporal variability can usually be traced back to meteorological processes that control precipitation and evaporation(Woods, 2005). Model studies suggest and observational evidence confirms that an intensified hydrological cycle is likely to be an important consequence of global climate change (Cahill, 2002; Tadic et al., 2016). However, relationship between physical characteristics and temporary trends of annual precipitation, and

runoff is very important and unique for each catchment area (Tadic et al., 2016). The intensification of water cycles is responsible for extreme events such as tropical storms, flash floods and droughts (Dars, 2013).

A comprehensive review of impacts is provided by IPCC (2013), indicates that climatic change is likely to increase runoff in higher latitude regions because of increased precipitation. Changes in flood frequencies are expected in some locations, particularly in northern latitudes and in catchments experiencing snowmelt flooding events. Changes in the hydrological regime that do occur are not expected to be equally distributed throughout the year (Burn & Elnur, 2002) .

2.5 Implication of hydro-climate variability on agriculture, reservoir operation, water storage, drought, flood

Extreme precipitation events are one of the major climate change concerns which can seriously influence the hydrology, agriculture, hydro-power generation and socio-economics

(Dars, 2013). For example, in Austria a study proved that droughts are strongly governed by combination of climate characteristics, increase of temperature and change of precipitation pattern, and catchment control. One of the most important climate elements is precipitation, strongly affecting water balance and quality of water resources (Tadic et al., 2016).

Future climate scenarios predict higher evapotranspiration rates, lower discharge rates, and groundwater levels (Visser et al., 2012). It means that, in the mostly agricultural areas, irrigation rates will increase, but the water resources could be questionable (Visser et al., 2012). As a consequence, serious water scarcity could be expected on the regional levels, meso and macro scale (Tadic et al., 2016).

In Uganda, agriculture is mainly subsistence and rain-fed therefore climate variability exacerbates the socioeconomic woes of Uganda especially in the light of pressures of trying to achieve food security and alleviate poverty(Nsubuga et al., 2014; Onyutha & Willems, 2015). In Eastern Uganda farmers report a general delay in the start of the rainy seasons, poor distribution within the season and sometimes early cessation (Kansiime et al., 2013). There is also variability in the intensity of rain which has resulted in increased frequency of drought, flash floods and landslides (Kansiime et al., 2013).

It has been found that precipitation variations may lead to greater changes in river runoff, especially for rivers which are not recharged by glaciers and snow melt Water Rivers (Men et al., 2019). Unlike precipitation changes, the increase in evaporation caused by rising temperatures has a slower impact on runoff (Men et al., 2019). These lead to fluctuation in streamflow, a sudden decrease of streamflow can have a large negative impact on the distribution of aquatic plants and animals as well as shipping and irrigation; furthermore, the significant increase of runoff can result in food disasters that seriously threaten lives and property (Chai et al., 2019). Furthermore, runoff variation is more sensitive to climate variability and human activities during extreme drought years. The variation characteristics of discharge become more complex under the effects of both climate variability and reservoir operation.

2.6 General methods to detect the hydro-climate variability

There are several methods developed by scholars to detect hydro-climatic variability. They can be divided into four types according to their basic ideas: data fitting, temporal domain-based test, frequency domain-based test and temporal and frequency domains-based test (Sang et al., 2013). These methods can also be classified statistical and graphical methods as briefly described below.

For the assessment of hydrological and climate variability and trends, different parametric (e.g., T-test, F-test, bootstrap and linear regression) and nonparametric methods can be used (Burn et al., 2010). Some of the nonparametric trend detection methods include the Mann-Kendall MK (Kendall, 1955; Mann, 1945) and the Spearman's rho tests. The slope m, of a monotonic trend can be given by the method of Sen, (1968)and Theil (1950). Although parametric methods are more powerful, their applications are restricted to normally distributed time series. Since most of the climatic time series, do not fulfill normality requirement, nonparametric methods are most frequently applied in trend analysis(Burn et al., 2004; Onyutha, 2016b, 2016a). In addition, the nonparametric methods are considered more robust than parametric methods against the outliers in a time series (Mahmood et al., 2019).

However, time series, specifically precipitation, are mostly considered difficult to predict because these consist of different components, such as trends, periodic patterns, cyclic behavior, and white noise (random component), which limit the application of simple and widely used forecasting methods as mentioned above(Mahmood et al., 2019).

Apart from the regression analysis, it is also not possible to calculate trend magnitude (slope), which brings additional assumptions for the theoretical validation in practical applications. Therefore, Sen proposed a new methodology on the basis of subsection time series plots derived from a given time series on a Cartesian coordinate system (Şen, 2012). The innovative-Şen approach yields trend categorizations as very low, low, medium, high, very high, which should be taken into consideration in future flood (very high) and drought (very low) studies (Dabanlı et al., 2016).

2.7 Previous similar studies in the basin

The Lake Kyoga basin is perhaps the least studied of the Nile tributaries yet it covers about 25% of the total area in Uganda (Brown & Sutcliffe, 2013). Some studies on precipitation (rainfall) trends have been done about the Nile basin which covers the Kyoga Basin. The study done by Onyutha & Willems(2015) to find the origin of the driving forces for the temporal variability in rainfall. This study included correlation analyses were carried out using global monthly sea level pressure (SLP) and sea surface temperature (SST). The investigation was supported by the use of 10 climate indices (IOD, NPI, Niño 3, Niño 3.4 among others). The results indicate that there is an increasing trend in the precipitation which is suspected to be influenced by the North Atlantic Ocean, Niño 3, Niño 3.4, and the Indian Ocean (Onyutha & Willems, 2015).

Further study of the Nile basin was done byOnyutha, in 2016, assessing changes in annual and seasonal potential evapotranspiration (PET) using the cumulative rank difference method. Trend was assessed both graphically and statistically. The results showed that there was a positive increasing trend in the PET (Onyutha, 2016b) .

Nyenje & Batelaan(2009), did a trend analysis of the climate in the Ssezibwa catchment a sub catchment of the Kyoga basin using trend Testing Tool. The study predicted that there will an increasing trend in temperature and decrease trend in discharge (approx. 50% per decade) but no significant trend in the precipitation. The Sen's T test indicated a slight downward trend in annual rainfall with a weak frequency fluctuation was detected in the Kyoga basin by Nsubuga et al (2014). Kansiime et al (2013) conducted a study in part of Lake Kyoga Basin on rainfall variability using (Mann-Kendall and Sen's T tests), coefficient of variation (CV), precipitation concentration index and drought severity index. The study found that there a general increase with greater variability during the rainy season that spans from August to November than that

which spans from May to June (Kansiime et al., 2013). This study also noted that there was higher variability in the rainfall in highlands as compared to the low lands (Kansiime et al., 2013).

Kyatengerwa et al (2020), assessed agricultural droughts for 1984–2017 in Uganda using SPI and SEDI, results showed increased drought frequency after 1999 and indicate that central and northwestern Uganda would face increasing drought risks in the future. The declining precipitation in Uganda has been attributed to rising surface temperatures of the Indian Ocean, and is expected to persist up to the next decade. This study suggested that droughts in major croplands could be often accompanied by high heat-wave temperatures in Uganda due to strong land-atmosphere coupling, and thus mortality risks in ecosystems could increase together with water stress.

ENSO accounts for about 50% of the East African seasonal rainfall variance and was also observed significant teleconnections between the SOI and seasonal rainfall over parts of East Africa (Ogallo, 1989). Indeje et al (2000), further confirm the relationships between seasonal rainfall in East Africa and phases of ENSO. The results showed relatively wet conditions were observed during the March–May and October–December rainfall seasons of the El Nin˜o years. Similar results were obtained during June–September of the post-ENSO (_1) years. Dry conditions dominate in June–September of the El Nin˜o onset years and the two seasons (March–May and October–December) of the post-ENSO (_1) years. Onyutha et al (2020) investigated the relationship between precipitation, potential evapotranspiration (PET) and ENSO indices in the Lake Kyoga Basin. Both seasonal and annual precipitation from 1960 to 2015 exhibited an insignificant decrease in most parts of the Basin. However, at some of the locations, PET exhibited an increasing (though insignificant $p > 0.05$) trend. Variance in annual precipitation and PET was found to be explained by the IOD, AMO and NAO, in decreasing order of influence respectively.

3. MATERIALS AND METHODS

3.1 Data Sets

3.1.1 Hydrological and meteorological datasets

The data used in this research include the climatic (temperature and precipitation) and hydrological (Streamflow). The catchment has over 100 meteorological stations, with varying record lengths. Relatively long spans of missing data exist for several stations varying from several months to years (Kigobe et al., 2011). The daily meteorological data of 12 stations with the least amount of missing data for the period ranging from 1974 – 2019 was collected from the Uganda National Meteorological Authority (UNMA) under the Ministry of Water and Environment (MWE). The selected stations are summarized in the table 1.1.

The stream flow data of 4 rivers within the basin was collected from the Directory of Water Resources Management under the MWE of Uganda. The gauged rivers are in the southern part of the basin and the details of the gauging stations is summarized the table 3.1. and figures 3.1 and 3.2 show the streamflow hydrograph and precipitation hyetograph of monthly data for the different sub-catchments.

Table 3.1: Selected river gaging stations in Kyoga Basin

Gauging station name	River	Lat (N)	Long (E)	H(m)	Q (m^3s^{-1})	Catchment area (km^2)
Mbulamuti	Victoria Nile	0.84	33.03	1030	1033.20	2321
Budumba	Mpologoma	0.83	33.79	1078	19.34	7519
Ssezibwa fall	Ssezibwa	0.37	32.87	1034	1.70	1509
Mbale- Moroto Road	Kelim (Greek)	1.60	34.54	1100	4.69	1930

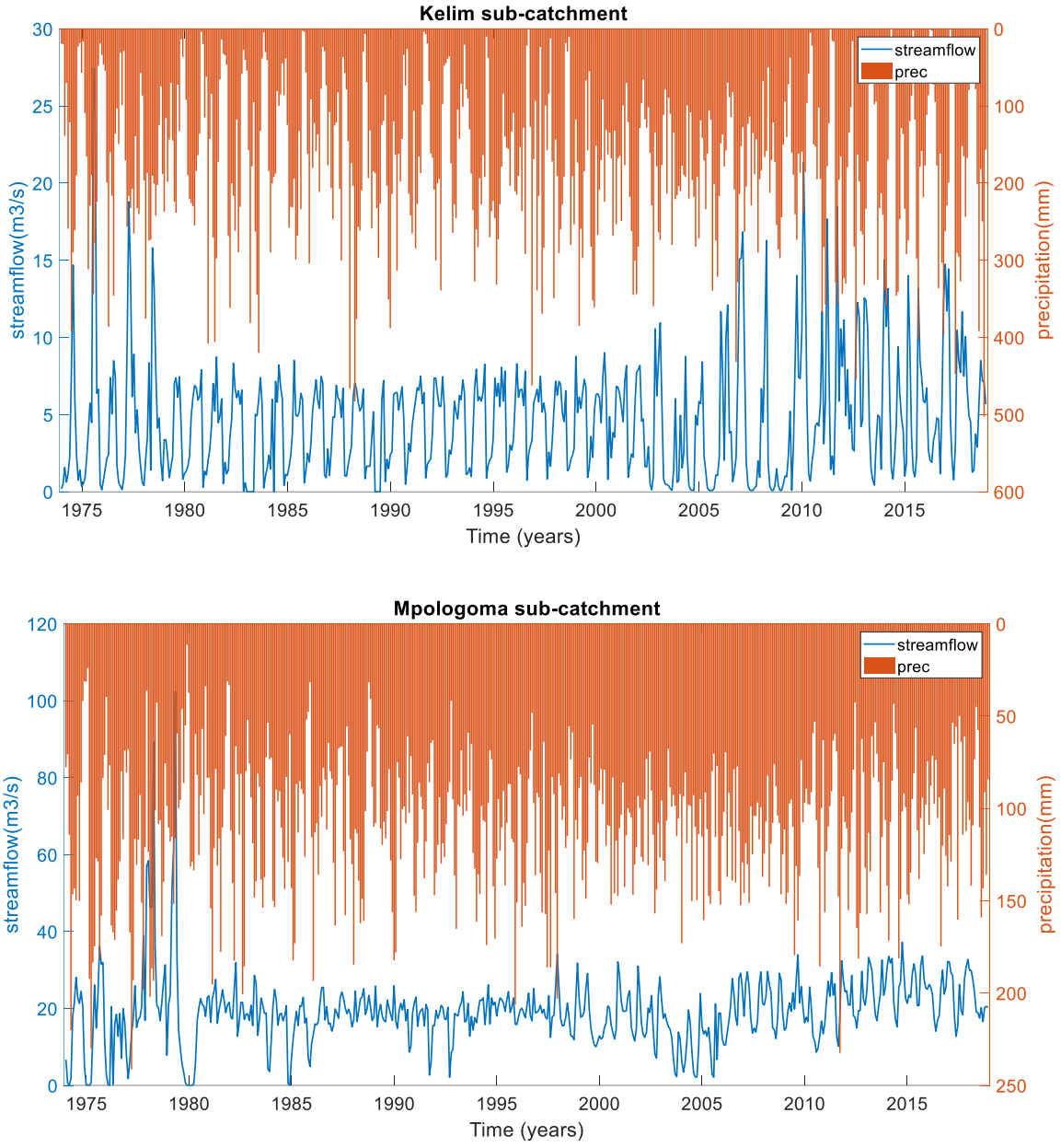


Figure 3.1: Streamflow hydrograph and precipitation hyetograph of Kelim and Mpologoma sub-catchments.

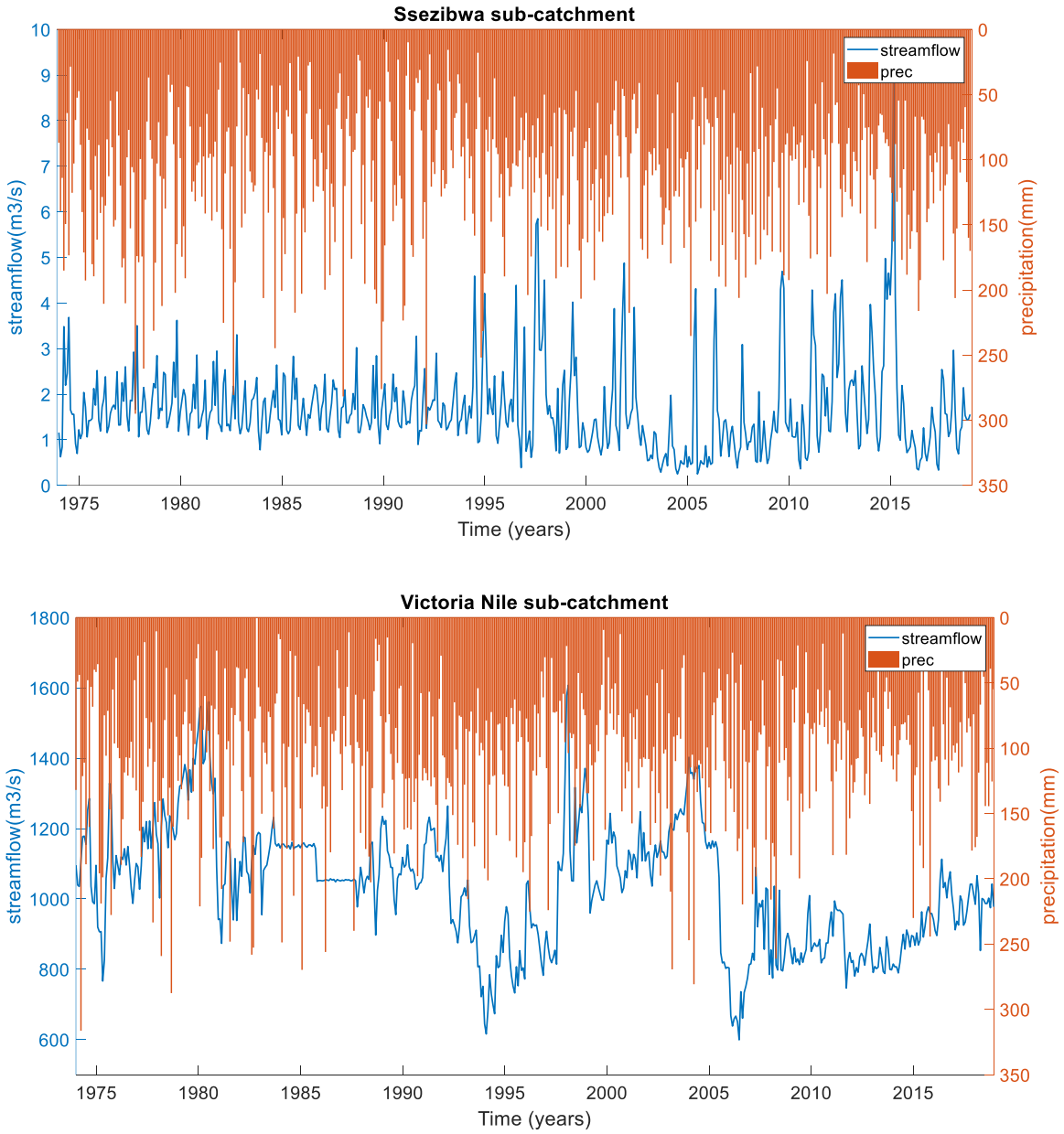


Figure 3.2: Streamflow hydrograph and precipitation hyetograph of Ssezibwa and Victoria Nile sub-catchments.

As developing countries, the quality of available climate and hydrological data status is not adequate with large missing value (Onyutha & Willems, 2017) . In this study, remote sensing datasets were used to fill the missing value of precipitation and temperature. The Daily gridded data of both precipitation and temperature data was accessed from the Princeton University Global Data Forcing (PGF) (downloaded from http://hydrology.princeton.edu/data/pgf/v3/0.25deg/) for the period of 45 years 1972 – 2016 and used to fill in the missing data. The PGF which provides a global coverage and spatial resolution of 0.25° × 0.25° was developed by merging the reanalysis datasets of the National

Centers for Environmental Prediction (NCEP) and National Center for Atmospheric Research (NCAR) and a collection of global observed database including the TRMM, the CRU TS2.0, the GPCP, and the NASA Langley Research Center SRB products.(Sheffield et al., 2006)

The missing values in the streamflow data were filled using predictive mean matching (PMM) regression model. In the PMM model, imputed values are sampled only from the observed values of the respective variable that match predicted values as closely as possible(Aguilera et al., 2020).

The areal precipitation and temperature values for each station were calculated using Thiessen polygon approach (Thiessen, 1911) summarized in equation 3.1 below:

$$V_a = \frac{A_1 * S_{V1} + A_2 * S_{V2} + \cdots + A_n * S_{Vn}}{(A_1 + A_2 + \cdots + A_n)} \qquad (3.1)$$

where V_a is the average rainfall or temperature, $A_{1, 2...}n$ is area of proximal polygons, $S_{V1, V2,...Vn}$ stand for station variables.

Many researchers used Thiessen method to estimate the spatial distribution of precipitation and temperature in several studies. This method can be used for the areas which have insignificant topographic differences and inadequate meteorological station density (Karaburun et al., 2011).

3.1.2 Climate Indices (NAO and ENSO indices)

Fluctuations in the sea level pressure (SLP), can reveal useful information on atmospheric circulation which brings about drier and wetter conditions (Onyutha & Willems, 2015). The North Atlantic Oscillation (NAO) was considered for this study. NOA is the normalized SLP difference between SW Iceland (Reykjavik), Gibraltar, and Ponta Delgada (Azores). The NAO (Hurrell, 1995; Jones et al., 1997) was obtained from the Climatic Research Unit (CRU) (https://www.esrl.noaa.gov/psd/gcos_wgsp/Timeseries/NAO/).

The ENSO phenomena are known to be a fundamental and quasi-periodic feature of the sea surface temperature (SST), with periodicities ranging from seasonal to about 8 years (Indeje et al., 2000). Changes in SST, can generate imbalance in the heat-flux field which can also bring about anomalous atmospheric circulation and rainfall patterns (Onyutha & Willems, 2015). Variations of SSTs over the Indian and South Atlantic oceans play a significant role in the variations of rainfall over the Nile Basin and East Africa (Indeje et al., 2000; Onyutha & Willems, 2015). For this study a number of readily and freely available climate indices were used. These indices are:- Area averaged Niño SST indices (Rayner et al., 2003; Trenberth,

1997) for the tropical Pacific regions described by Niño 3 (90–150Wand 5N–5S) and Niño 3.4 (120–170W and 5N–5S), were also obtained from CRU (https://www.esrl.noaa.gov/psd/gcos_wgsp/Timeseries/NAO/).

3.2 Methods

3.2.1 Estimation of potential evapotranspiration (PET)

Potential evapotranspiration (PET) was estimated using the Hargreaves equation since it requires only two easily accessible parameters, temperature and solar energy. The Hargreaves equation is expressed as follows:

$$PET = 0.0023 * (S_O/\lambda) * (T + 17.8) * (T_{max} - T_{min})^{0.5} \quad (3.2)$$

PET is the daily potential evapotranspiration rate(mm/month), S_0 is the extra-terrestrial solar radiation (kJ/m^2/month), T is the mean daily temperature (^{0}C), λ is the latent heat of evaporation (kJ/kg), T_{max} is the daily maximum temperature (^{0}C), T_{min} is the daily minimum temperature (^{0}C). The 1985 Hargreaves equation has a minimum weather data requirement, using mainly maximum and minimum air temperature (Hargreaves & Samani, 1985).

The equation self-compensates for the lack of Rs (global solar radiation at the surface) and humidity data required by the Penman and Penman-Monteith methods. The parameter of temperature range (Tmax -Tmin) in equation 3.2 implicitly accounts for effects of cloudiness in that temperature range generally decreases with increasing cloudiness. In addition, temperature range correlates with relative humidity and vapor pressure deficit and is inversely influenced by wind run.(Hargreaves & G, 2003)

3.2.2 Standardised Precipitation Indices (SPI)

SPI is a drought index that shows the catchment drought status based on precipitation. The (SPI) for any location is calculated based on the long-term precipitation record for a desired period. This long-term record is fitted to a probability distribution, which is then transformed to a normal distribution so that the mean SPI for the location and desired period is zero (McKee et al., 1993). The fundamental strength of SPI is that it can be calculated for a variety of time scales, it exhibits statistical consistency, and has the ability to present both short-term and long-term droughts over time scales of precipitation variation (Belayneh & Adamowski, 2013) . This versatility allows SPI to monitor short-term water supplies, such as soil moisture which is important for agricultural production, and long-term water resources, such as groundwater

supplies, streamflow, and lake and reservoir levels. Soil moisture conditions respond to precipitation anomalies on a relatively short scale.

The 3-month accumulated precipitation in the SPI for a short-term or seasonal drought index, a 12-month SPI for an intermediate-term drought index, and 48 months for a long-term index (McKee et al., 1993).

The length of precipitation record and nature of probability distribution play an important role for calculating SPI. The length of a precipitation record has a significant impact on the SPI values. Similar and consistent results are observed when the SPI values, computed from different lengths of record, have similar gamma distributions over different time periods. However, to identify key dry periods, it is important to analyse data for time scales greater than 6 months. This is because the high frequency of SPI values at shorter time scales conceal the critical dry periods. For time scales shorter than 6 months, there is insignificant autocorrelation while for time scales greater than 6 months, the autocorrelation increases significantly (Belayneh & Adamowski, 2013; Wambua et al., 2014) (. When SPIs are calculated for long time scales (longer than 24 months) fitting a distribution might be biased due to the limitation in data length and it is true that when finer resolutions of spatial analysis need to be investigated, long data sets are not available in many catchments around the world.

For dry climates where precipitation is seasonal in nature and zero values are common, there are too many zero precipitation values in a particular season. In these climatic zones, the calculated SPI values at short time scales may not be normally distributed because of the highly skewed underlying precipitation distribution and because of the limitation of the fitted gamma distribution. This may be prone to large errors while simulating precipitation distributions in dry climates from small data samples.

Table 3.2 Drought intensities as per SPI values Adopted from Agnew & Chappell (1999)

SPI/SSI Classes	Condition
>1.65	Extremely wet
>1.28	Severely wet
>0.84	Moderately wet
>-0.84 and <0.84	Normal
<-0.84	Moderately drought
<-1.28	Severe drought
<-1.65	Extremely drought

3.2.3 Standardised Streamflow index (SSI)

The Standardized Streamflow Index (SSI) allows accurate spatial and temporal comparisons of the hydrological conditions of a stream or a set of streams (Telesca et al., 2012). SSI uses the same principle as the SPI, therefore the calculations of SSI is the same as the process of calculating SPI, the only difference is that instead of precipitation data, streamflow data are used. (Barker et al., 2015; Shamshirband et al., 2020; Vicente-Serrano et al., 2012). In contrast to precipitation and SPI calculation, numerous probability distributions have been fitted to streamflow data for SSI calculation. This is because stream flows are characterized by spatial variability larger than that of climatic variables and the seasonality is subjected to intense changes (Telesca et al., 2012). This variability makes rather difficult to select the most appropriate distribution in order to calculate a streamflow drought index over a wide area (Telesca et al., 2012).

In this study the gamma distribution was used to fit streamflow. This distribution has been used in previous studies to fit streamflow datasets (Nkiaka et al., 2017; Vogel & Wilson, 1996; Zhang et al., 2015).

3.2.4 Aridity index (AI)

Aridity index (AI) is the ratio of PET and precipitation as described by Budyko (1974) and can be expressed as

$$\text{AI} = {}^{PET}/_{P} \quad (3.3)$$

where PET is the potential evapotranspiration (mm) and P is the precipitation (mm). For this study, the AI was calculated on an annual scale.

Regions where aridity index is greater than unity are broadly classified as dry since the evaporative demand cannot be met by precipitation. The climate in these areas tends to suffer from drought and water resource shortages (Li et al., 2017). Regions with AI less than unity are broadly classified as wet. The aridity index may also be related to climatic regimes in a broad sense, e.g. arid, semi-arid, sub-humid, and humid regions are defined by the aridity index ranges of 12 < AI ≤ 5; 5 < AI≤ 2; 2 < AI≤ 0.75; and 0:75 < AI ≤ 0.375; respectively (Arora, 2002; Ponce et al., 2000).

3.2.5 Hydro-climatic Indices

The indices for precipitation are the maximum 5-day precipitation amount during a year (RX5day) and the 95th percentile of precipitation on wet days (R95). RX5day can be expressed as, let RR_{kj} be the precipitation amount for the 5-day interval ending k, period j. Then maximum 5-day values for period j are;

$$Rx5day_j = \max\left(RR_{kj}\right) \quad (3.4)$$

RX5day can be used as a flood indicator, because generally floods are not caused by a single heavy thunderstorm event, but more likely, by long-lasting heavy precipitation events that are extended over a large region (Sillmann & Roeckner, 2008). The increase in the Rx5day increases the maximum quantity of total precipitation which in turn improves hydrological cycle (Ruiz-Alvarez et al., 2020).

The R95 can be described by letting RR_{wj} be the daily precipitation amount on a wet day w (RR ≥ 1.0mm) in period i and let $RR_{wn}95$ be the 95^{th} percentile of precipitation on wet days in the study period. If W represents the number of wet days in the period, then:

$$R95 = \sum_{w=1}^{W} RR_{wj} \quad (3.5)$$

Where $RR_{wj} > RR_{wn}95$

R95 characterizes and is suitable for analysing changes in the upper tail of the precipitation distribution. It implicitly takes into account the trends in the total amount of precipitation. Key

to note is that the R95 index is not sensitive to changes in the number of wet days (Tank & Konnen, 2003).

Q95(the 5-percentile flow) is the discharge that is exceeded 95% of all the time. This low flow characteristic is used worldwide and has been chosen because of its relevance for numerous water resources management applications (Laaha & Blöschl, 2007). These include;

1. Water quality management for issuing discharge permits and locating treatment plants.
2. Water supply planning to determine allowable water transfers and withdrawals
3. For hydropower development it's used for determining environmental flows
4. In an environmental context for streamflow habitat assessment

The table 3.4 below show a list of the hydroclimatic indices considered for this study

Table 3.3: The list of hydro-climatic indices used in this study

Index	Description	Units
SPI	Standardised Precipitation Index	
RX5day	Maximum 5-day precipitation amount during a year	mm
R95	very wet days	Days
Q95	95^{th} streamflow quantile	m^3s^{-1}
SSI	Standardised Streamflow Index	
AI	Aridity Index	

3.2.6 Persistence of Hydroclimatic Indices (Hurst exponent)

Persistence is the presence in a time series of significant dependence between observation as long time span a part (Hosking, 1984) . The *H* exponent was used in this study, it is a useful statistical method for understanding the properties of a time series without making assumptions about statistical restrictions. The method of rescaled-range (R/S) analysis (Peters, 1994) is used in the present study. The first step of this method is to divide a time series into a number of shorter time series. Hurst(1951) stated that the distance that a random particle covers increases with the square root of time within those shorter time series as in the following expression:

$$R = \sqrt{T} = T^{0.5} \qquad (3.6)$$

where R is the distance covered (range) and T is a time index. The dimensionless form is obtained by dividing R by the standard deviation (S) of the time series. Hurst(1951) found that the intensity level of a trend and the level of noise in a time series can be measured by how the R/S scales with time. That is, by how high the H value is above (below) 0.5. To interpret the operation of R/S, take a time series, x_i (i=1, …, N). In the first step, each of the shorter time series is normalized by subtracting the sample mean of x:

$$y_i = x_i - \bar{x} \tag{3.7}$$

where the remaining series, y_i (i=1, …, N), has a mean of zero. The following step makes a cumulative time series as:

$$Z_j = \sum_{i=1}^{j} y_i, j = 1, \dots, N \tag{3.8}$$

The range (R_N) is set as the distance that a system travels in time of the index N (Hurst 1951), and it is achieved by:

$$R_N = \max(Z_1, Z_2, \dots, Z_N) - \min(Z_1, Z_2, \dots, Z_N) \tag{3.9}$$

Hurst (1951) stated that if N =T, then applying Equation (3.4) provides that the time series, x_i (i=1, …, N), is independent for increasing values of N. Hurst (1951) proposed a more general form of Equation (3.4) because this equation can only be applied to the time series that is in Brownian motion:

$$(R/S)_N = c.N^H \tag{3.10}$$

where, the subscript, N, for $(R/S)_N$ denotes the duration of the individual short time series and c is a constant. The Hurst exponent is just the slope of the ordinary line equation that is obtained by plotting the $\log(R/S)_N$ versus $\log(N)$ as:

$$log(R/S)_N = logc + HlogN \tag{3.11}$$

If a system or a process has a uniform probability distribution, then the H value will be close to 0.5. On the contrary, an H value above 0.5 indicates that each observation carries a persistence of all the cases that preceded it, and a value below 0.5 points to anti-persistence (or short-time persistence as in the periodic series).

3.2.7 Trend of Hydroclimatic Indices (Modified Mann-Kendell Test)

The MK is a well-known nonparametric test that was introduced by Mann, (1945) and developed by Kendall(1955). The Mann-Kendell test has 2 parameters that are of importance

to trend detection. These parameters are significance level that indicates the trend's strength, and the slope magnitude estimate that indicates the direction as well as magnitude of trend.(Burn & Elnur, 2002) . The advantage of the Mann–Kendall test is that it could be applied for non-normally distributed data and time series including outliers and nonlinear trends (Palizdan et al., 2016). Furthermore, it is robust to the impact of inhomogeneous time series and can cope with missing values and values below a detection limit (Yan et al., 2007). The test is usually recommended for the situations when a single study uses data from various stations (Nourani et al., 2018). However, it doesn't include the effect of autocorrelation of the time series. To incorporate the information of the auto-correlation of the precipitation, temperature and streamflow, in this study, the modified MK approach was used.

For a given time series of n data points where the Xj symbolizes the data point at the time j, the MK statistic (S) is defined as the summation of the number of positive differences minus the number of negative differences (Nourani et al., 2018):

$$S = \sum_{i=1}^{n-1} \sum_{j=i+1}^{n} sgn(X_j - X_i) \qquad (3.12)$$

Where X_j and X_i are the data values in years j and i, respectively, with j > i, and sgn (X_j - X_i) is the sign function given by

$$sgn(X_j - X_i) = \begin{cases} 1 & if\ X_j - X_i > 0 \\ 0 & if\ X_j - X_i = 0 \\ -1 & if\ X_j - X_i < 0 \end{cases} \qquad (3.13)$$

The magnitude of S represents the strength of trend in data. While a very high positive value of S denotes an increasing trend, a very low negative value reveals a decreasing trend.

However, the MK test is sensitive to the existence of serial correlation in the time series which is often found in hydro-climatic data (Burn & Elnur, 2002; Palizdan et al., 2016). The presence of serial correlation can complicate the identification of trends in that a positive serial correlation can increase the expected number of positive false outcomes for a Mann-Kendell test(Burn & Elnur, 2002). A time series exhibiting positive autocorrelation causes the effective sample size to be less than the actual sample size, thereby increasing the variance and the possibility of detecting significant trends when in fact, there are no trends (Adarsh et al., 2016). On contrary, the existence of negative autocorrelation in a time series enhances the possibility of accepting the null hypothesis (absence of significant trends), when actually, there are significant trends (Adarsh et al., 2016; Ehsanzadeh et al., 2011). Several approaches have been

suggested for removing the serial correlation from a data set prior to applying trend test. These include pre-whitening and prune among other modified approaches. Pre-whitening involves calculating the serial correlation and removing the correlation if the calculated serial correlation is significant at 5% level(Burn & Elnur, 2002) .

Hamed & Rao (1998) proposed a modified approach, in which the calculation of the variance of the test statistics S is altered as given by an empirical formula. The significance of trends is tested by comparing the standardized test statistic in equation 3.12 with the standard normal variate Z at the desired significance level.

$$Z = S/\sqrt{Var(S)} \qquad (3.14)$$

The variance of the test statistic can be computed as follows:

$$Var(S) = \frac{n(n-1)(2n+5)}{18}\left(\frac{n}{n^*}\right) \qquad (3.15)$$

where n is the actual number of observations and n* is the effective number of sample size needed in order to account for the autocorrelation factor in the dataset. The ratio n/n* is the factor that represents the correction associated with the autocorrelation of the data. Empirically, the correction is expressed by Hamed & Rao (1998) as follows:

$$\left(\frac{n}{n^*}\right) = 1 + \frac{2}{n(n-1)(n-2)} \sum_{i=1}^{n=1}(n-i)(n-i-1)(n-i-2)\rho(i) \qquad (3.16)$$

where ρ (i) is the autocorrelation function of the ranks of the observations.

The test result, which is the standardized test statistic Z, gives not only the information about stationarity or nonstationary but also whether the trend is upward or downward. If the computed value of $|Z| > Z_{\alpha/2}$, then the null hypothesis of no trend is rejected at a level of significance in a two-sided test (i.e., the trend is significant). A positive value of Z indicates an increasing trend and a negative value of Z indicates a decreasing trend.

3.2.8 Change point Detection (Pettit Test)

Hydrological time series are assumed to be consistent and stationary which is not the reality (Xie et al., 2014). Several hydrological data series demonstrate significant non-consistency or non-stationarity, due to the influence of climate change and/or large-scale human activities on the water resources systems (Xie et al., 2014). The stationarity assumption typically focuses on

either trend analysis or change point analysis, which detect evidence of change-either gradual change (trend) or abrupt change (jump).

The Pettitt test(Pettitt, 1979) is one of the most widely used tests in hydro-climatological studies to detect abrupt changes in the mean of the variable of interest (Mallakpour & Villarini, 2015) . The main reasons for the popular use of this method include: (1) it combines the searching and testing of the potential change point; (2) compared to other nonparametric methods, the significance of the test can be obtained using the approximated limiting distribution(Xie et al., 2014).

The Pettitt test is based on the Mann-Whitney two-sample test (rank based), and allows the detection of a single shift at an unknown time t. The null hypothesis is no change in the distribution of a sequence of random variables; the alternative hypothesis is that the distribution function $F_1(x)$ of the random variables from X_1 to X_t is different from the distribution function $F_2(x)$ of the random variables from X_{t+1} to X_T. Let

$$D_{ij} = sgn(X_i - X_j) = \begin{cases} -1 \ (X_i - X_j) < 0 \\ 0 \ (X_i - X_j) = 0 \\ +1 \ (X_i - X_j) > 0 \end{cases} \quad (3.17)$$

here X_i and X_j are random variables with Xi following X_j in time. The test statistic $U_{t,T}$ depends on D_{ij} as

$$U_{t,T} = \sum_{I=1}^{t} \sum_{j=t+1}^{T} D_{ij} \quad (3.18)$$

The statistic $U_{t,T}$ is the same as the Mann-Whitney statistic for analyzing when the two samples $X_1,\ldots,X_t$ and $X_{t+1}\ldots,X_T$ arise from the same population. The test statistic $U_{t,T}$ is assessed for all random variables from 1 to T; then the most significant change point is selected where the value of $|U_{t,T}|$ is the largest:

$$K_T = max_{1 \le t < T} |U_{t,T}| \quad (3.19)$$

A change point occurs at time t when the statistic K_T is significantly different from zero at a given level. The approximate significant level is given by

$$p = 2.exp\left[\frac{-6K_T^2}{T^2+T^3}\right] \quad (3.20)$$

Once the p-value is less than the pre-assigned significance level α, (α=5% is used in this study) the null hypothesis is rejected and the data is divided into two sub-series (before and after the location of the change point) with two different distribution functions.

3.2.9 Wavelet transformation coherent

The wavelet transformation coherence (WTC) here was proposed by Torrence & Webster, (1999), and modified by Lachaux et al (2002) and Grinsted et al(2004). WTC is worked based on two variables. According to Grinsted et al (2004), the continuous wavelet transform of two time series X and Y of length n with uniform time step Δt are denoted as $W_n^x(s)$ and $W_n^y(s)$:

$$w_n^x = \sqrt{\frac{\Delta t}{s}} \sum_{n=1}^{N} X_n \varphi_o[(n'-n)\frac{\Delta t}{s}] \qquad (3.21)$$

Where φ_o is the dimensionless frequency

The wavelet power is $|W_n^X(s)|^2$. The complex argument of $W_n^X(s)$ can be interpreted as the local phase.

The WTC can be calculated using the following equation (3.20) adopted from Grinsted et al., (2004):

$$R^2(Y,X) = \frac{|S^m(S^{-1}W_n^{XY}(S))|^2}{S^m((S^{-1}|W_n^x|^2)(S^{-1}|W_n^Y(s)|^2))} \qquad (3.22)$$

Where S^m is a smoothing operator both in the scale axis and time domain. W_n^{XY} is cross wavelet transform (XWT) of two time series Xn and Yn.

$$S^m(W) = S_{scale}(S_{time}(W_n(s))) \qquad (3.23)$$

where S_{scale} denotes smoothing along the wavelet scale axis and S_{time} smoothing in time. It is natural to design the smoothing operator so that it has a similar footprint as the wavelet used.

It is important to note that coherence between two wavelet spectra does not indicate correlation at high power, but that similar oscillations are occurring in each series at the frequency of interest(Carey et al., 2010) .

4. RESULTS AND DISCUSSION

4.1 Data consistency

The quality of the raw rainfall and stream gaging data was examined after filling in the missing data. The consistency, homogeneity and persistence were tested and the results are discussed below.

A double-mass curve shown in figure 4.1 was fitted for the collected precipitation data to test for its consistency. The cumulative total precipitation was computed for each station and then plotted against the cumulative total of an adjacent stations. There were insignificant changes in some station curves and this was neglected thus the data was considered to be consistent.

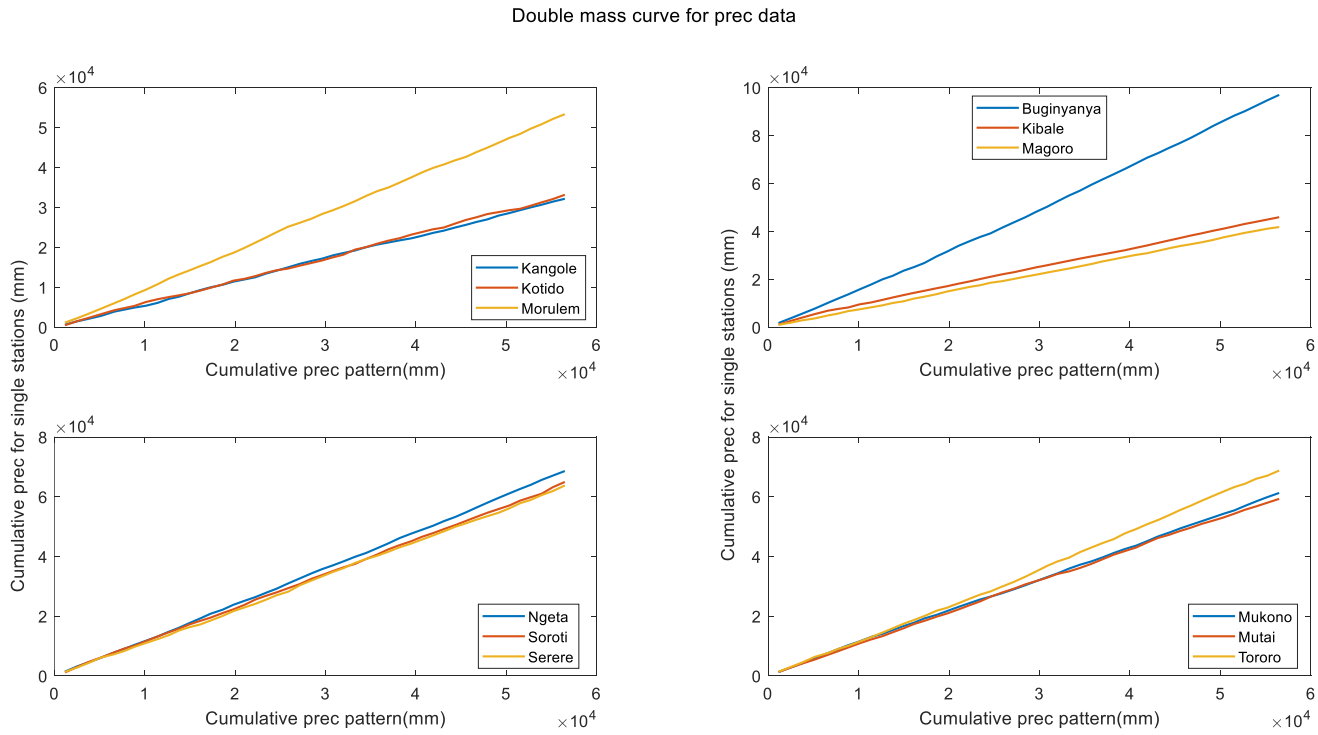


Figure 4.1: Double mass curve for precipitation data of the selected stations in LKB

Thereafter, areal precipitation and temperature contributed by each weather station was calculated using Thiessen polygon approach. The figure 4.2 below shows the Thiessen polygon and the respective weighting factors for each station. The Mpologoma and Okere sub

catchments had more than one station so further analysis for the weights of the different stations was done and also shown in figure 4.2.

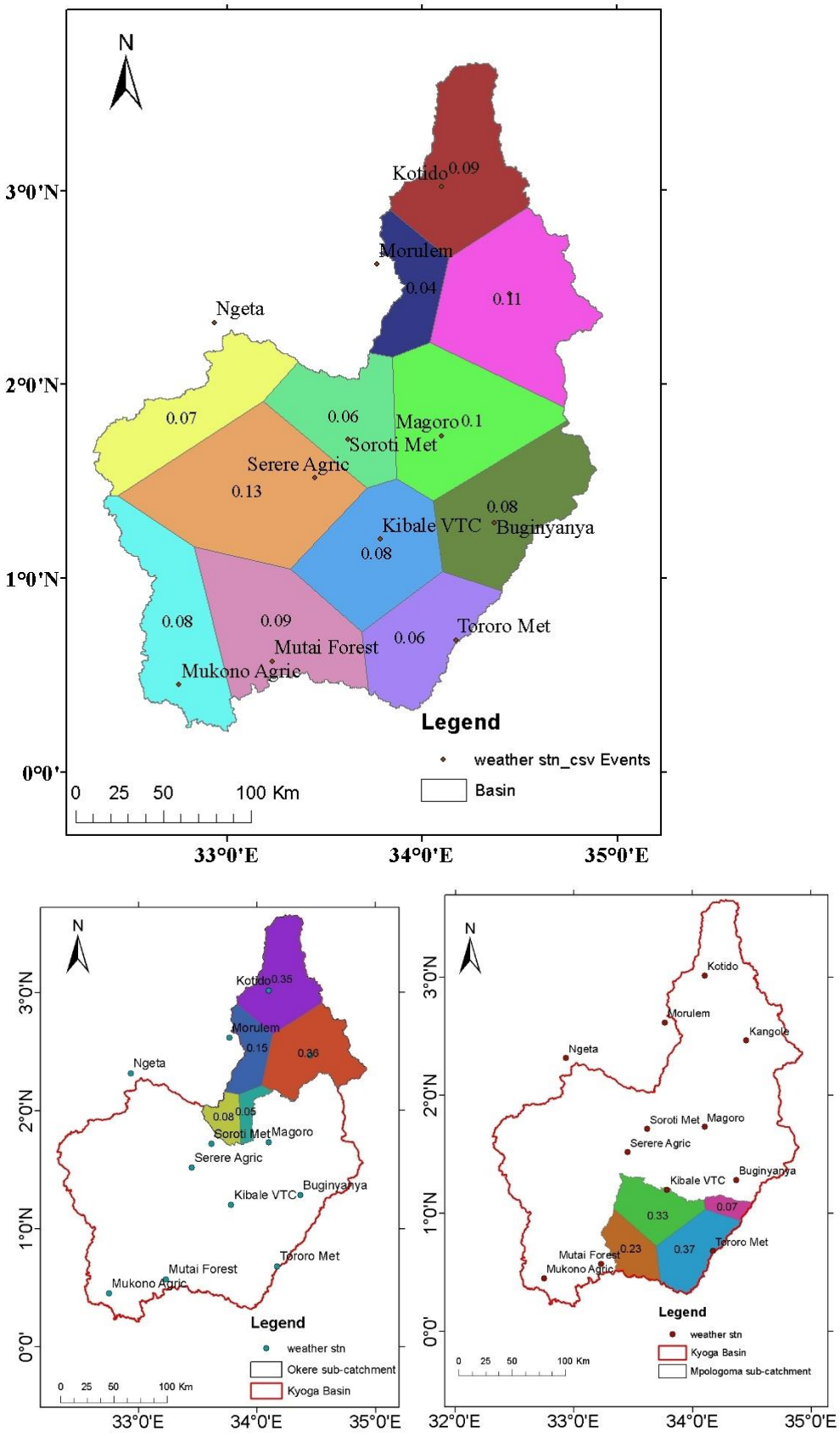


Figure 4.2: Thiessen polygon showing the weighting factor for each selected station in the Kyoga basin, Okere and Mpologoma sub-catchments

4.2 Extracted indices from precipitation, temperature and streamflow

The indices were extracted for each weather station and stream gage where applicable. The results are presented and discussed in this section.

4.2.1 Standardised Precipitation Index (SPI) and Standardised Streamflow Index (SSI)

The precipitation and streamflow data were approximated to a gamma distribution and the 3-month SPI (SPI-3) and SSI (SSI-3) were calculated for each station per each sub-catchment. SPI-3 and SSI-3 reflect short- and medium-term moisture conditions and provides a seasonal estimation of precipitation and streamflow. The plots of the seasonal variations per station are shown in the figures 4.3 and table 4.1 is a summary of the drought years and drought categories in the different sub-catchments

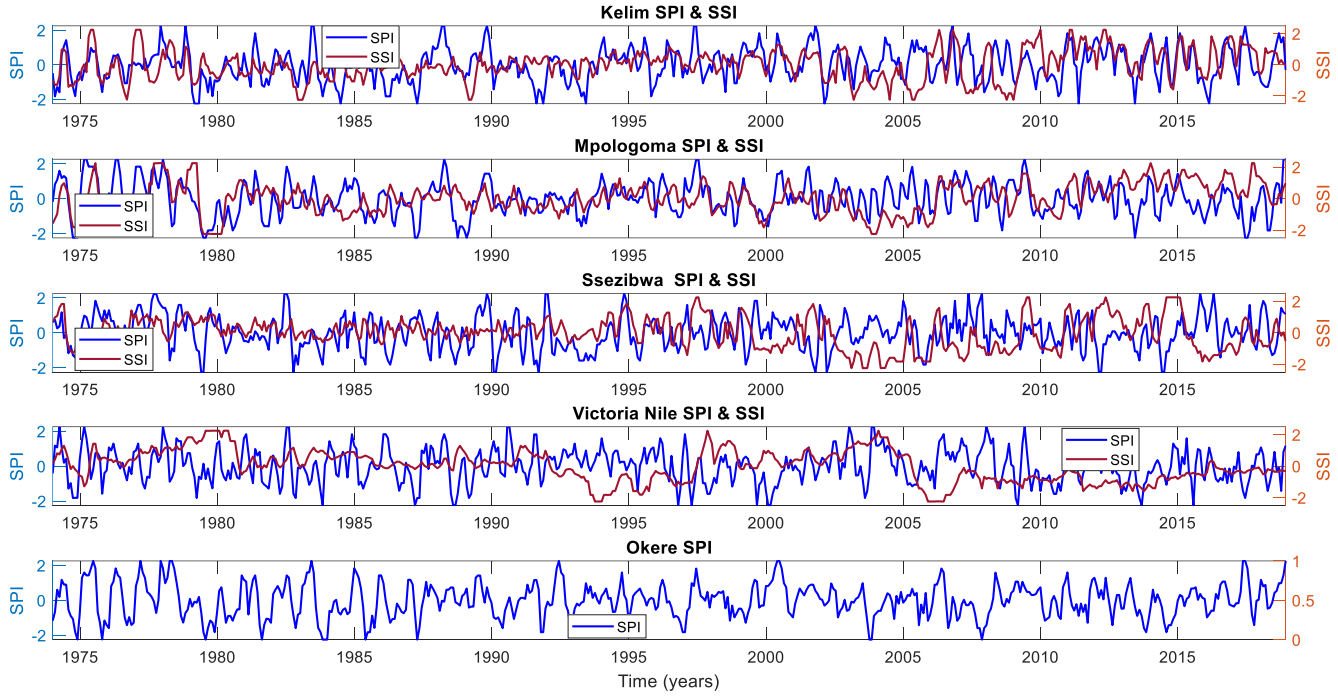


Figure 4.3: SPI and SSI of the Kelim, Mpologoma and Ssezibwa sub-catchments in LKB

Table 4.1: The number of droughts and categories in the different years per sub-catchment

	Kelim sub-catchment								Mpologoma								Ssezibwa								Victoria Nile								Okere			
	SPI				SSI				SPI				SSI				SPI				SSI				SPI				SSI				SPI			
Year	Extreme	Severe	Moderate	Sum	Extreme	Severe	Moderate	Sum	Extreme	Severe	Moderate	Sum	Extreme	Severe	Moderate	Sum	Extreme	Severe	Moderate	Sum	Extreme	Severe	Moderate	Sum	Extreme	Severe	Moderate	Sum	Extreme	Severe	Moderate	Sum	Extreme	Severe	Moderate	Sum
1974		2		2			3	3	2			2		2		2			3	3			1	1		2	1	3				0	1		1	2
1975		1	1	2			1	1			1	1		3	1	4				0				0		1		1			1	1	1		1	2
1976			1	1	1		1	2			1	1		2	2	4				0				0				0				0		1	2	3
1977				0			2	2				0				0				0				0			1	1				0				0
1978				0				0		1		1				0		1	1	2				0				0				0			1	1
1979	2	2		4			1	1	1	2		3	2	1		3	1			1				0		1	1	2				0	1	2	1	4
1980				0				0		2		2	1		1	2			1	1				0				0				0			2	2
1981			2	2				0		2		2				0				0				0			1	1				0	1		1	2
1982		1	2	3	1			1			1	1				0	1	1	1	3				0		3		3				0		1		1
1983		1	1	2	1			1				0			1	1		1		1				0	1		2	3				0	1	1		2
1984	1			1				0				0			2	2			1	1				0				0				0	1			1
1985			1	1			2	2			2	2			1	1		1	1	2				0			2	2				0	1	2		3
1986		2	2	4				0		1		1			1	1		1	1	2				0			1	1				0			2	2
1987	1			1				0	1	1		2				0		1		1				0	1	1		2				0	1			1
1988				0				0	1		1	2				0		1	1	2				0	1	2		3				0				0
1989				0	1	1		2	1	1		2				0			1	1				0		2	1	3				0				0
1990			1	1				0				0				0	1		1	2				0				0				0		1	2	3
1991	2		1	3				0				0				0	1	3		4				0			2	2				0		1		1
1992			1	1				0				0			1	1			2	2				0				0				0			1	1
1993	1	1		2				0		1	2	3				0		3	2	5				0				0	1	1		2				0
1994				0				0				0				0			1	1				0				0	1	2		3			1	1
1995		1	1	2				0			1	1				0		1		1				0		1		1		3	1	4				0
1996				0				0				0				0			2	2				0	1			1			1	1		1		1
1997			1	1				0		1	1	2				0				0			1	1	1	1	1	3			1	1				0
1998		1	1	2				0				0			1	1				0				0			1	1				0			1	1
1999				0				0		1	2	3		1		1		1		1			1	1	1		2	3				0			1	1
2000				0				0			1	1		1		1				0			3	3	1		1	2				0				0
2001				0			1	1				0			1	1	1		1	2				0			1	1				0				0
2002	1			1			2	2				0				0	1		1	2		1	1	2				0				0				0
2003		1		1	1	1		2			3	3		1	1	2				0	1		1	2		1		1				0	1			1
2004				0	1			1			1	1	1	2	1	4				0	2	2		4				0				0			1	1
2005			2	2	1	2		3			1	1		3	1	4		2		2		3		3			3	3	1		1	2			2	2
2006			1	1			1	1				0		1	1	2				0			1	1			1	1	1	1		2		1	2	3
2007		1	1	2		2	3	5			1	1				0				0		2	1	3				0			1	1	1	2		3
2008				0	1	2		3		1	1	2			1	1			1	1			4	4				0			1	1			1	1
2009			2	2	1			1				0				0				0				0	1	1	2	4			1	1				0
2010		1		1				0			1	1			2	2			1	1		1	1	2		1	1	2				0			2	2
2011	1			1				0			1	1				0		1	1	2				0			1	1		1		1			1	1
2012				0				0			1	1				0	1			1				0		1	1	2			2	2			1	1
2013	1			1				0	1			1				0		1	1	2				0	1		1	2		2		2		2		2
2014		1	1	2		1	1	2			1	1				0	1		1	2				0			1	1			2	2		1	2	3
2015				0				0			1	1				0				0		1	2	3	1			1				0				0
2016	1			1				0				0				0			1	1		1	2	3				0				0				0
2017			1	1				0	1	1	2	4				0				0			1	1		1		1				0			1	1
2018			1	1				0		1		1				0			1	1				0			2	2				0				0
Sum	11	16	25	52	9	9	18	36	8	16	27	51	4	17	19	40	8	19	28	55	3	11	20	34	10	19	31	60	4	10	12	26	10	16	30	56

In the sub-catchments Kelim, Mpologoma, Ssezibwa and Victoria Nile, SSI and SPI showed similar patterns of variation in the plot presented above though it should be noted that on several incidents the SSI was overlapping the SPI (when the SPI decreased, the SSI decreased more

than the SPI and vice versa). The number of droughts per year, including the drought categories per sub-catchment for the period of 1974-2018 are shown in table 4.1. Generally, more seasonal meteorological droughts were experienced from SPI whereas less hydrological droughts were experienced from the SSI. The high frequency of meteorological droughts is due to the high variability of precipitation compared to streamflow.

Kelim sub-catchment experienced extreme drought conditions (SPI or SSI<-1.65) in the follwing years. For SPI in 1979, 1984, 1987, 1991, 1993, 2002, 2011, 2013 and 2016, SSI in 1976,1982, 1983, 1989, 2003, 2004, 2006, 2008 and 2009.

Mpologoma catchment had extreme hydrological drought conditions in SSI in 1979-1980, 2004 and in the SPI in 1974,1979, 1987-89, 2012 and 2017. Ssezibwa sub-catchment experienced extreme meteorological drought in 1979, 1982, 1990, 1991, 2001, 2002, 2012, 2014, extreme hydrologic drought in 2003 and 2004. Victoria Nile sub-catchment experienced extreme metrologicaldrought conditions in 1983, 1988, 1996-1997, 2000, 2009, 2013 and 2015, in SSI 1993, 2005 and 2006. The Okere sub-catchment experienced extreme metrological drought conditions in 1974-1975, 1980-1985, 1991, 1994, 1996, 2003, 2007, 2010 and 2014 as shown in table 4.2. For this sub-catchment the extremely dry conditions were more frequent compared to the other sub-catchments.

The SPI and SSI in all the sub-catchments were able to capture the severely dry conditions (drought) in 1977-1979 and those in the period 1991-2000. These observations are consistent with those of the government meteorologists who affirm that droughts in the, northern and north-eastern districts (which are part of LKB) are becoming more frequent(GoU, 2007; Nyasim et al., 2016). They also logged seven droughts between 1991 and 2000, with a particularly long and severe drought in 1999–2000(GoU, 2007). SPI and SSI depicted that the frequency of extremely dry condition (drought) was increasing from 5-7 years return period to 1-3 years return period. This result agrees with that of Bernard et al.,(2013) where it was concluded that return period of these events has dropped from 4 to 10-year period to a 1–3 year period.

Given that agriculture is the main activity in the LKB, most crops take up to 6 months to be fully developed, a water deficiency accumulation of at least 3 months, during the growing season, will adversely impact crop yields. Since drought develops over time, it can be assumed that the extended period of drought at longer timescales may be a result of the after-effects of accumulation of antecedent water scarcity over time and this situation may be amplified with

persistent and continuous periods of no rainfall. In addition, a drought can occur if there is a shift in seasonal rainfall such that the rains are delayed thus causing impairment on activities that normally depend on the onset of a rainfall event.

4.2.2 The maximum 5-day precipitation during a year (Rx5day), the 95th percentile of precipitation on wet days (R95) and the 5-percentile flow (Q95)

The Maximum 5-day precipitation amount in millimetres during a year, the 95th percentile of precipitation on wet days (R95) per year and the 5-percentile flow for each sub-catchment was calculated and summarised in the figure 4.2 below.

For each sub-catchment all Rx5, R95 and Q95 showed similar patterns, when the Rx5 was low both the R95 and Q95 were low too and all were high in the same year. This implies that all have similar effect on the catchment.

Very high values depicting floods are seen for Kelim in 1983, 1998, 2007and 2012. For the northern part of Mpologoma Catchment high values were seen in 1975, 1978, 1982, 1988, 1989, 2005, 2010 and 2016. Ssezibwa high values in 1979, 1981, 1989, 1992, 2000, 2007and 2010. Victoria Nile in 1975, 1991, 2000, 2007 and 2018.

Rx5 and R95 can be used as flood indicator because severe floods, the more the Rx5 the higher the susceptibility of the area to get floods. Q95 on the other hand is a low flow index used to indicated low flow conditions and determine environmental flows. The amount of Rx5 was ranging from 30-200mm. Kelim sub-catchment and parts of Mpologoma showed Rx5 above 100mmin the period between 1976-1978 this coincides with the period in which Uganda experienced floods in most parts of the country. Okere sub-catchment had the least values of Rx5 which implies that it is the least prone to flooding. The Rx5 and R95 were able to capture the floods in 97/98, 2007 and 2010 which were also recorded by Bernard et al (2013) and Nyasim et al (2016).

The Q95 of the different rivers was also calculated, low values indicating hydrological drought in each sub-catchment were recorded in the following years. Kelim sub-catchment in 1976, 2004 and 2009, Mpologoma river in 1980, 1992 and 2004, Ssezibwa in 1975, 2000, 2004, 2000, 2007 and 2017 and in the Victoria Nile in 1994, 1997, 2001, 2006 and 2009 after which the flows keep increasing. Ssezibwa river generally has low flows hence most prone to hydrological drought. The droughts captured by Q95 perfectly match those identified using SSI. These very low flows imply that the amount of environmental flow is reduced hence

adverse effects on the ecology downstream. Also, other water requirements downstream are affected.

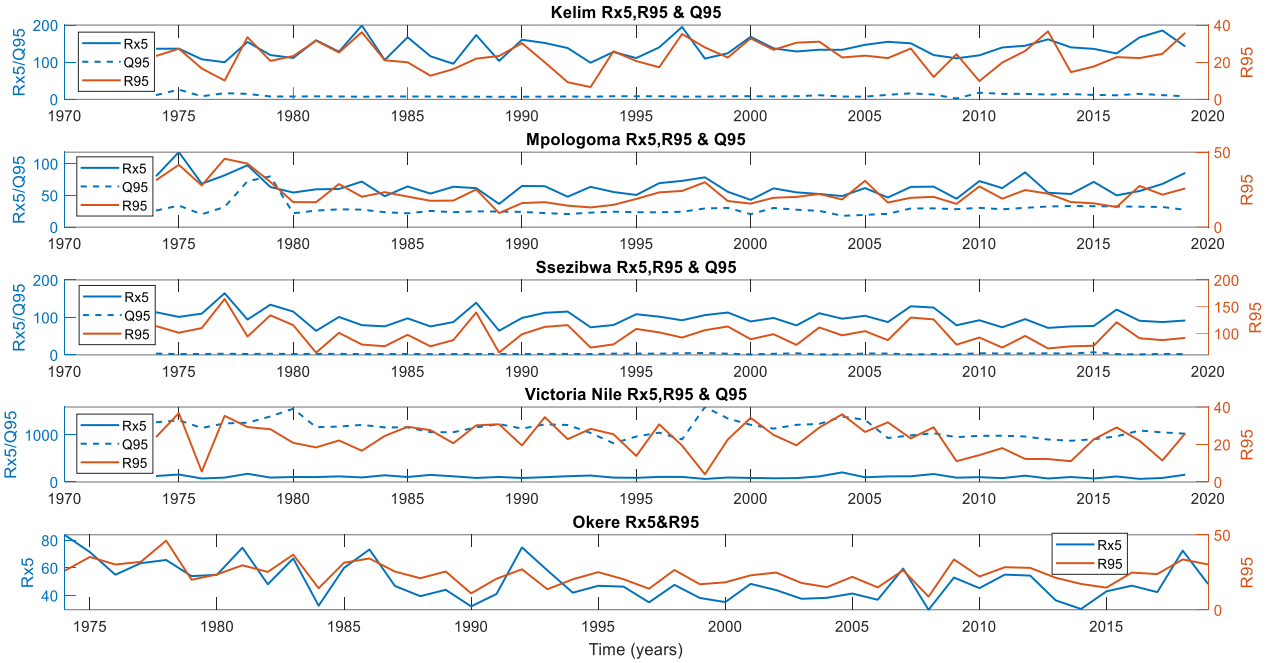


Figure 4.4: The Rx5, R95 and Q95 of the selected sub-catchments in LKB

4.2.3 Aridity Index

The annual aridity index of each station was calculated and the results are presented in the figure 4.5 below. The Okere sub-catchment found in the North Eastern part of Kyoga basin exhibited aridity ranging from 2-4 which indicate that this part of the basin is semi-arid. The rest of the sub-catchments except Kelim had values ranging between 1-2, this indicates that the larger part of the LKB is sub-humid. Kelim had AI ranging between 0.5-1 which shows that it is humid.

The two components used to calculate AI are precipitation and evapotranspiration, these are crucial variables in the hydrological cycle reflecting the availability water and energy. Furthermore, these components are vital in estimating the water balance of a catchment, the multi-year streamflow, without considering the water storage change is the difference between precipitation and evapotranspiration. This implies that as aridity increases the amount of water in the system decreases. Therefore, the Okere sub-catchment that is semi-arid has high rates of evapotranspiration compared to the amount of precipitation it receives hence it less favorable for agriculture unlike the rest that are semi-humid and humid.

In the years 1979/80 for Kelim, Mpologoma and Okere the AI is notably high (the evapotranspiration was higher than the rate of precipitation received), this coincides with the drought faced in those sub-catchments.

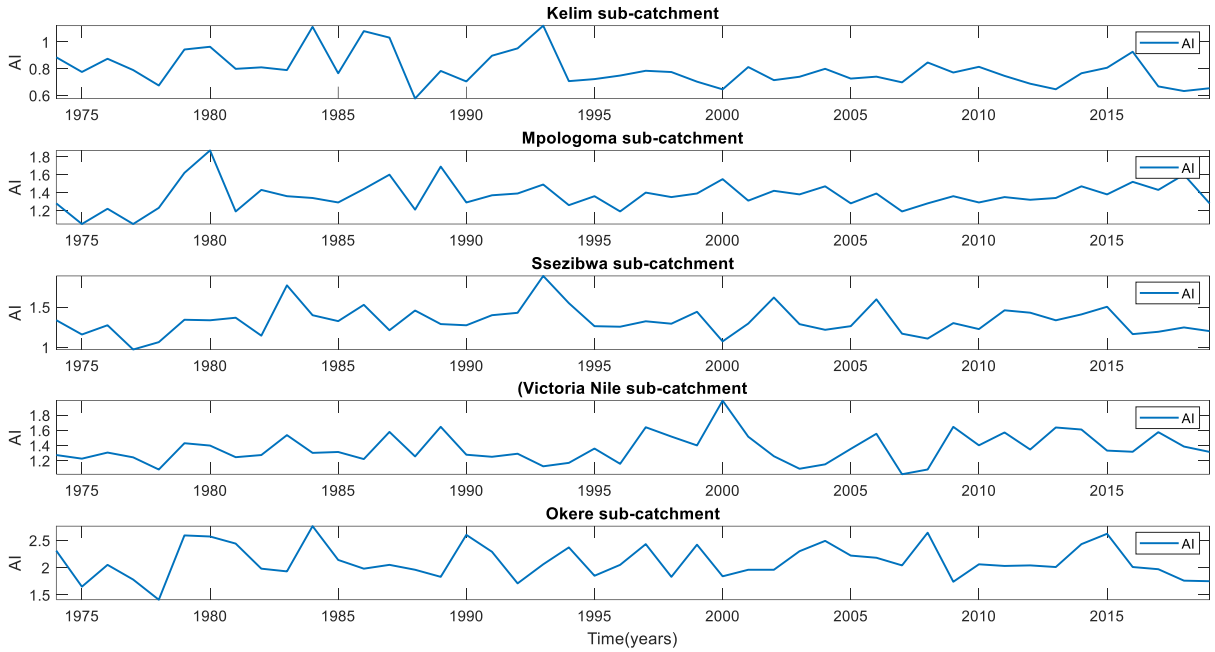


Figure 4.5: The AI of the selected sub-catchments in LKB

4.3 Homogeneity and Persistence of indices

4.3.1 Homogeneity Analysis of the Indices (break point analysis)

The Pettitt test method was used at a level of confidence of 95% (alpha=0.05) to determine the homogeneity of the indices. The results show that all the indices have breaking points in the periods indicated. This implies that indices are inhomogeneous and the breaks per station are in the years indicated in table 4.1

Table 4.2 : Break point analysis results for all indices

SPI-3	SSI	Rx5	R95	Q95	AI
Kelim Sub-catchment					
1994 (Feb)	2010(Mar)	1995	1996	2005	1993
Mpologoma Sub-catchment					
1979 (Jan)	2006(Nov)	1979	1985	2006	1977
Ssezibwa					
1979 (Feb)	2000(Jan)	1980	2008	1993	2004
Victoria Nile Sub-catchment					
2008 (Oct)	2006(Jan)	1993	2008	2005	2004
Okere Sub-catchment					
1978(Aug)		1986	1987		1977

4.3.2 Persistence Analysis of the Indices

The presentence was analysed using the Hurst persistence method, the Hurst values for the different sub-catchments and indices are summarised below in table 4.3.

All the Rx5 Hurst values are great or equal to 0.5 reflecting persistence in the index. Buginyanya however has a Hurst value below 0.5 meaning there is no persistence. All the values of Hurst index for all indices are above 0.5 except Kelim SPI which implies that series are correlated for all streams. The Kelim SSI-3 returned an inconclusive value of Hurst index so it not certain whether the series is persistent or not.

Table 4.3: Persistence analysis results for all indices

SPI-3	SSI	Rx5	R95	Q95	AI
Kelim sub-catchment					
0.75		0.36	0.64	0.89	0.8
Mpologoma sub-catchment					
0.69	0.7	0.78	0.84	0.72	0.67
Ssezibwa sub-catchment					
0.59	0.78	0.66	0.73	0.79	0.69
Victoria Nile sub-catchment					
0.60	0.84	0.69	0.61	0.78	0.65
Okere sub-catchment					
0.53		0.87	0.86		0.53

Kelim sub-catchment showed persistent AI conditions and meteorological drought, there was no persistence in the Rx5 hence floods were not persistent in this sub-catchment. Notably low flows were persistent in the Kelim river according to the Q95. This means the rate of evaporation is less than that of precipitation, which would imply high stream flows or even drought but that is not the case. This could be because the catchment is generally at high altitude or could be influenced by other factors like anthropogenic activities and soil moisture among others that have not been explored in this study.

Mpologoma Sub-catchment showed general persistence in aridity conditions, meteorological drought and floods, persistence is higher (close to 1) in the northern part of the sub-catchment. Hydrological drought and low flows were persistent in the river Mpologoma. The persistence of both drought and floods is due the seasons, the rainy seasons receiving excessive rainfall and the dry seasons being very dry with minimal rain. However, it should be noted that most of the floods were moderate.

Ssezibwa and Victoria Nile sub-catchment showed persistence in all the indices, meaning AI conditions, floods, both meteorological and hydrological droughts plus low flow conditions. Meteorological drought was least persistence in both catchments.

Okere sub-catchment showed persistence of all the indices implying that droughts, floods and AI conditions were experienced in this catchment.

4.4 Trend Analysis of the Indices (p-value, Z, H)

The modified Mann-Kendall method suggested by Hamed and Rao (1998) was used to detect the trend in the series the different indices. A 95% confidence interval was used (alpha=0.05) and the null hypothesis (H_o) was that there is no monotonic trend and the alternative hypothesis was that there is a trend in the series (H_1). The p value indicated the significance of the trend and Z shows the direction of the trend.

The trend test was conducted on the time series of each index per station and the p, Z values and hypothesis H are summaries in table 4.4 below. Additionally, wavelet decomposition was done on the indices and the trend patterns plotted to enhance the modified Mann-Kendall results. The trend patterns were further plotted to emphasize the MMK results

Table 4.4: Trend analysis results for all the indices

SPI-3 p(Z)H	SSI p(Z)H	Rx5 p(Z)H	R95 p(Z)H	Q95 p(Z)H	AI p(Z)H
Kelim Sub-catchment					
<0.05(3.17)1	<0.05 (2.71) 1	0.13 (1.53)0	0.11(1.610)0	0.05(1.99)1	<0.05 (-3.05)1
Mpologoma Sub-catchment					
0.70(-0.38)0	<0.05 (5.12)1	0.34(-0.95)0	0.16(-1.401)0	0.09(1.72)1	0.19(1.31)0
Ssezibwa					
0.82 (-0.22)0	0.1533(-1.43)0	<0.05(-2.08)1	1.64(-1.6096)0	050 (0.68)0	0.81(-0.24)0
Victoria Nile Sub-catchment					
<0.05 (0.00)1	0(-11.66)1	0.05(-1.90)1	0.11(-1.61)0	<0.05(-3.84)1	0.099(1.65)1
Okere Sub-catchment					
0.73(0.35)0		<0.05(-5.54)1	0.03(-2.12)1		0.78(-0.28)0

The Kelim sub-catchment that is located in the eastern part of the LKB positive trends for all indices except the AI. There was significant increasing in the precipitation indices (SPI, Rx5, R95) and insignificant increasing trend in the stream flow indices (SSI and Q95). The AI showed significantly decreasing trend. The Kelim sub-catchment had significant increasing in the precipitation indices, insignificant increasing trend in the stream flow indices and

significantly decreasing trend in AI. This is very logical, because as precipitation increases the aridity decreases.

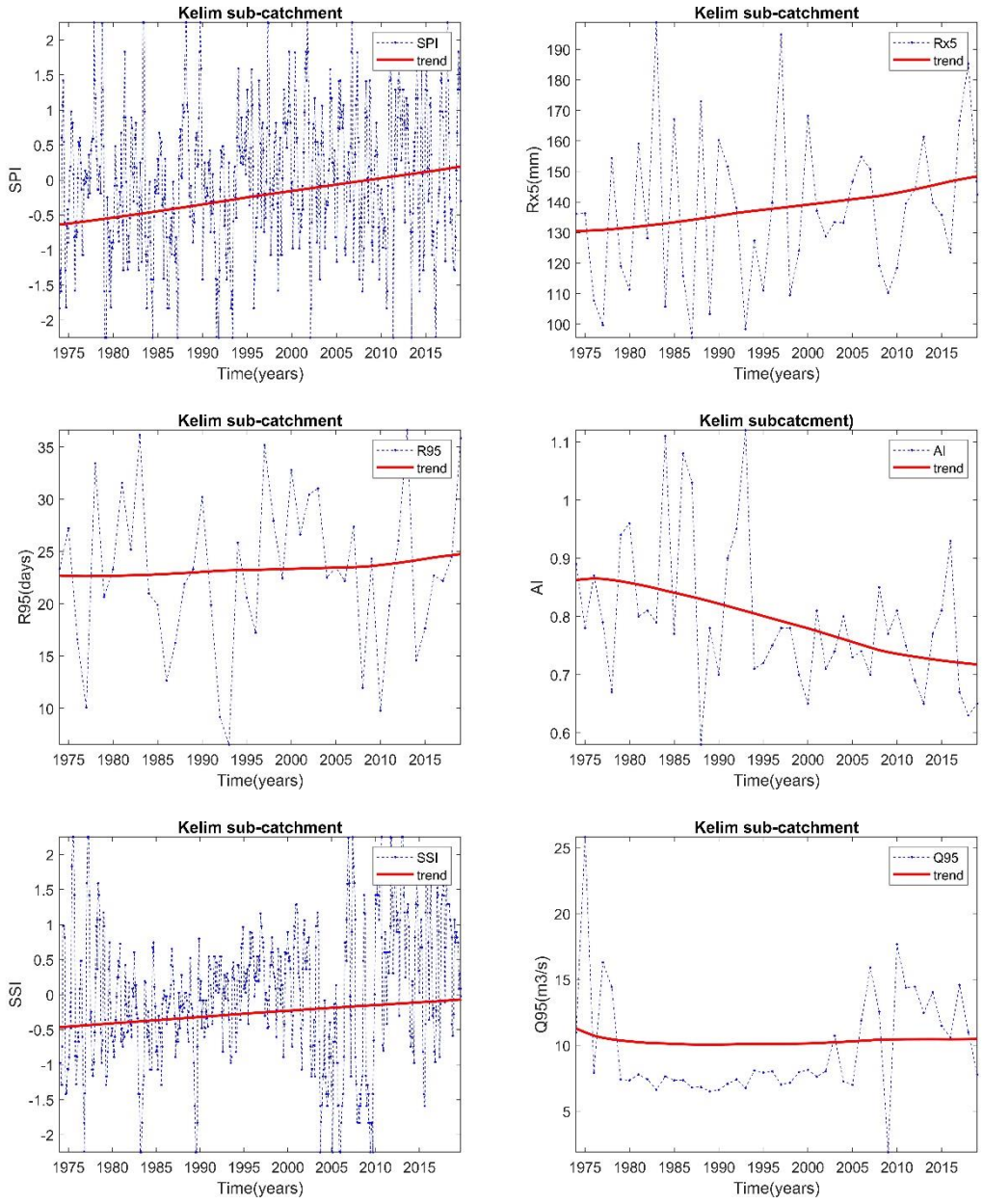


Figure 4.6: Trend of indices in the Kelim sub-catchment

The Mpologoma sub-catchment that covers the most of the south-eastern part of LKB the catchment showed decreasing trends for some precipitation indices (insignificant SPI, significant for Rx5 and R95) and a significantly increasing trend of AI. The streamflow indices are however increasing, the SSI is increasing significantly and the Q95 insignificantly. The precipitation indices results agree with Mubialiwo et al (2020) on the precipitation of Mpologoma sub-catchment. The SSI showed a decreasing trend, however Q95 showed an

insignificant increasing and AI showed a decreasing trend which also showed a sharp decrease in 2009.

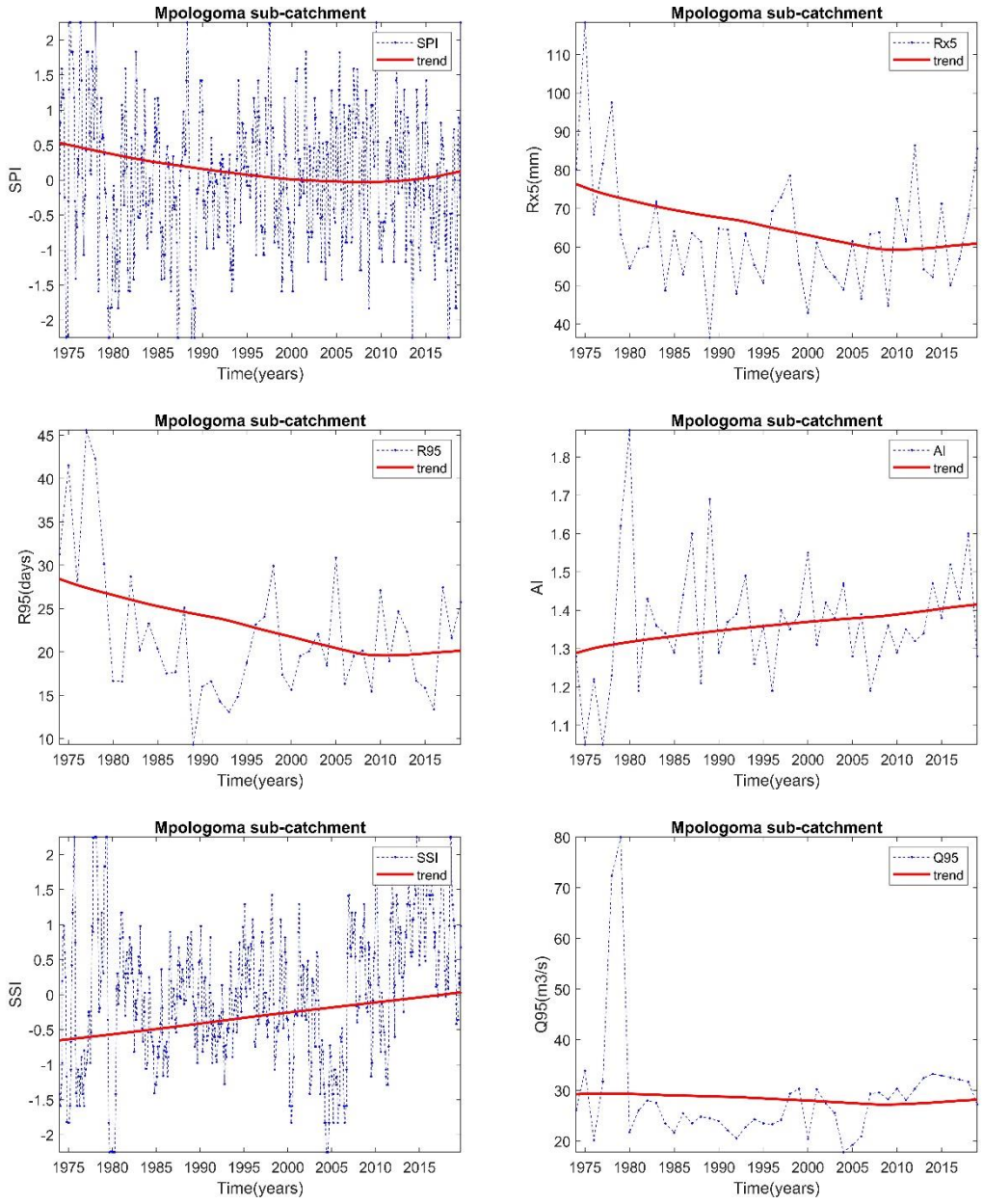


Figure 4.7:Trend of indices in the Mpologoma sub-catchment

Ssezibwa sub-catchment in the southern-western part showed decreasing trends for Rx5 and R95 and an insignificant increasing trend of SPI. The SSI showed a decreasing trend, however Q95 showed an insignificant increasing trend from 1974 up to 2009 when it started showing a decreasing trend. The AI showed a decreasing trend which also showed a sharp decrease in 2009.

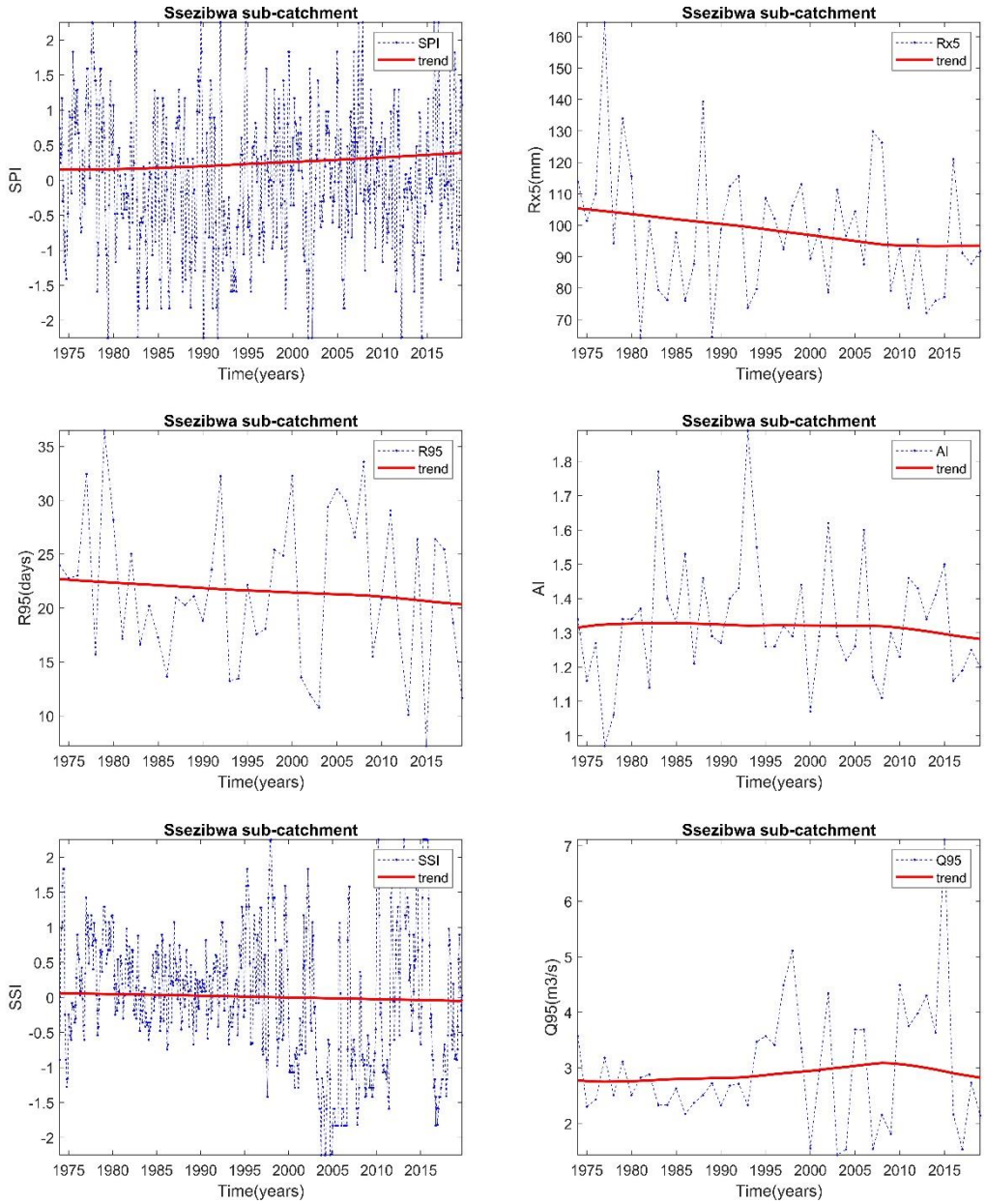


Figure 4.8:Trend of indices in the Ssezibwa sub-catchment

Victoria Nile showed decreasing trends of precipitation indices, the SPI being insignificant and the others significant. The AI had a significant increasing trend while the streamflow indices had decreasing trends. In 2009, there was a sharp change in the trends in the respective directions as shown in figure 4.9

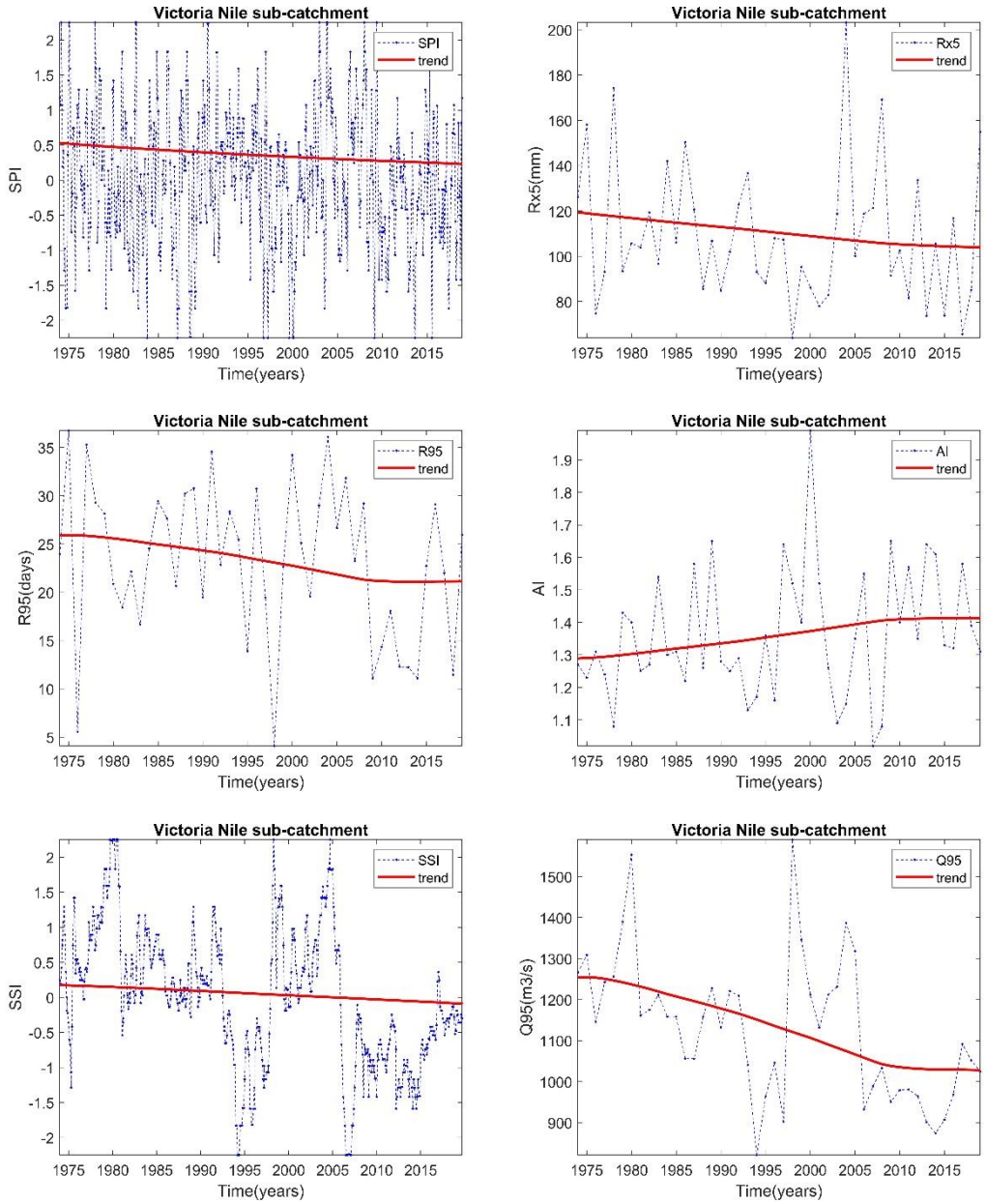


Figure 4.9: Trend of indices in the Victoria Nile sub-catchment

There was no flow data for the Okere sub-catchment but the precipitation indices and AI were considered (figure 4.10). This catchment occupies the North-eastern part of the LKB. The SPI showed an insignificantly increasing trend while Rx5 and Rx95 showed significant decreasing trend till 2010 where their trends started increasing while that of AI was insignificantly increasing till 2010 when it started decreasing. It should be noted however that there was a sharp change of direction in 2009 for the trends in this catchment.

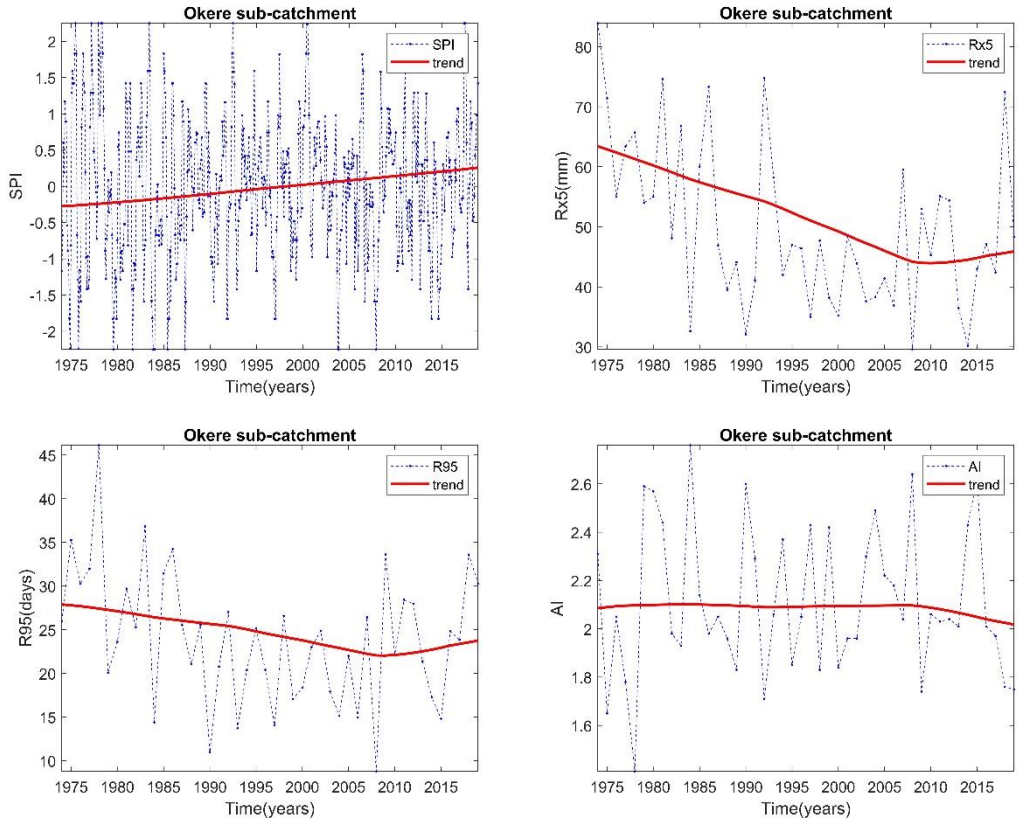


Figure 4.10: Trends of indices in the Okere sub-catchment

4.5 Climate teleconnections

NAO, Nino3.4 and Nino were considered for this study. The indices for the period of 1974-2019 were downloaded from CRU as earlier mentioned in chapter 3. Each index was analyzed to come up with the annual and seasonal values to be compared with the hydro-climatic indices. The 3 months moving average of each index were also calculated and these were used to analyze the interaction with SPI-3 and SSI-3. The annual variation and variation of 3 months moving average of the climate indices were plotted and are shown in figures 4.8 and 4.9 respectively.

The annual NAO varies between -1 and 1 but goes beyond -2 in 2010. Annual values of Nino3 range -1 and 1.5, while those oh Nino3.4 range between -1 and 1. The moving averages portray similar patterns to those of the annual vales of the climate indices.

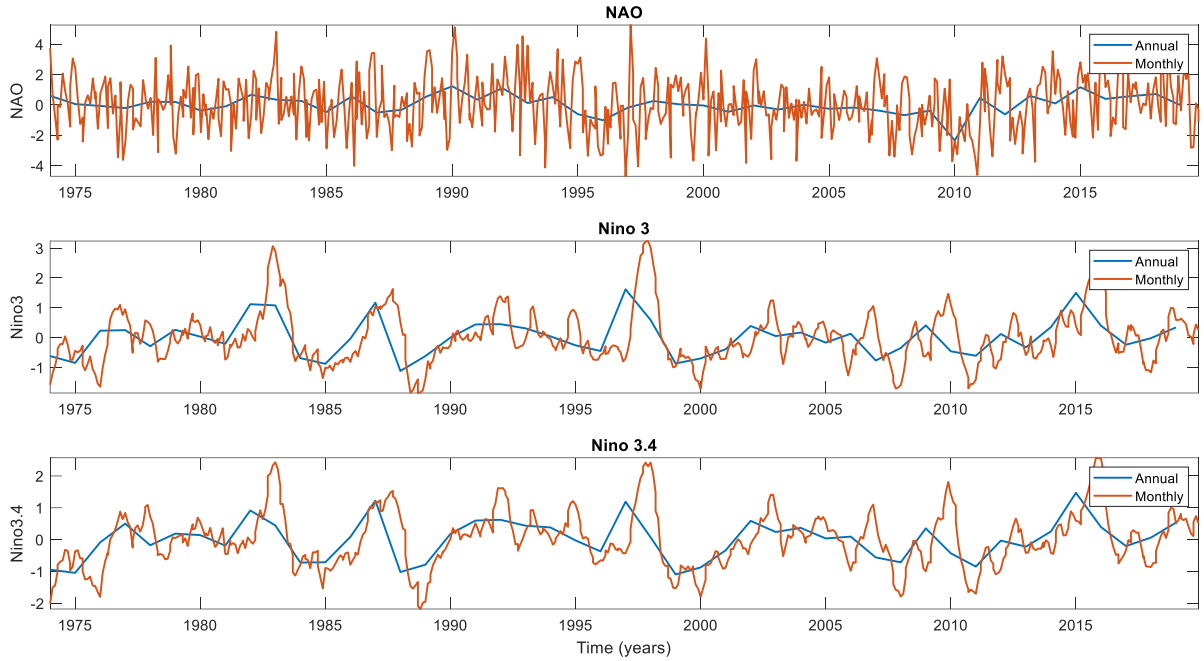


Figure 4.11: Monthly and annual variation of climate teleconnections

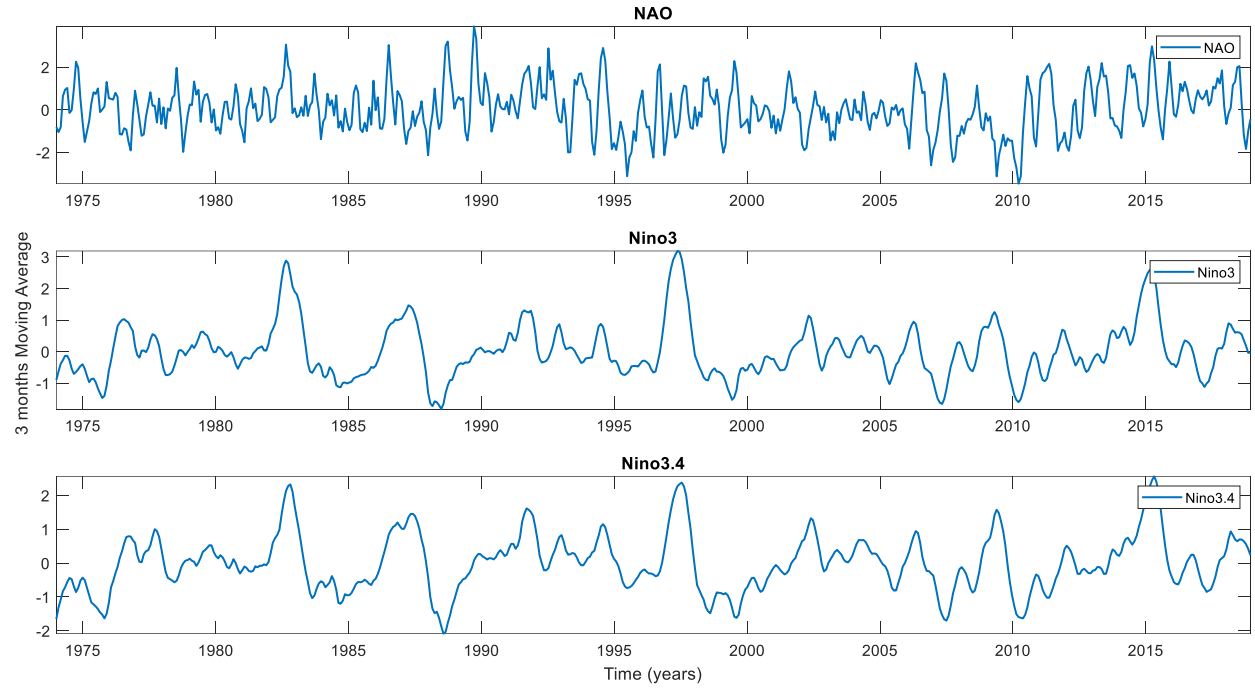


Figure 4.12: Three months moving average of the climate teleconnections

4.6 Interaction among the indices

The Wavelet coherence method was used to assess the interaction (synchrony and coupling) between the various indices. The covariation of the power spectra of indices was calculated

using the wavelet coherence MATLAB package presented in Grinsted et al (2004). This approach computes the wavelet power spectra using the Morlet wavelet, which has found widespread application in hydrology due to its frequency resolution and ability to detect both time-dependent amplitude and phase for different frequencies in the time series.

The Cone of Influence (white dotted line) defines areas in full color that are not influenced by edge effects of the wavelet spectra. The colors indicate the strength of the coherence, with orange and yellow areas within the white lines significant at the 95% (alpha=0.05) level against yellow noise. 1 (yellow) means the two signals are highly correlated and 0 (blue) means no correlation. Directions of the arrows indicate the degree to which the 2 series X and Y are in phase. Right arrows indicate the series are completely in phase, left indicate they are completely out of phase (180_ phase angle), and down arrows indicate Y lags X by 90_ (one fourth of the cycle at that period).

4.6.1 Interaction between SPI-3 and SSI-3

The SSI-3 of the different streams were interacted with the SPI-3 of the weather stations in the sub-catchments.

In the figure 4.13 below showing the WC between Kelim SSI-3 and SPI-3, the x- axis shows the Time in years with 0 corresponding to 1974 and 45 with 2019. The two series show a high level of coherence in the periods of 0-2 years. There are significant peaks in the ~0.5-year band around 1975, 1979 and 2014. The SPI-3 over laps SSI-3 in all the 3 cases.

In the Ssezibwa sub-catchment SSI-3 and SPI-3 showed coherence in the periods of 1-8 years. There are such there as the significant peak in the mentioned period band around 1975, 1979-80 and 2017-19. In 1974 and 79-80 the two indices are in phase as the arrows point in to the right, however in the 2017-2019 period they are completely out of phase.

In the Mpologoma sub-catchment SSI-3 and SPI-3 showed coherence in the periods of 0-2 years. There are such there as the significant peak in the mentioned period band around 1979-80 and 2015-17.

The coherence between Victoria SSI-3 and Mutai SPI-3 showed a high level of coherence in the periods of 8-16 years. Indicating interannual coherence.

Results indicate that the coherence between these two variables generally was ranging between 0-0.8. This is mainly attributed to the fact that although precipitation is a primary contributor to streamflow, other factors such as changes in land use, land degradation, and the construction

of reservoirs for hydro power production in the case of Victoria Nile all affect the hydrological characteristics of the basin in the lower reach.

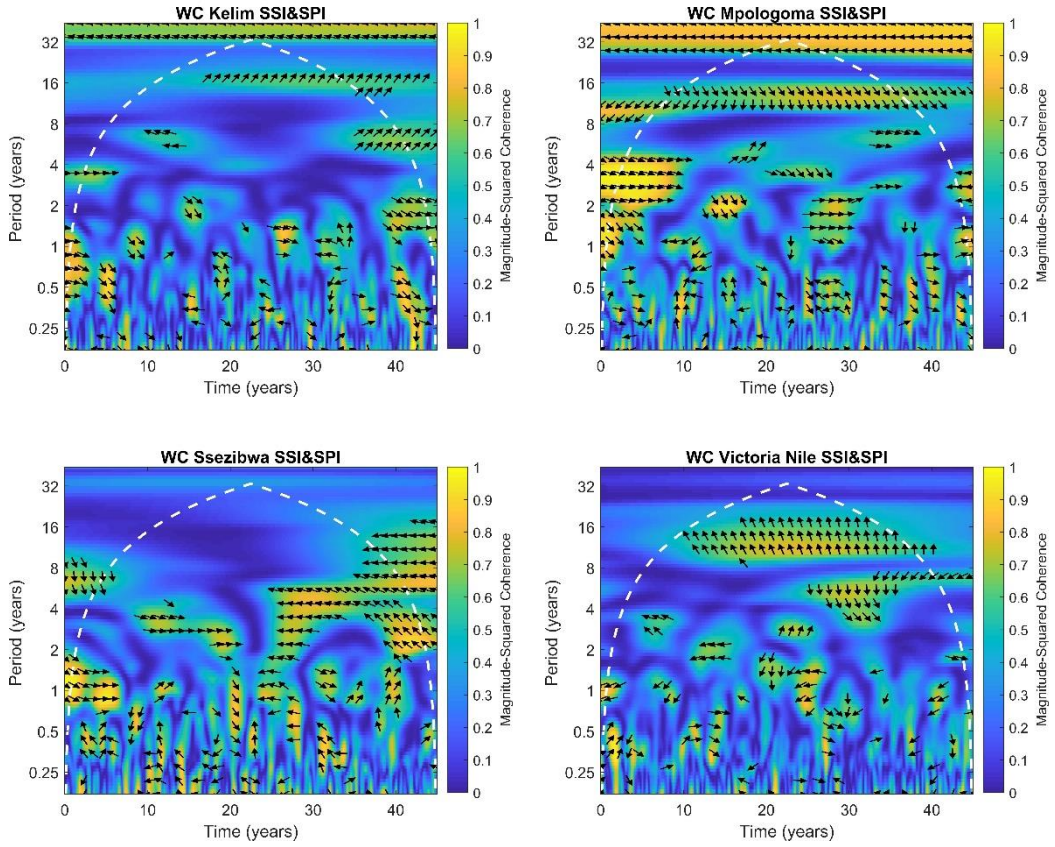


Figure 4.13: Wavelet coherence between SPI and SSI for the different sub-catchments

4.5.2 Interaction between R95 and AI

Coherence between the annual Rx95 and annual AI for each sub-catchment was done. Most of the sub-catchments exhibited interannual coherence in the period of 0-4years in the 1976-1983 and 2013 -17(figure 4.14). Kelim sub-catchment has high out of phase coherence in the 6-10 period throughout the whole period. Mpologoma sub-catchment had coherence in the period of 0-4 years in 1976-1994 then it shifted to the period of 8-16 years in 1995-2005. The Ssezibwa showed the least coherence only in the 0-4 years period in 1974-76 and 1994-1995. Victoria Nile showed coherence of about 0.6-0.7 in the periods of 0-4 years and 8-16 years. In the Okere sub-catchment coherence was mostly completely out of phase and in the 0-8 years period.

The high out of phase coherence between the Rx95 and AI is an implication that as the precipitation increases the Aridity decreases and vice versa.

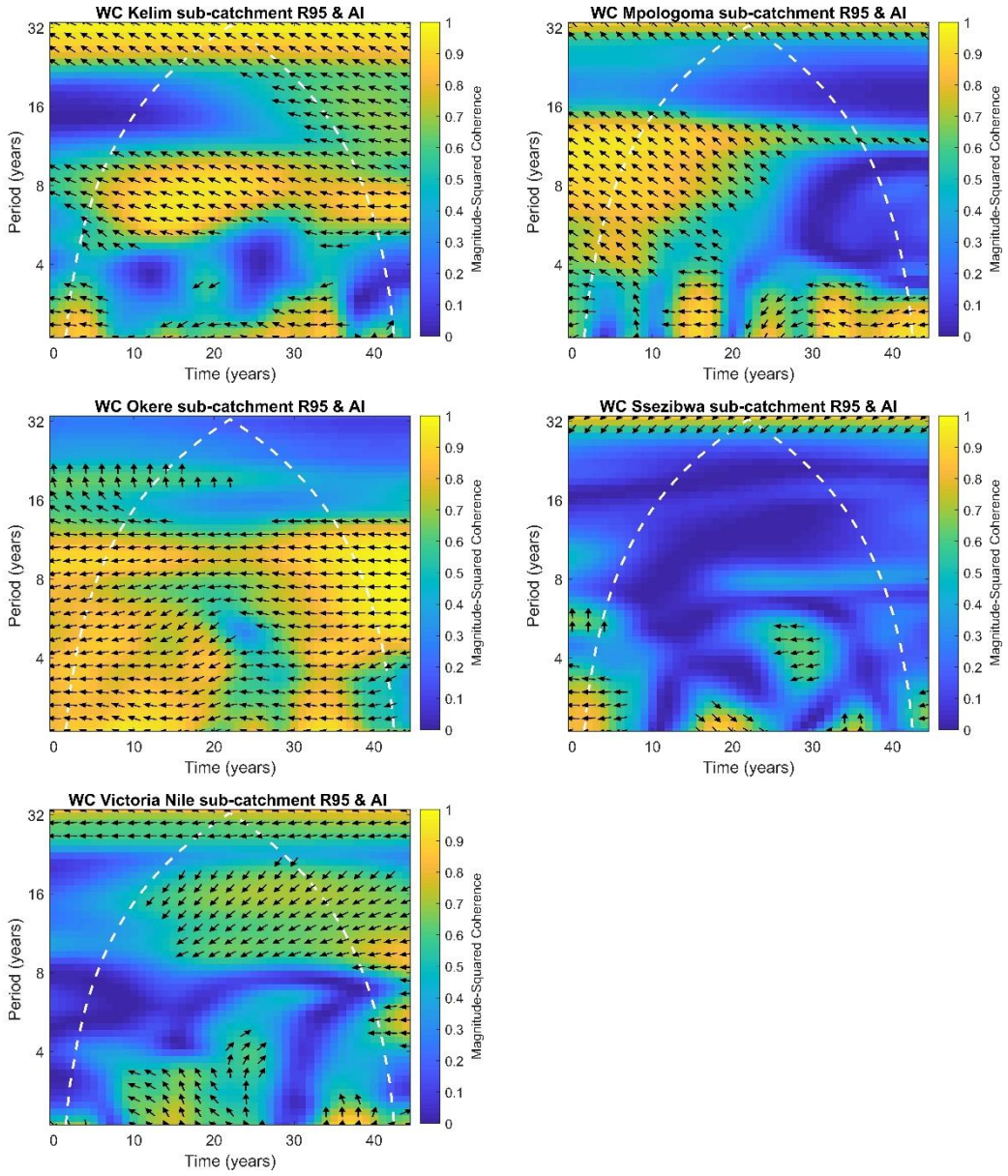


Figure 4.14: Wavelet coherence between R95 and AI

4.6.2 Interaction between NAO and Hydro-climatic indices

Each of the 6 hydroclimatic indices in the 6 sub-catchments were interacted with the NAO climate index and the results are reported in this section. The SPI-3 and SSI-3 were tested against the 3 months moving average of NAO and the rest against the annual NAO.

4.6.2.1 Interaction between NAO and precipitation- based indices

The coherence SPI-3, Rx5 and Rx95 with NAO was evaluated. The SPI-3 of all sub-catchments showed coherence in the periods of 0-2 years, this may indicate inter seasonal coherence. Some sub-catchments (Victoria Nile, southern part of Mpologoma, Ngeta and Soroti areas) showed

coherence in the 8-16 years period. Most of the coherence was in phase as shown in figure 4.15.

Coherence of NAO and Rx5 was least in Victoria Nile sub-catchment. The coherence was significant in the period of 0-2 years in 1985-94 and 2005-10. Coherence was also seen 10-16 years in 1985-2019. The coherence was both in and out of phase. Figure 4.16 shows the coherence of NAO with Rx5.

Figure 4.17 shows the coherence patterns of NAO and R95 which is the major reflection of the coherence of most stations. High coherence in the 0-4 years period in 1984-99 and 2005-13, then 12-16 years for 2000-18

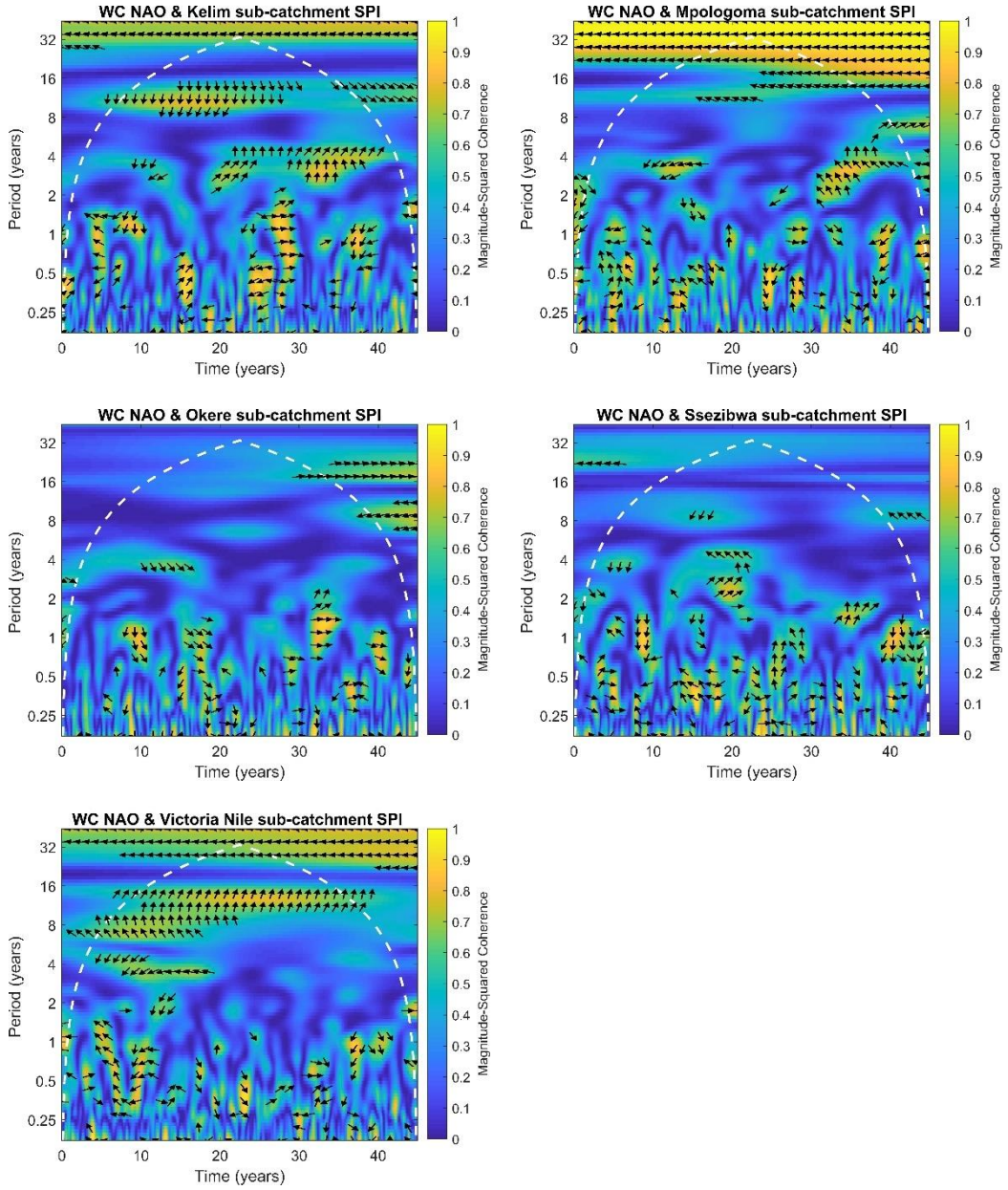


Figure 4.15: Wavelet coherence between NOA and SPI

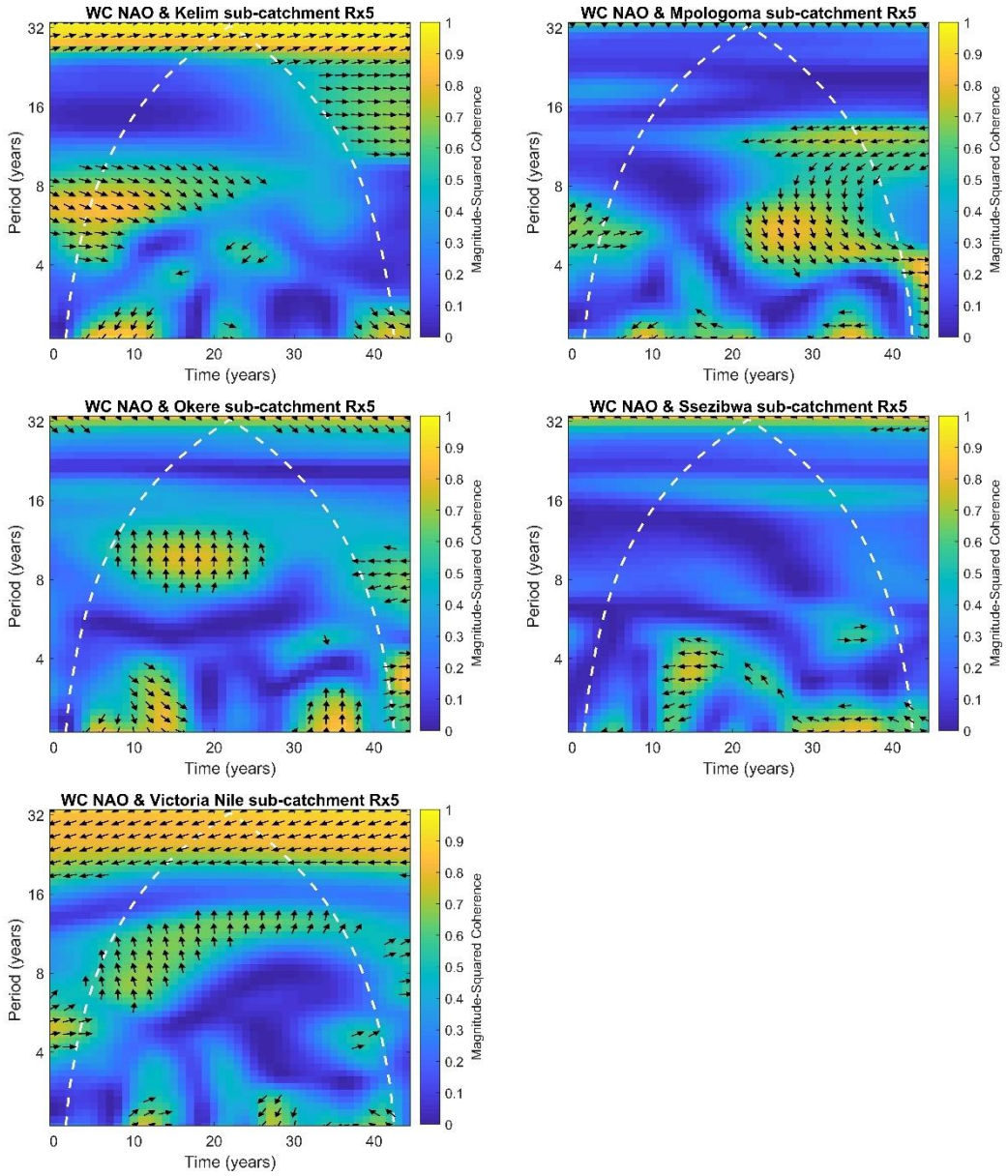


Figure 4.16: Wavelet coherence between NAO and Rx5

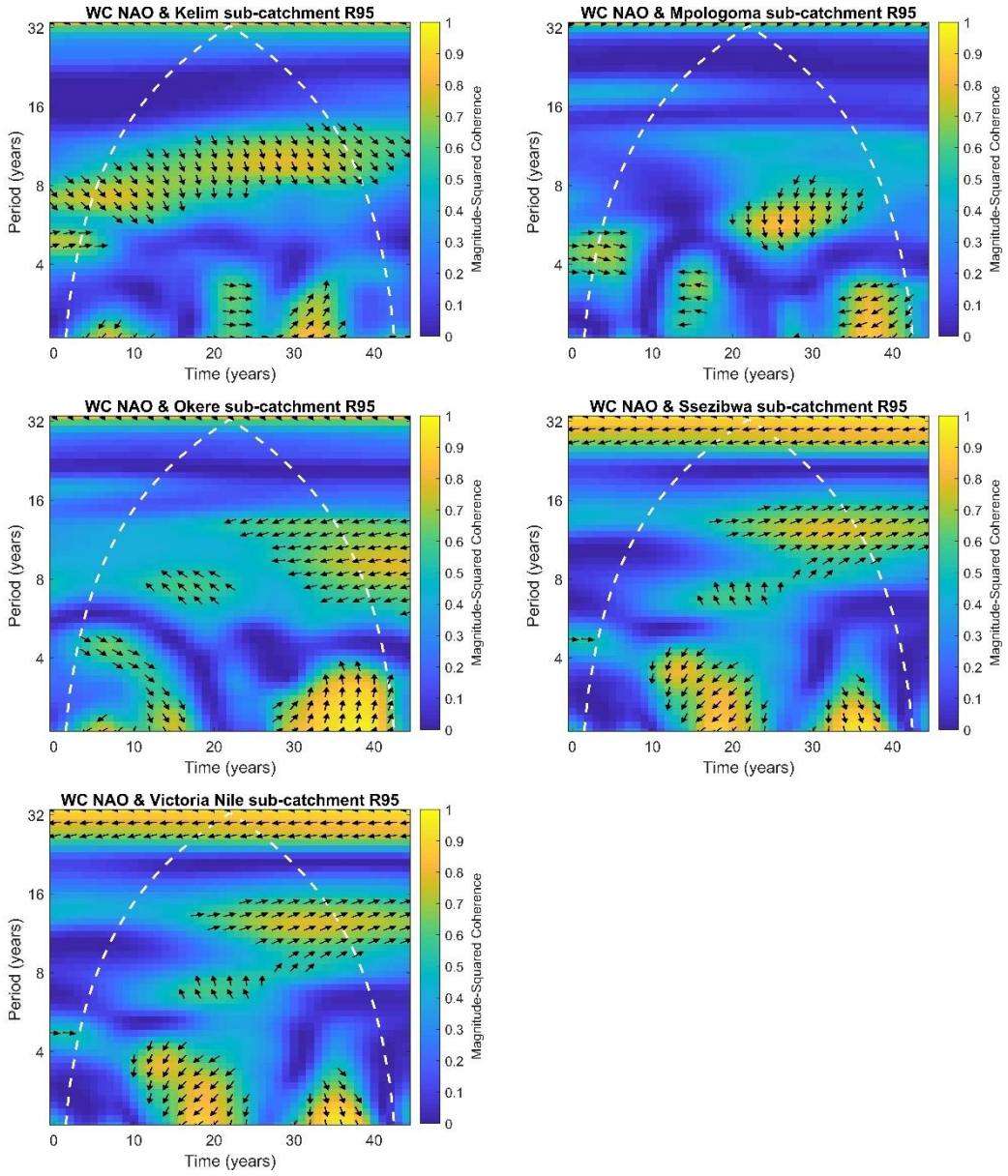


Figure 4.17: Wavelet coherence between NAO and Rx95

4.6.2.2 Interaction between NAO and aridity index

The annual NOA was evaluated with the AI. For this relationship each station had a unique pattern of coherence between the 2 indices but there was coherence for sub-catchment. Serere area showed the least coherence. Figure 4.18 showed the coherence of NAO and all the stations, significant coherence was seen in 3-5 years in the of 1996-2000. The AI over laps the NAO.

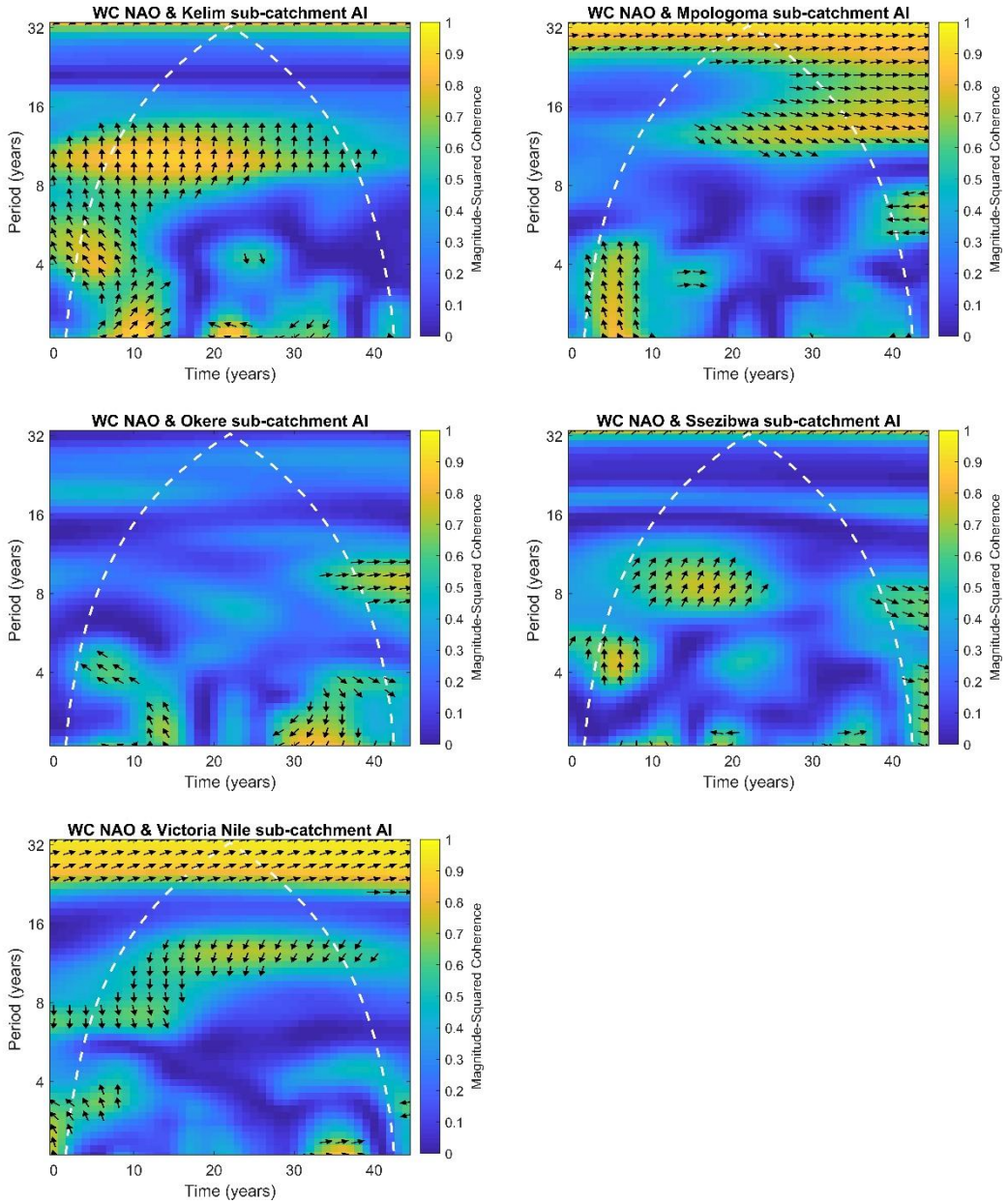


Figure 4.18: Wavelet coherence between NAO and AI

4.6.2.3 Interaction between NAO and streamflow- based indices

The Q95 showed high coherence in the period of 6-12 years in 1984-94 as illustrated in figure 4.19 below for the Victoria Nile. Kelim sub-catchment showed the least coherence seen in the period of 0-4 years in 2006-2019.Mpologoma showed coherence similar to that of Kelim but in 1978-1983. Ssezibwa showed coherence in the period of 4-8 years in 1983-1994.

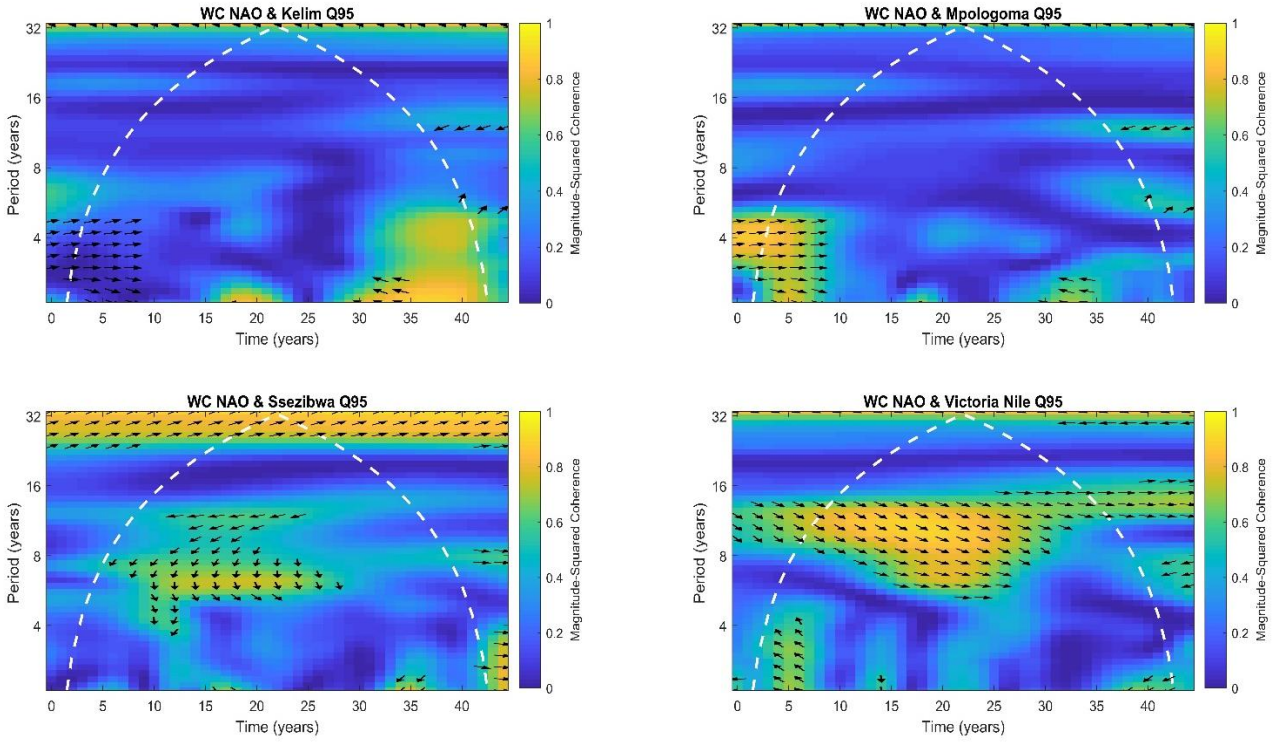


Figure 4.19: Wavelet coherence between NAO and Q95

The SSI-3 showed high coherence in the 0-2 years period, as shown for all sub-catchments in figure 4.20.

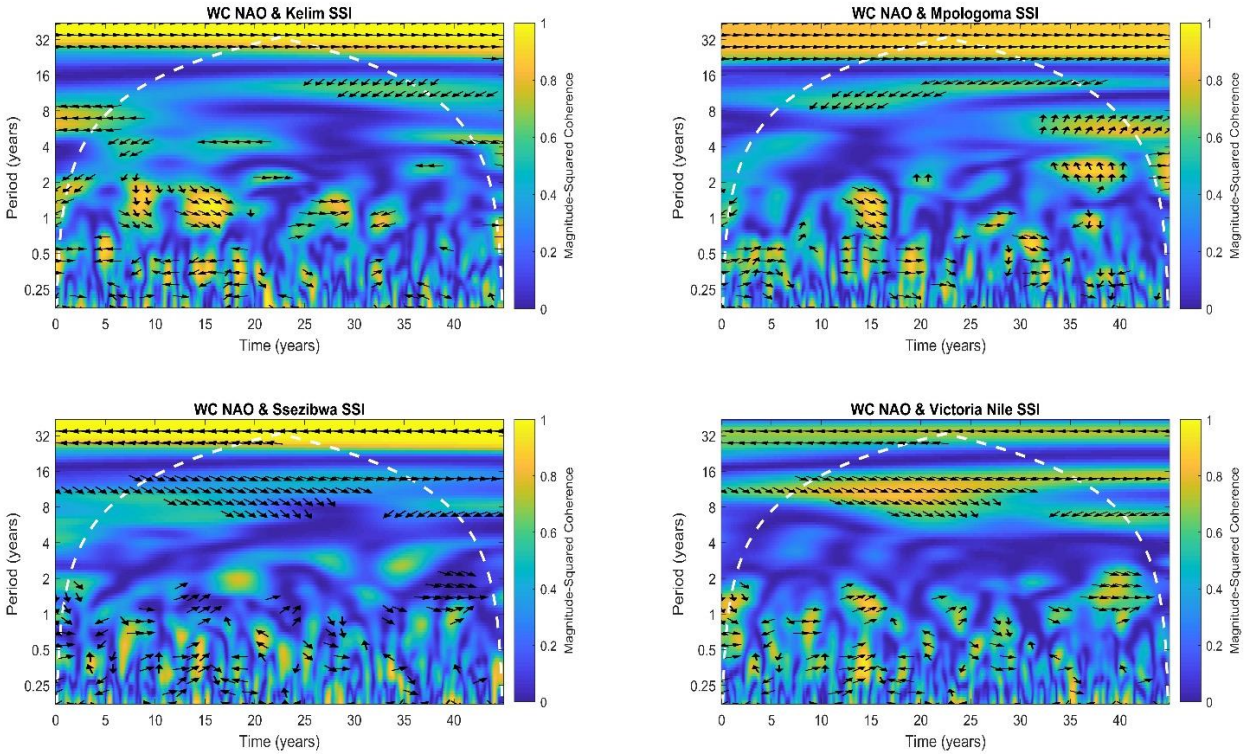


Figure 4.20: Wavelet coherence between NAO and SSI

4.5.3 Interaction between Niño 3.4 and Hydro-climatic indices

The interaction between the Niño 3.4 climate index and the 6 hydroclimatic indices was explored using the wavelet coherent method and the results are recorded in this section below.

4.6.2.4 Interaction between Niño 3.4 and SPI and SSI

The interaction of Niño 3.4 with all the 3 precipitation indices for each station was explored and the results are shown in figures 4.21, 4.22, 4.23 for SPI-3, Rx5 and R95 respectively.

The interaction between Niño 3.4 and SPI was relatively high and out of phase coherence in the period of 0-0.5 years (0-6months) over the years for all the sub-catchments, there is also inter annual coherence of 2-8 years for southern part of Okere and Mpologoma. Interannual coherence of 8-16 years for all sub-catchments.

R95 was coherent with Niño 3.4 in the period of 0-8 years for all the sub-catchments.

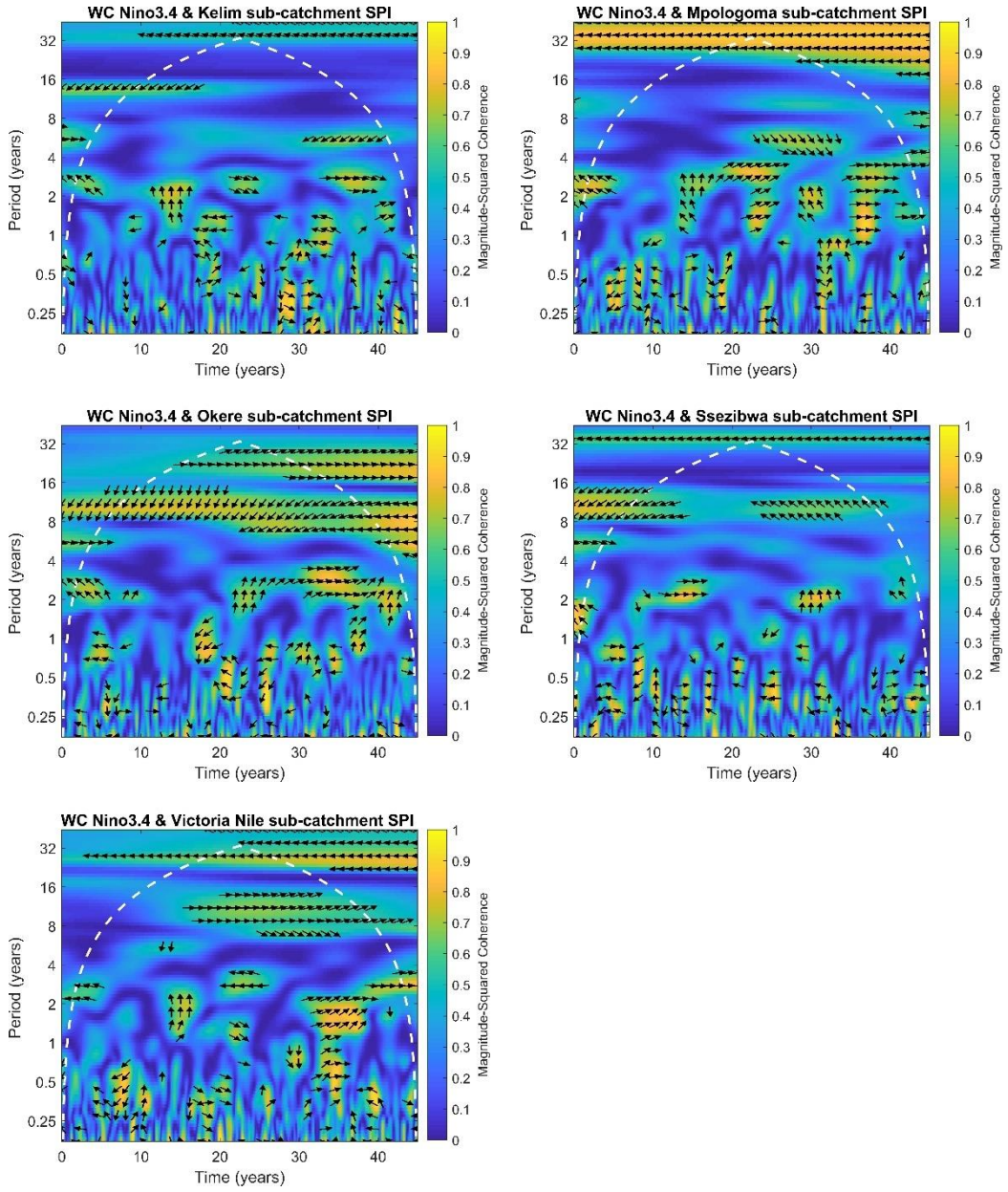


Figure 4.21: Wavelet coherence between Niño 3.4 and SPI

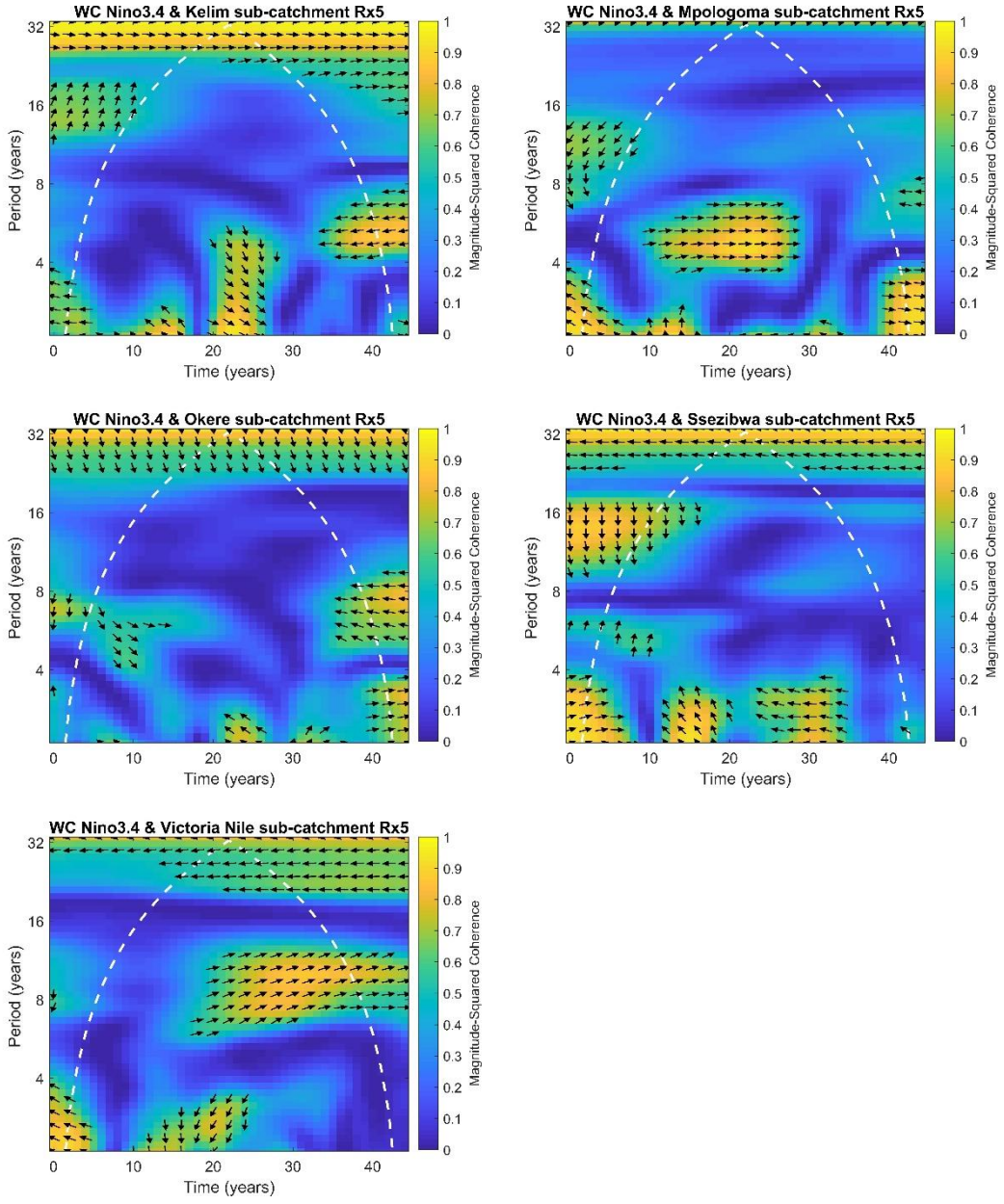


Figure 4.22: Wavelet coherence between Niño3.4 and Rx5 of selected stations in LKB

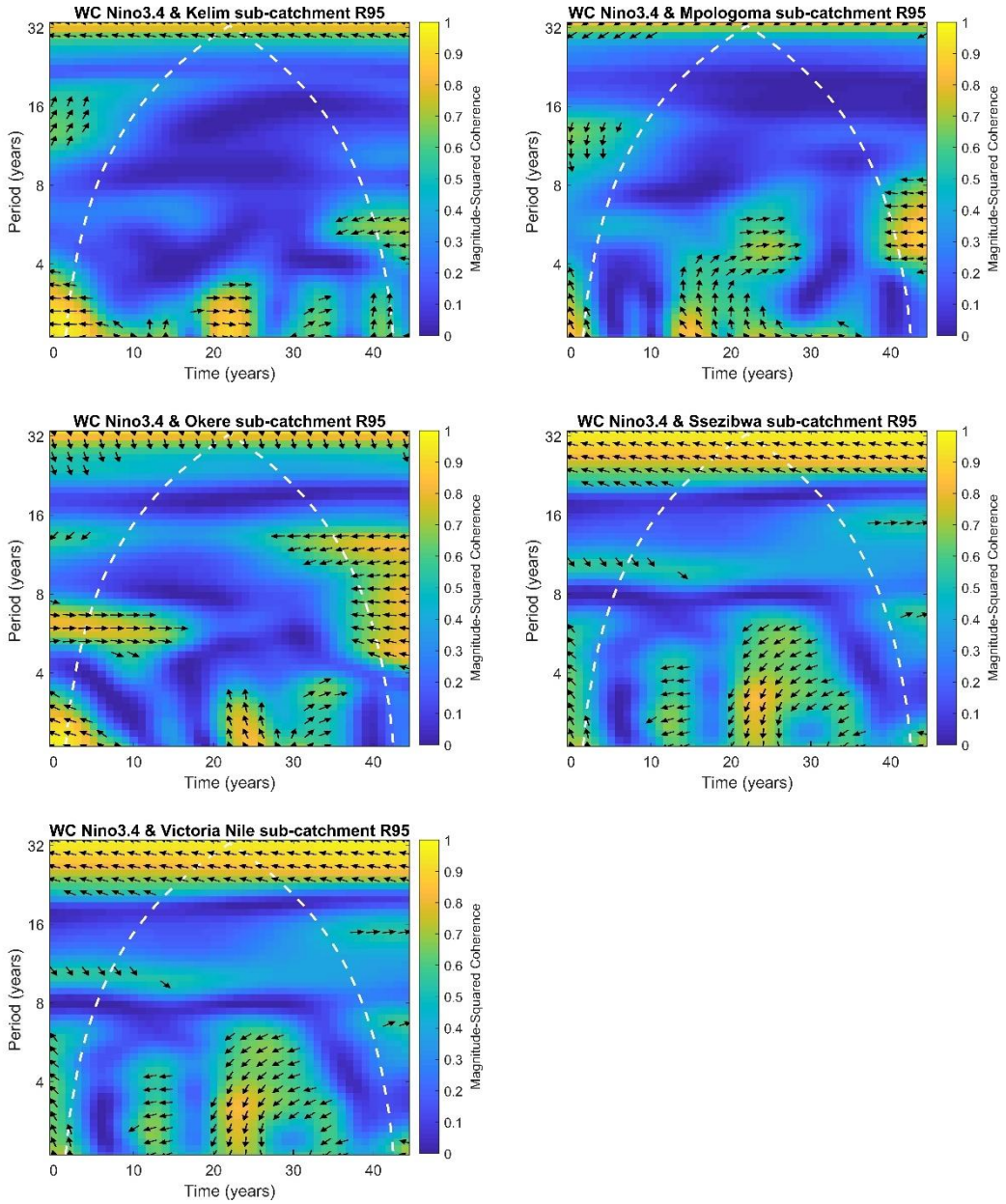


Figure 4.23: Wavelet coherence between Niño3.4 and R95 of selected stations in LKB

4.5.4.2 Interaction between Niño 3.4 and evapotranspiration- based indices

The interaction between Niño 3.4 and AI showed minimal coherence for the following southern part of Okere (Kangole), Kelim sub-catchment, Magoro, Ngeta and Southern part of Mpologoma. The following stations rather showed high coherence in all the periods; Northern part of Okere, Northern part of Mpologoma, Soroti and Victoria Nile. These resulted are summarized in figure 4.24.

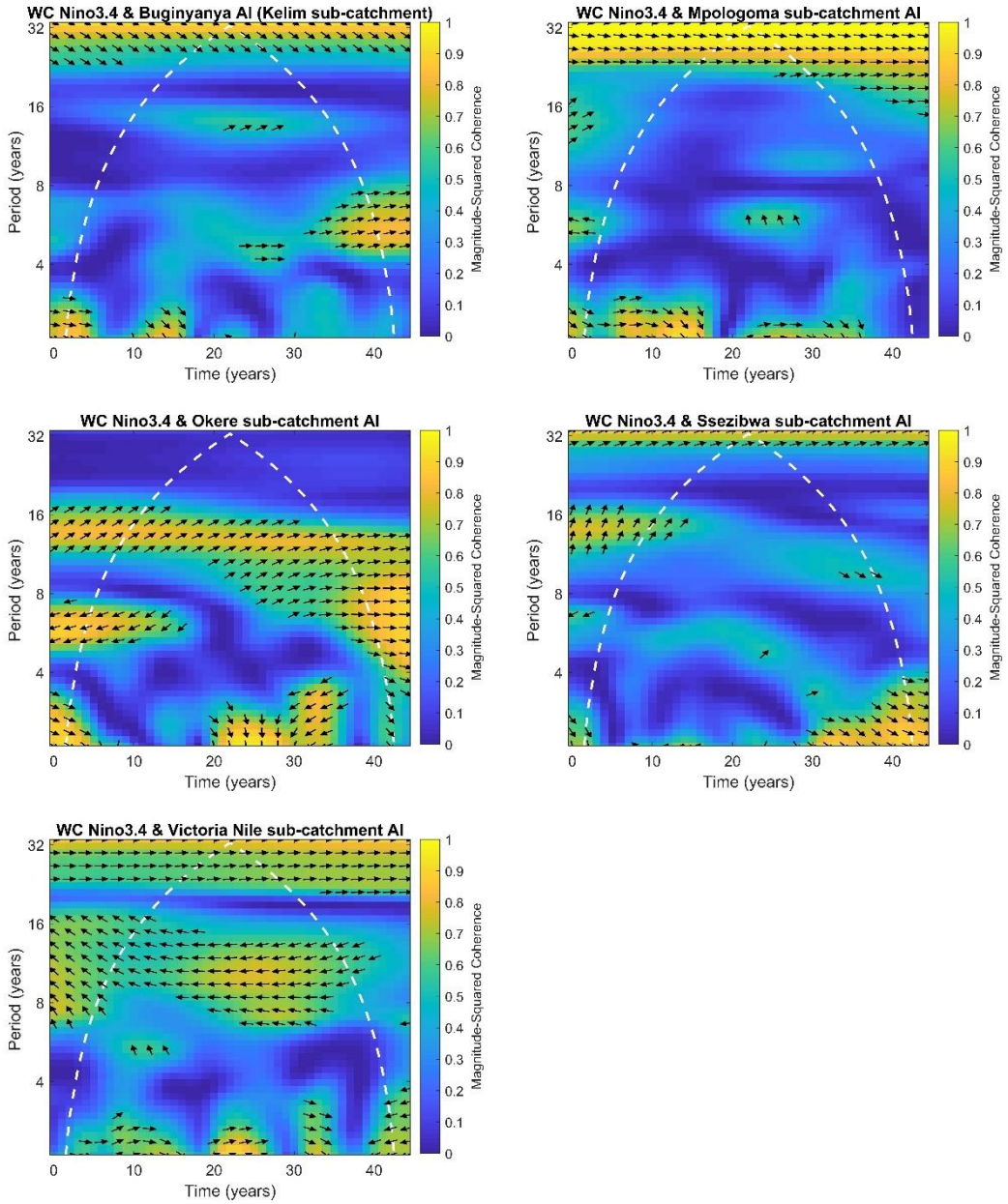


Figure 4.24: Wavelet coherence between Niño 3.4 and AI of selected stations in LKB

4.6.2.5 Interaction between Niño 3.4 and streamflow- based indices

Two streamflow indices, that is SSI and Q95 were interacted with Niño 3.4. The results are in figure 4.25 and 4.26. Victoria Nile showed the least coherence of all the 4 sub-catchments. The rest of the sub-catchments showed coherence in the periods of 0-4 years with marked coherence in the period of 1-4 years in the years of 2006-2010.

Ssezibwa catchment has almost no coherence with Niño 3.4 while the other catchments have isolated coherences with Niño 3.4. Kelim showed a coherence in the period of 0-4 years in

2012-2015, Mpologoma showed coherence in the period of 0-2 years in 1978-1984 while Victoria Nile showed coherence in the period of 0-4 years in 1992-1998.

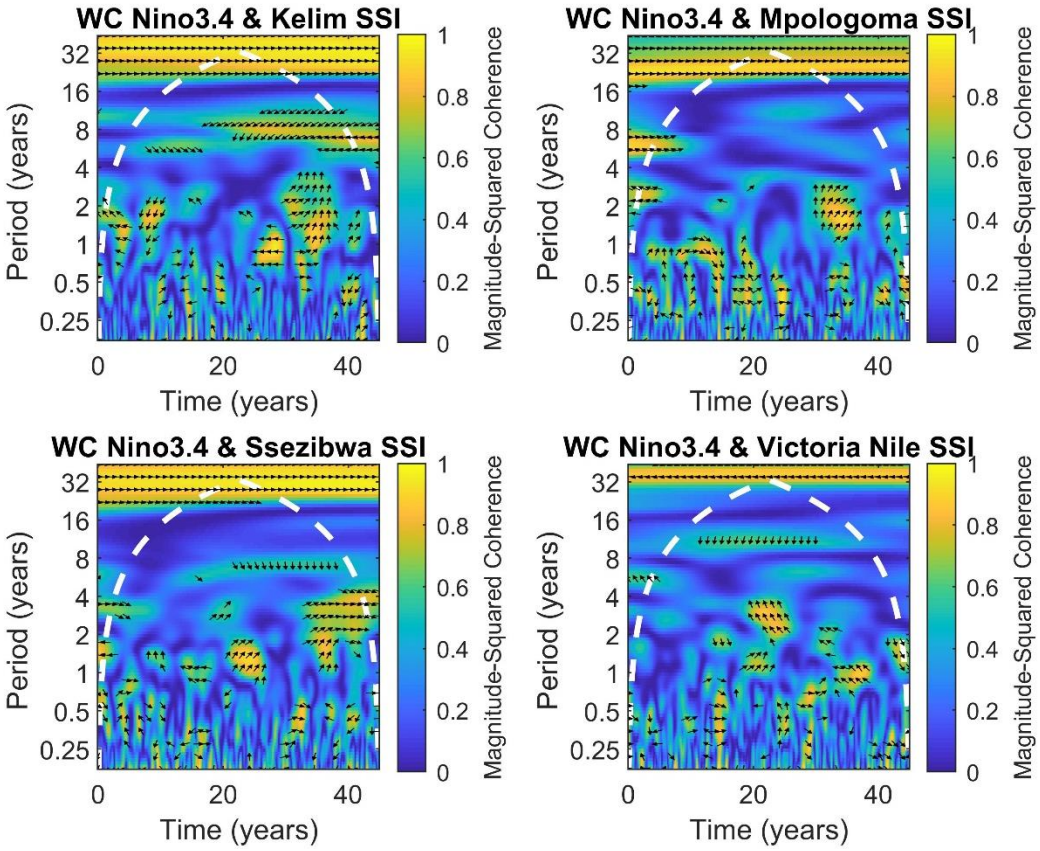


Figure 4.25: Wavelet coherence between Niño 3.4 and SSI

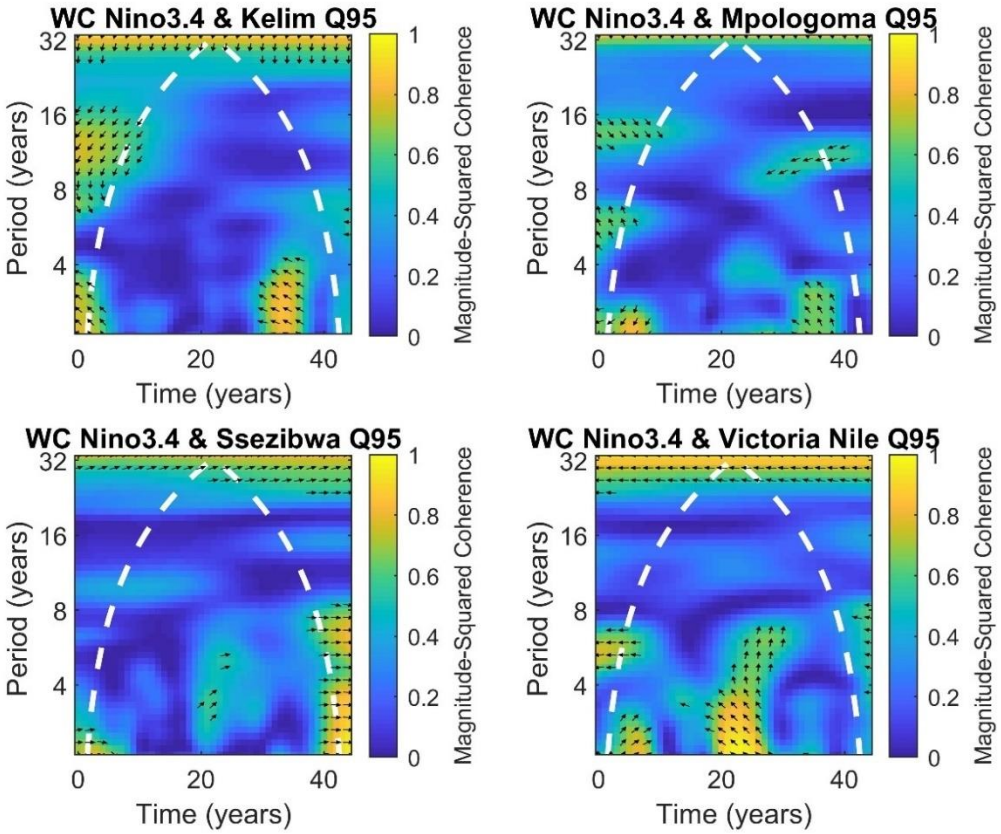


Figure 4.26: Wavelet coherence between Niño 3.4 and Q95

4.5.4 Interaction between Niño 3 and Hydro-climatic indices

Like the rest of the climate indices, Niño 3 was interacted with the 6 hydro-climatic indices and the results are presented in this section

4.6.2.6 Interaction between Niño 3 and precipitation- based indices

The interaction between Niño 3 and the 3 precipitation indices is summarised in the figures 4.27, 4.28 and 4.29. The SPI showed inconsistent coherence for the periods of 0-6 months for all the stations. Okere showed coherence in the period of 2-4 years in 1995-1998, while Mpologoma showed coherence in the periods of 5-8 years in 1995-2002.

Rx5 showed localised coherences especially in the 0-4 years period for all sub-catchments.

R95 showed very little coherence in the Okere and Kelim sub-catchment, the coherence is seen minimumly in the period of 0-4 yrs. The other sub-catchment showed coherence in the period of 8-16 years.

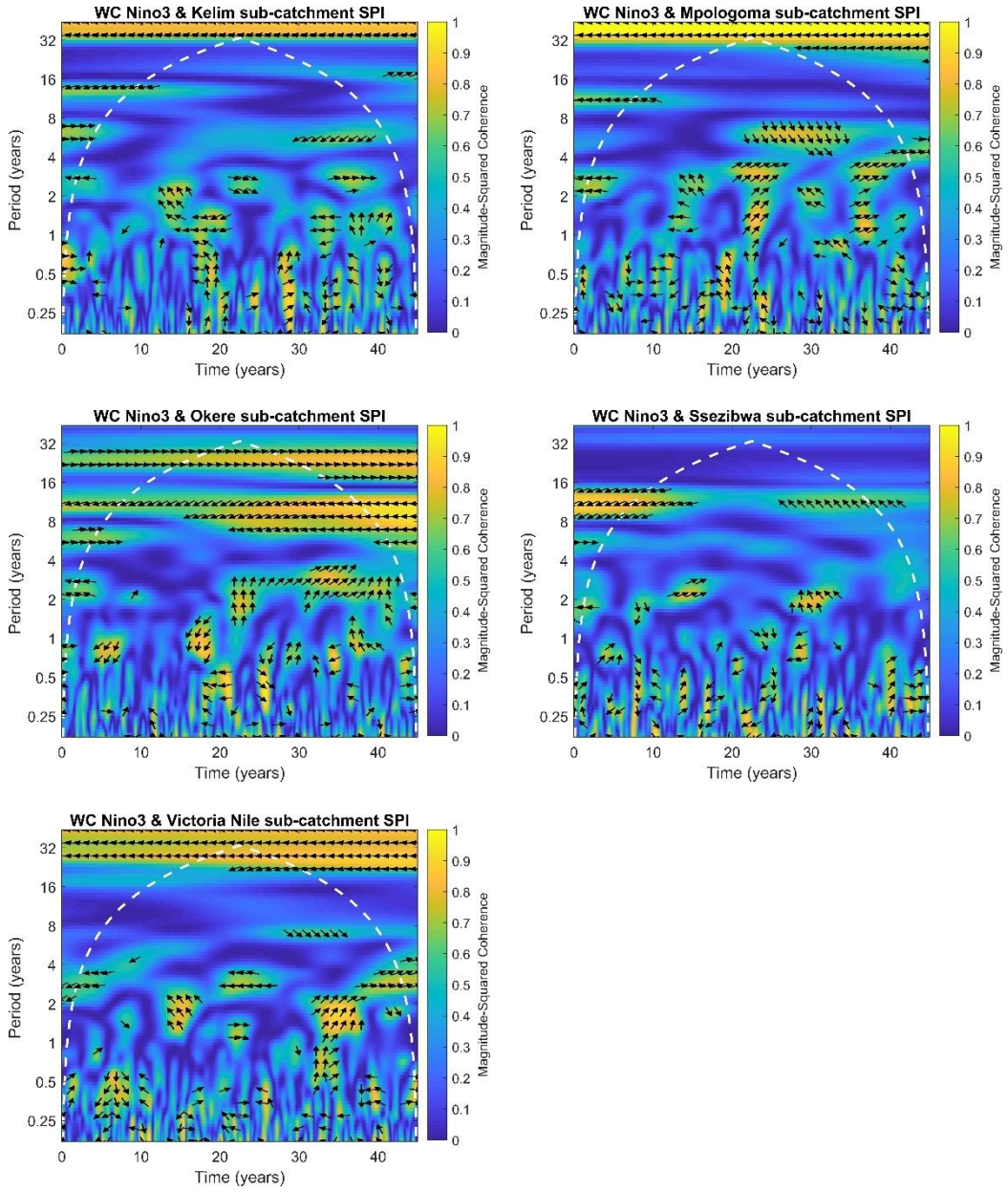


Figure 4.27: Wavelet coherence between Niño 3 and SPI of the selected stations in LKB

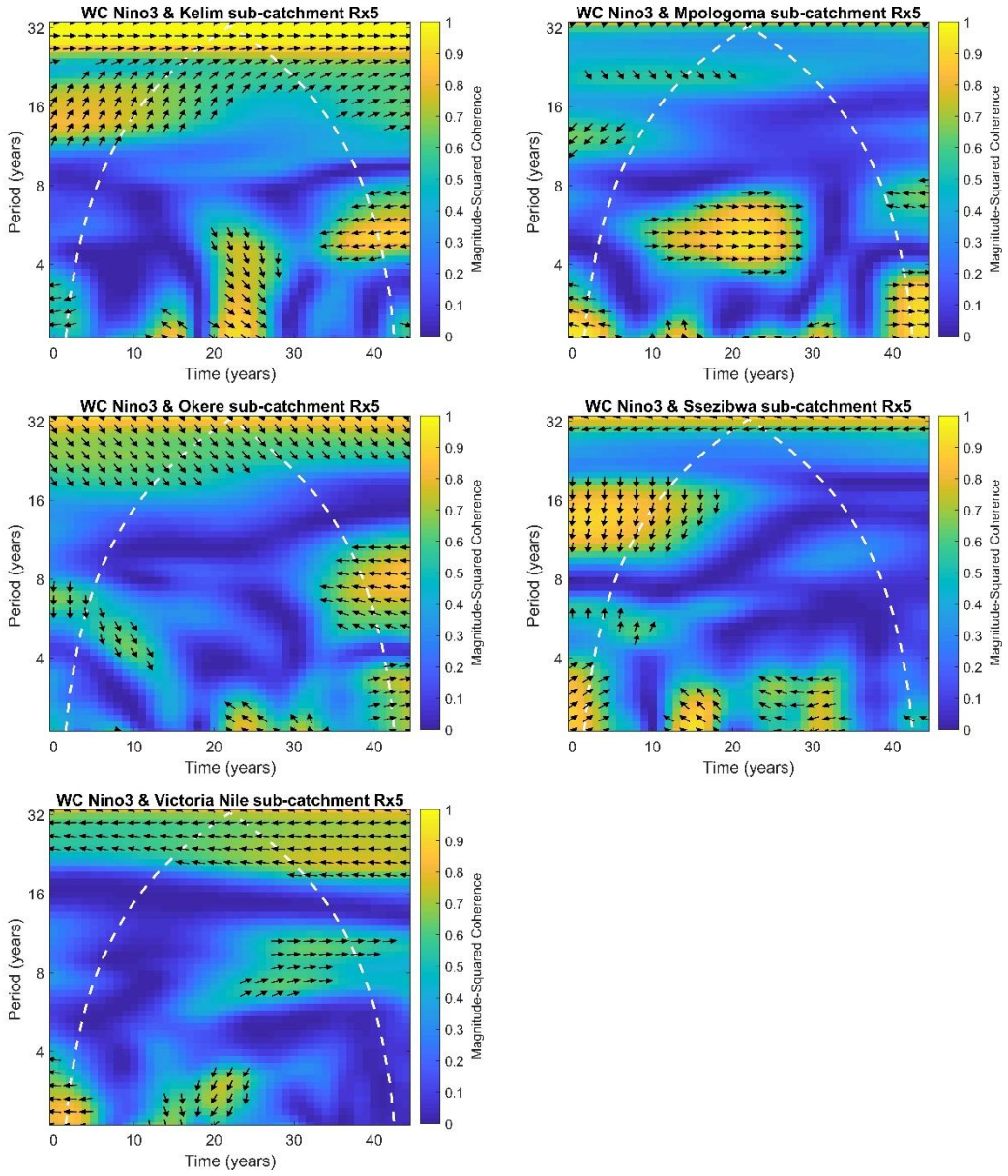


Figure 4.28: Wavelet coherence between Niño 3 and Rx5 of selected stations in LKB

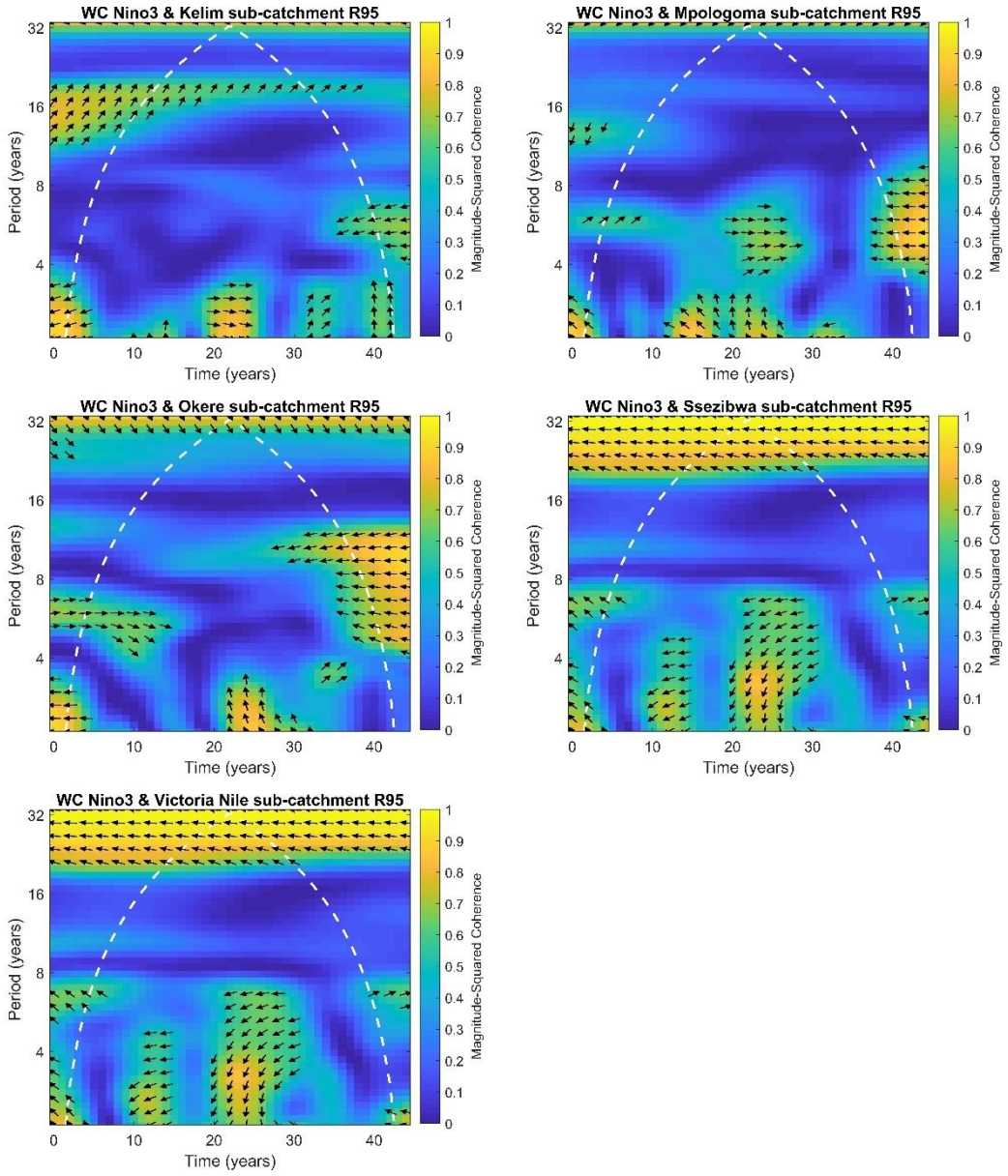


Figure 4.29: Wavelet coherence between Niño3 and R95 for selected stations in LKB

4.6.2.7 Interaction between Niño 3 and evapotranspiration- based indices

Figure 4.30 shows the interaction of AI an evapotranspiration index with Niño 3. Most of the stations show very little coherence in the 0-4 years period. Okere sub-catchment showed coherence in all the periods.

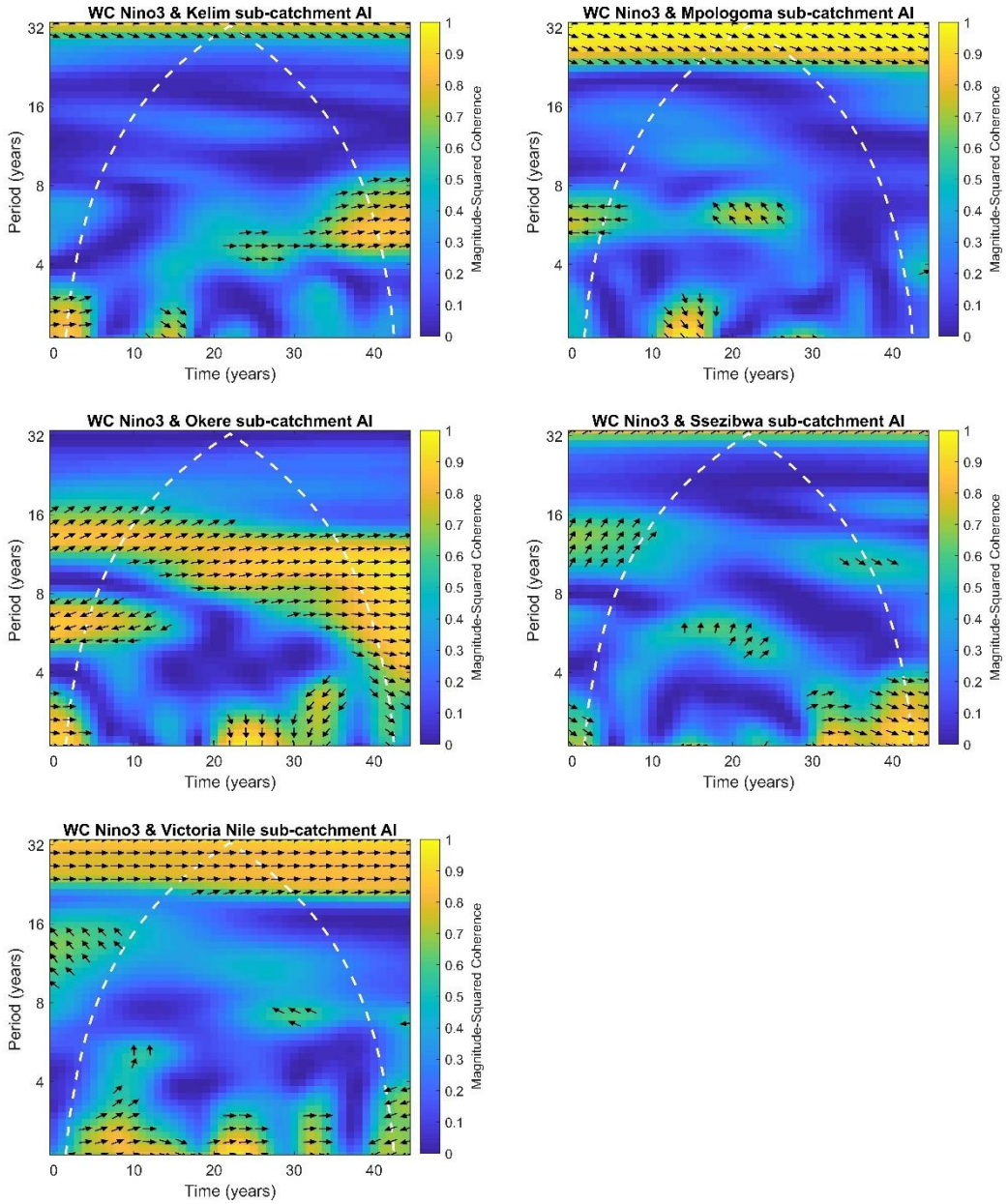


Figure 4.30: Wavelet coherence between Niño 3 and AI for selected station in LKB

4.6.2.8 Interaction between Niño 3 and streamflow- based indices

The 2 streamflow indices were interacted with Niño 3 and the results are shown in figure 4.31 and 4.32.

For SSI, Victoria Nile showed the least coherence with Niño 3 with high coherence seen in the period of 2-4 years in 1994-1996. The other 3 sub-catchments show uneven coherence in the periods of 0-6months. They further show isolated coherence of 1-4 years, for Kelim and Mpologoma its was 208-2010 whereas for Ssezibwa it was in 1994-1996.

The Q95 of Ssezibwa showed the least coherence, followed by Mpologoma, Kelim and Victoria Nile showing the highest coherence with in the 0-4 years period.

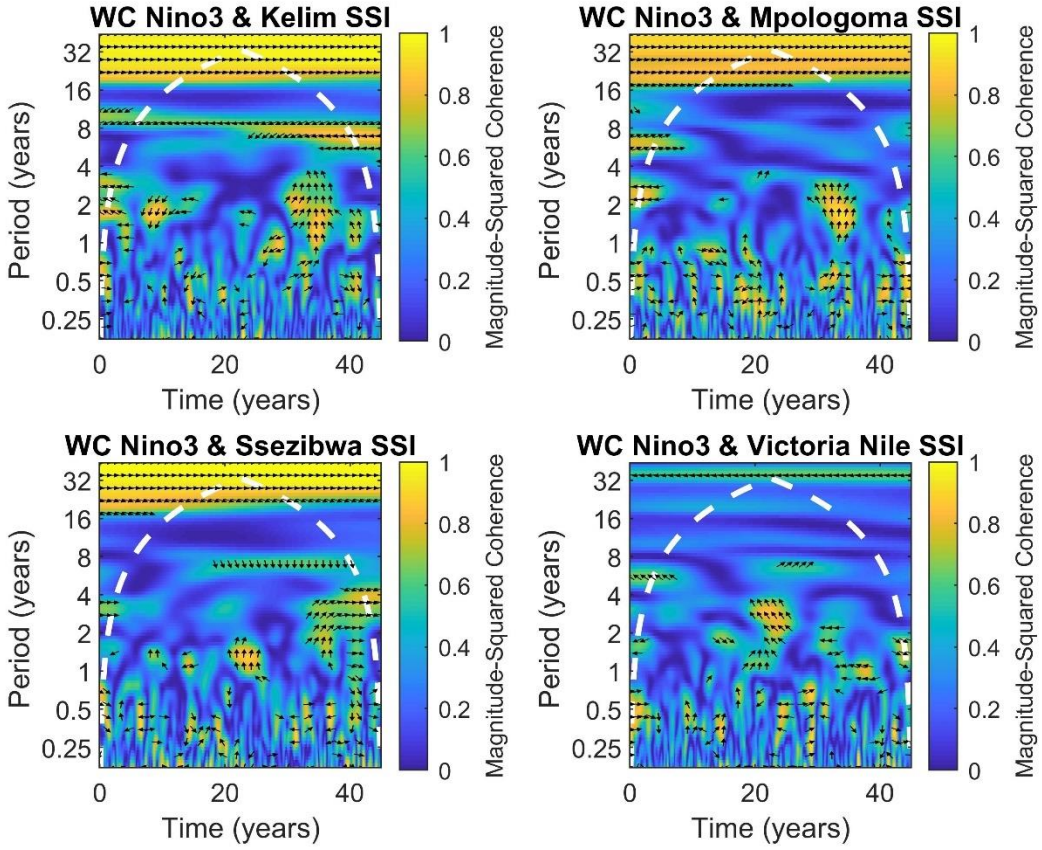


Figure 4.31: Wavelet coherence between Niño3 and SSI of the gauged sub-catchments in LKB

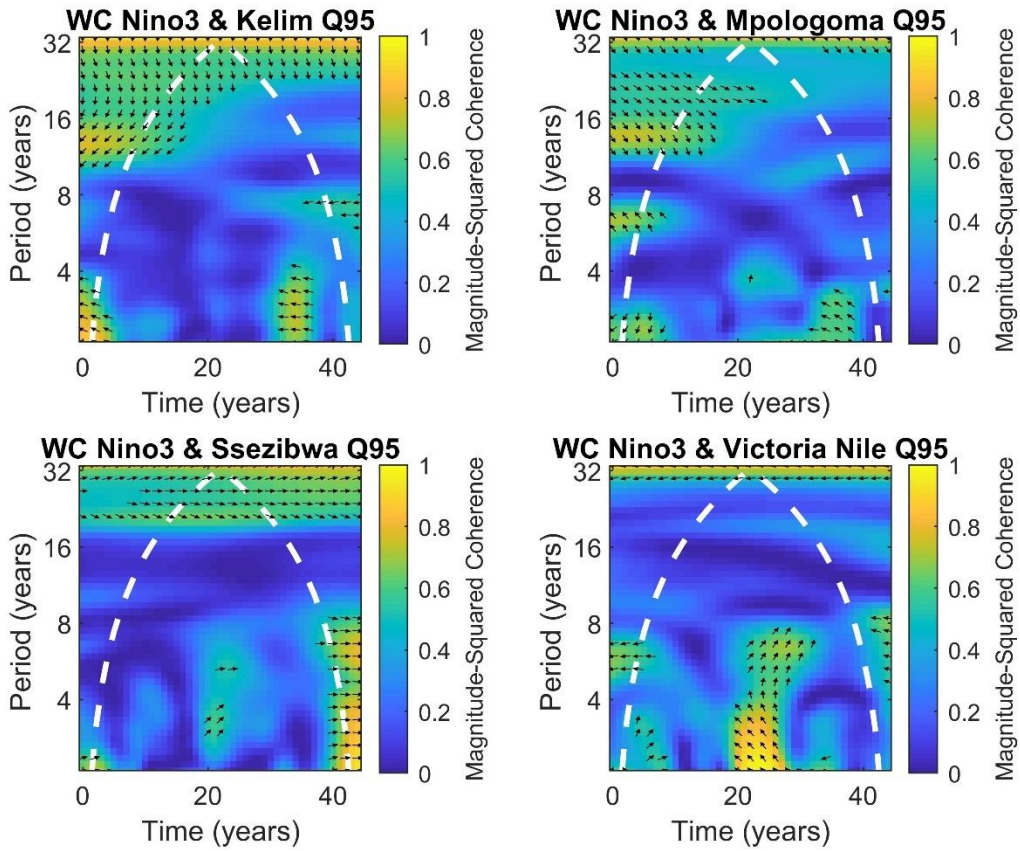


Figure 4.32: Wavelet coherence between Niño 3 and Q95 of the gauged sub-catchments in LKB

5. CONCLUSION AND RECOMMENDATION

5.1 Conclusion

The results obtained from this study are an indication of climate variability in the LKB, exhibiting extremes events of both drought and floods. Both extremes have an impact on the river flows as floods can be associated with soil erosion, land slides among others and prolonged droughts with water and food scarcity. Significant seasonal variability negatively affects crop and livestock production. This greatly affects farmers' decisions and yields at the end of the seasons. It calls for mitigation practices, adaptation methods and great involvement and support from the government.

In most parts of the LKB precipitation is decreasing while aridity is increasing. Therefore, it might be urgent to prepare countermeasures to rising drought risks in the country, particularly for areas in which climate has been semi-humid but expected to become drier and the semi-arid become arid. Persistence of climate variability was noted which may be an indication that the occurrence of extreme events will continue both in predictable and unpredictable ways.

The decreasing precipitation in LKB has been attributed to the climatic teleconnection which might imply that the teleconnections have a cause in the variations of the hydro-climatic indices, Ogallo (1989), Indeje et al (2000) Onyutha (2016a) and Onyutha (2020) also confirm this. This is one of the causes of climate variability among others which can be confirmed through future research. The streamflow however, did not have strong relationship with the climate teleconnections. The cause of this indicates a need for further study.

The coherence between the precipitation and streamflow was not as strong as expected, this implies that there are other factors that contribute to streamflow let alone factors that influence precipitation being converted in to streamflow. These could include anthropogenic activities like land use land cover changes, soil properties, slope among others.

The relationship between the precipitation and aridity was inverse but very strong. It calls for attention though because the decreasing precipitation is resulting in increasing aridity in various parts of the LKB. If not mitigated it will result in a complete change of climate in the region.

5.2 Recommendation

The following recommendations are made:

The results indicate an increase in the frequency and magnitude of meteorological droughts as compared to the hydrological droughts, the government, and farmers should consider drought in their plans. Also, employment of drought resistant crops is highly recommended. Additionally, improvement of agricultural and land use best practices in order to cope with the changing environment as a way of adaptation.

Water resource managers should consider effective and efficient methods of water distribution and usage with in the basin. Options like rainwater harvesting, storage of excess water during the rainy season and flood seasons plus encouraging water users to considerably use the water well.

Future research should consider the impacts of human activities on extreme events (drought and floods) to provide better tools for enhancing community drought and floods preparedness.

The use of indices in the LKB studies should be explored more on 3 fronts;

- comparing indices like SPI and SSI at variable scales in order to capture various feature of extreme that were not captured at the scale of 3.
- Making projections of future scenarios the different indices which is very vital for planning
- Coupling the indices with other factors which cause variation in hydroclimatic indices. These factors may be the anthropogenic activities which cause changes in land use and land cover. Soil properties can also be explored as they affect the recharge of streams.
- Investigating the different indices and quantifying their contribution to streamflow is also recommended as it will improve the prediction and management to water resource

REFERENCES

Adarsh, S., VishnuPriya, M. S., Narayanan, S., Smruthi, M. S., George, P., & Benjie, N. M. (2016). Trend analysis of sediment flux time series from tropical river basins in India using non-parametric tests and multiscale decomposition. *Modeling Earth Systems and Environment*, *2*(4), 1–16. https://doi.org/10.1007/s40808-016-0245-0

Agnew, C. T., & Chappell, A. (1999). Drought in the Sahel. *GeoJournal*, *48*(4), 299–311. https://doi.org/10.1023/A:1007059403077

Aguilera, H., Guardiola-Albert, C., & Serrano-Hidalgo, C. (2020). Estimating extremely large amounts of missing precipitation data. *Journal of Hydroinformatics*, *22*(3), 578–592. https://doi.org/10.2166/hydro.2020.127

Arora, V. K. (2002). The use of the aridity index to assess climate change effect on annual runoff. *Journal of Hydrology*, *265*(1–4), 164–177. https://doi.org/10.1016/S0022-1694(02)00101-4

Barker, L. J., Hannaford, J., Chiverton, A., & Svensson, C. (2015). From meteorological to hydrological drought using standardised indicators. In *Hydrology and Earth System Sciences Discussions* (Vol. 12, Issue 12). https://doi.org/10.5194/hessd-12-12827-2015

Basalirwa, C. P. K. (1995). Delineation of Uganda into climatological rainfall zones using the method of principal component analysis. *International Journal of Climatology*, *15*(10), 1161–1177. https://doi.org/10.1002/joc.3370151008

Bawden, A. J., Linton, H. C., Burn, D. H., & Prowse, T. D. (2014). A spatiotemporal analysis of hydrological trends and variability in the Athabasca River region, Canada. *Journal of Hydrology*, *509*(2014), 333–342. https://doi.org/https://doi.org/10.1016/j.jhydrol.2013.11.051

Belayneh, A., & Adamowski, J. (2013). Drought forecasting using new machine learning methods. *Journal of Water and Land Development*, *18*(9), 3–12. https://doi.org/10.2478/jwld-2013-0001

Bernard, B., Vincent, K., Frank, M., & Anthony, E. (2013). Comparison of extreme weather events and streamflow from drought indices and a hydrological model in River Malaba, Eastern Uganda. *International Journal of Environmental Studies*, *70*(6), 940–951. https://doi.org/10.1080/00207233.2013.862463

Brown, E., & Sutcliffe, J. V. (2013). The water balance of Lake Kyoga , Uganda The water balance of Lake Kyoga , Uganda. *Hydrological Sciences Journal*, *58*(2), 342–353. https://doi.org/10.1080/02626667.2012.753148

Budyko, I. M. (1974). *Climate and Life* (D. H. Miller (ed.); Vol. 18, Issue 2). Academic Press.

Burn, D. H., Abdul Aziz, O. I., & Pietroniro, A. (2004). A Comparison of Trends in Hydrological Variables for Two Watersheds in the Mackenzie River Basin. *Canadian Water Resources Journal*, *29*(4), 283–298. https://doi.org/10.4296/cwrj283

Burn, D. H., & Elnur, M. A. H. (2002). Detection of hydrologic trends and variability. *Journal of Hydrology*, *255*, 107–122.

Burn, D. H., Sharif, M., & Zhang, K. (2010). Detection of trends in hydrological extremes for Canadian watersheds. *Hydrological Processes*, *24*(13), 1781–1790. https://doi.org/10.1002/hyp.7625

Cahill, A. T. (2002). Determination of changes in streamflow variance by means of a wavelet-based test. *Water Resources Research*, *38*(6), 1-1-1–13. https://doi.org/10.1029/2000wr000192

Carey, S. K., Tetzlaff, D., Seibert, J., Soulsby, C., Buttle, J., Laudon, H., McDonnell, J., McGuire, K., Caissie, D., Shanley, J., Kennedy, M., Devito, K., & Pomeroy, J. W. (2010). Inter-comparison of hydro-climatic regimes across northern catchments: Synchronicity, resistance and resilience. *Hydrological Processes*, *24*(2010), 3591–3602. https://doi.org/10.1002/hyp.7880

Chai, Y., Li, Y., Yang, Y., Zhu, B., Li, S., Xu, C., & Liu, C. (2019). Influence of Climate Variability and Reservoir Operation on Streamflow in the Yangtze River. *Scientific Reports*, *9*(1), 1–10. https://doi.org/10.1038/s41598-019-41583-6

Conway, D., Pereschino, A., Ardoin-Bardin, S., Hamandawana, H., Dieulin, C., & Mahé, G. (2009). Rainfall and water resources variability in sub-Saharan Africa during the twentieth century. *Journal of Hydrometeorology*, *10*(1), 41–59. https://doi.org/10.1175/2008JHM1004.1

Dabanlı, İ., Şen, Z., Yeleğen, M. Ö., Şişman, E., Selek, B., & Güçlü, Y. S. (2016). Trend Assessment by the Innovative-Şen Method. *Water Resources Management*, *30*(14), 5193–5203. https://doi.org/10.1007/s11269-016-1478-4

Dars, G. H. (2013). *Climate Change Impacts on Precipitation Extremes over the Columbia River Basin Based on Downscaled CMIP5 Climate Scenarios* [Portland State University]. https://doi.org/10.15760/etd.979

De Lima, M. I. P., Carvalho, S. C. P., & P. De Lima, J. L. M. (2010). Investigating annual and monthly trends in precipitation structure: An overview across Portugal. *Natural Hazards and Earth System Science*, *10*(11), 2429–2440. https://doi.org/10.5194/nhess-10-2429-2010

Ehsanzadeh, E., Ouarda, T. B. M. J., & Saley, H. M. (2011). A simultaneous analysis of gradual and abrupt changes in Canadian low streamflows. *Hydrological Processes*, *25*(5), 727–739. https://doi.org/10.1002/hyp.7861

Fan, H., & He, D. (2015). Temperature and precipitation variability and its effects on streamflow in the upstream regions of the Lancang-Mekong and Nu-Salween Rivers. *Journal of Hydrometeorology*, *16*(5), 2248–2263. https://doi.org/10.1175/JHM-D-14-0238.1

Filahi, S., Tanarhte, M., Mouhir, L., Morhit, M, E., & Tramblay, Y. (2016). Trends in indices of daily temperature and precipitations extremes in Morocco. *Theor Appl Climatol*, *124*(2016), 959–972. https://doi.org/10.1007/s00704-015-1472-4

Gedefaw, M., Wang, H., Yan, D., Song, X., Yan, D., Dong, G., Wang, J., Girma, A., Ali, B. A., Batsuren, D., Abiyu, A., & Qin, T. (2018). Trend analysis of climatic and hydrological variables in the Awash river basin, Ethiopia. *Water (Switzerland)*, *10*(11), 1–14. https://doi.org/10.3390/w10111554

GoU. (2007). *Climate change: National Adaptation Programmes of Action*.

Greve, P., Roderick, Michael, L., & Seneviratne, Sonia, I. (2017). Simulated changes in aridity from the last glacial maximum to 4xCO2. *Environmental Research Letters*, *12*(11), 1–8. https://doi.org/https://doi.org/10.1088/1748-9326/aa89a3

Greve, P., Roderick, M. L., Ukkola, A. M., & Wada, Y. (2019). The aridity Index under global warming. *Environmental Research Letters*, *14*(12), 1–11. https://doi.org/10.1088/1748-9326/ab5046

Grinsted, A., Moore, J. C., & Jevrejeva, S. (2004). Application of the cross wavelet transform and wavelet coherence to geophysical time series. *Nonlinear Processes in Geophysics*,

11(5/6), 561–566. https://doi.org/10.5194/npg-11-561-2004

Gudmundsson, L., Do, H. X., Leonard, M., & Westra, S. (2018). The Global Streamflow Indices and Metadata Archive (GSIM)-Part 2: Quality control, time-series indices and homogeneity assessment. *Earth System Science Data*, *10*(2), 787–804. https://doi.org/10.5194/essd-10-787-2018

Hamed, K. H., & Rao, A. R. (1998). A modified Mann-Kendall trend test for autocorrelated data. *Journal of Hydrology*, *204*, 182–196.

Hargreaves, G. H., & G, A. R. (2003). History and evaluation of Hargreaves evapotranspiration equation. *Journal of Irrigation and Drainage Engineering*, *129*(1), 53–63. https://doi.org/10.1061/(ASCE)0733-9437(2003)129:1(53)

Hargreaves, G. H., & Samani, Z. A. (1985). Reference Crop Evapotranspiration From Ambient Air Temperature. *Applied Engineering in Agriculture*, *1*(2), 96–99. https://doi.org/10.13031/2013.26773

Hosking, J. R. M. (1984). Modeling persistence in hydrological time series using fractional differencing. *Water Resources Research*, *20*(12), 1898–1908. https://doi.org/10.1029/WR020i012p01898

Huang, H., Han, Y., Cao, M., Song, J., & Xiao, H. (2016). Spatial-Temporal variation of aridity index of China during 1960-2013. *Advances in Meteorology*, *2016*, 1–10. https://doi.org/10.1155/2016/1536135

Hurrell, J. W. (1995). James W. Hurrell. *Science*, *269*(5224), 676–679. https://doi.org/10.1126/science.269.5224.676

Hurst, E. H. (1951). Long-term storage capacity of reservoirs. *Transactions of the American Society of Civil Engineers*, *116*(1), 770–799.

Husain, A., & Hamid, A. T. (2012). Climate Change Impact on Hydro-meterological Variables : A Review. *International Journal of Emerging Technology and Advanced Engineering*, *2*(9), 48–54.

Indeje, M., Semazzi, F. H. M., & Ogallo, L. J. (2000). ENSO SIGNALS IN EAST AFRICAN RAINFALL SEASONS. *International Journal of Climatology*, *20*(1), 19–46. https://doi.org/https://doi.org/10.1002/(SICI)1097-0088(200001)20:1<19::AID-JOC449>3.0.CO;2-0

IPCC. (2013). *Summary for Policymakers. In: Climate Change 2013: The Physical Science Basis. Contribution of Working Group I to the Fifth Assessment Report of the Intergovernmental Panel on Climate Change[Stocker, T.F., D. Qin, G.-K. Plattner, M. Tignor, S.K. Allen, J.* https://doi.org/10.1038/446727a

JICA. (2011). *The Development Study on Water Resources Development and Management for Lake Kyoga Basin in the Republic of Uganda*.

Jones, P. D., Jonsson, T., & Wheeler, D. (1997). Extension to the North Atlantic oscillation using early instrumental pressure observations from Gibraltar and south-west Iceland. *International Journal of Climatology*, *17*(13), 1433–1450. https://doi.org/10.1002/(sici)1097-0088(19971115)17:13<1433::aid-joc203>3.3.co;2-g

Kansiime, M. K., Wambugu, S. K., & Shisanya, C. a. (2013). Perceived and Actual Rainfall Trends and Variability in Eastern Uganda : Implications for Community Preparedness and Response. *Journal of Natural Sciences Research*, *3*(8), 179–194. www.iiste.org

Karaburun, A., Demirci, A., & Kara, F. (2011). Analysis of spatially distributed annual, seasonal and monthly temperatures in Istanbul from 1975 to 2006. *World Applied Sciences Journal*, *12*(10), 1662–1675.

Kayendeke, E. J., & French, H. K. (2019). Characterising the Hydrological Regime of a Tropical Papyrus Wetland in the Lake Kyoga Basin, Uganda. In L. R. Bamutaze Y., Kyamanywa S., Singh B., Nabanoga G. (Ed.), *Agriculture and Ecosystem Resilience in Sub Saharan Africa. Climate Change Management* (pp. 213–236). Springer. https://doi.org/10.1007/978-3-030-12974-3_10

Kendall, M. G. (1955). Rank correlation methods, 2nd ed. In *Rank correlation methods, 2nd ed.*

Khalid, S., Rehman, S. U., Shah, S. M. A., Naz, A., Saeed, B., Alam, S., Ali, F., & Gul, H. (2013). Hydro-meteorological characteristics of Chitral River basin at the peak of the Hindukush range. *Natural Science*, *05*(09), 987–992. https://doi.org/10.4236/ns.2013.59120

Kigobe, M., McIntyre, N., Wheater, H., & Chandler, R. (2011a). Multi-site stochastic modelling of daily rainfall in Uganda. *Hydrological Sciences Journal*, *56*(1), 17–33. https://doi.org/10.1080/02626667.2010.536548

Kigobe, M., Wheater, H., & McIntyre, N. (2014). Statistical Downscaling of Precipitation in the Upper Nile: Use of Generalized Linear Models (GLMs) for the Kyoga Basin. In *Nile River Basin: Ecohydrological Challenges, Climate Change and Hydropolitics* (pp. 421–449). https://doi.org/https://doi.org/10.1007/978-3-319-02720-3_22

Kundzewicz, Z. W., & Robson, A. J. (2004). Change detection in hydrological records - A review of the methodology. *Hydrological Sciences Journal*, *49*(1), 7–20. https://doi.org/10.1623/hysj.49.1.7.53993

Kyatengerwa, C., Kim, D., & Choi, M. (2020). A national-scale drought assessment in Uganda based on evapotranspiration deficits from the Bouchet hypothesis. *Journal of Hydrology*, *580*(November 2019), 124348. https://doi.org/10.1016/j.jhydrol.2019.124348

Laaha, G., & Blöschl, G. (2007). A national low flow estimation procedure for Austria. *Hydrological Sciences Journal*, *52*(4), 625–644. https://doi.org/10.1623/hysj.52.4.625

Lachaux, J. P., Lutz, A., Rudrauf, D., Cosmelli, D., Le Van Quyen, M., Martinerie, J., & Varela, F. (2002). Estimating the time-course of coherence between single-trial brain signals: An introduction to wavelet coherence. *Neurophysiologie Clinique*, *32*(3), 157–174. https://doi.org/10.1016/S0987-7053(02)00301-5

Li, Y., Feng, A., Liu, W., Ma, X., & Dong, G. (2017). Variation of aridity index and the role of climate variables in the Southwest China. *Water*, *9*(743), 1–14. https://doi.org/10.3390/w9100743

M Wambua, R., Mutua, Benedict, M., & Raude, James, M. (2014). Drought Forecasting Using Indices and Artificial Neural Networks for Upper Tana River Basin, Kenya-A Review Concept. *Journal of Civil & Environmental Engineering*, *04*(04), 1–12. https://doi.org/10.4172/2165-784x.1000152

Mahmood, R., Jia, S., & Zhu, W. (2019). Analysis of climate variability, trends, and prediction in the most active parts of the Lake Chad basin, Africa. *Scientific Reports*, *9*(1), 1–18. https://doi.org/10.1038/s41598-019-42811-9

Mallakpour, I., & Villarini, G. (2015). A simulation study to examine the sensitivity of the Pettitt test to detect abrupt changes in mean. *Hydrological Sciences Journal*, *61*(2), 245–254. https://doi.org/10.1080/02626667.2015.1008482

Mann, Henry, B. (1945). Nonparametric Tests Against Trend Author *Econometrica*, *13*(3),

245–259. http://www.jstor.com/stable/1907187

McKee, T. B., Doesken, N. J., & Kleist, J. (1993). The relationship of drought frequency and duration to time scales. *Eighth Conference on Applied Climatology*, *17*(22), 179–183. https://climate.colostate.edu/pdfs/relationshipofdroughtfrequency.pdf

Men, Y., Li, P., Zhou, J., Cheng, G., Chen, S., & Luo, W. (2019). Tailoring the Electronic Structure of Co2P by N Doping for Boosting Hydrogen Evolution Reaction at All pH Values [Research-article]. *ACS Catalysis*, *9*(4), 3744–3752. https://doi.org/10.1021/acscatal.9b00407

Meresa, H. K., & Gatachew, M. T. (2019). Climate change impact on river flow extremes in the upper blue nile river basin. *Journal of Water and Climate Change*, *10*(4), 759–781. https://doi.org/10.2166/wcc.2018.154

Meresa, H. K., Romanowicz, R. J., & Napiorkowski, J. J. (2017). Understanding changes and trends in projected hydroclimatic indices in selected Norwegian and Polish catchments. *Acta Geophysica*, *65*(4), 829–848. https://doi.org/10.1007/s11600-017-0062-5

Mubialiwo, A., Onyutha, C., & Abebe, A. (2020). Historical Rainfall and Evapotranspiration Changes over Mpologoma Catchment in Uganda. *Advances in Meteorology*, *2020*, 1–19. https://doi.org/10.1155/2020/8870935

Nashwan, M. S., & Shahid, S. (2019). Spatial distribution of unidirectional trends in climate and weather extremes in Nile river basin. *Theoretical and Applied Climatology*, *137*(2019), 1181–1199. https://doi.org/https://doi.org/10.1007/s00704-018-2664-5

Nkiaka, E., Nawaz, N. R., & Lovett, J. C. (2017). Using standardized indicators to analyse dry/wet conditions and their application for monitoring drought/floods: a study in the Logone catchment, Lake Chad basin. *Hydrological Sciences Journal*, *62*(16), 2720–2736. https://doi.org/10.1080/02626667.2017.1409427

Nourani, V., Danandeh Mehr, A., & Azad, N. (2018). Trend analysis of hydroclimatological variables in Urmia lake basin using hybrid wavelet Mann–Kendall and Şen tests. *Environmental Earth Sciences*, *77*(5), 1–18. https://doi.org/10.1007/s12665-018-7390-x

Nsubuga, F., Botai, O, J., Olwoch, Jane, M., Rautenbach, dew, C, J., Bevis, Y., & Adetunji, Adebayo, O. (2014). The nature of rainfall in the main drainage sub- basins of Uganda. *Hydrological Sciences Journal*, *59*(2), 278–299.

https://doi.org/10.1080/02626667.2013.804188

Nsubuga, F. N. W., Namutebi, E. N., & Nsubuga-Ssenfuma, M. (2014). Water Resources of Uganda: An Assessment and Review. *Journal of Water Resource and Protection*, *6*(2014), 1297–1315. https://doi.org/10.4236/jwarp.2014.614120

Ntale, H. K., & Gan, T. Y. (2003). Drought indices and their application to East Africa. *International Journal of Climatology*, *23*(11), 1335–1357. https://doi.org/10.1002/joc.931

Nyasim, M., Radney, M., Mungai, C., & Kamini, C. (2016). *Uganda's National Adaptation Programme of Action: Implementation, Challenges and Emerging Lessons.* https://doi.org/https://hdl.handle.net/10568/79935

Nyeko-ogiramoi, P., Willems, P., & Ngirane-katashaya, G. (2013). Trend and variability in observed hydrometeorological extremes in the Lake Victoria basin. *Journal of Hydrology*, *489*(2013), 56–73. https://doi.org/10.1016/j.jhydrol.2013.02.039

Nyenje, P. M., & Batelaan, O. (2009). Estimating the effects of climate change on groundwater recharge and baseflow in the upper Ssezibwa catchment , Uganda. *Hydrological Sciences Journal*, *54*(4), 713–726. https://doi.org/10.1623/hysj.54.4.713

Ogallo, L. F. (1989). the Spatial and Temporal Patterns of the East African Seasonal Rainfall Derived From. *International Journal of Climatology*, *9*(2), 145–167. https://doi.org/https://doi.org/10.1002/joc.3370090204

Onyutha, C. (n.d.). Statistical Uncertainty in Hydrometeorological Trend Analyses. *Advances in Meteorology*, *2016*, 1–26. https://doi.org/https://doi.org/10.1155/2016/8701617

Onyutha, C. (2016a). Identification of sub-trends from hydro-meteorological series. *Stochastic Environmental Research and Risk Assessment*, *30*(2016), 189–205. https://doi.org/http://dx.doi.org/ 10.1007/s00477-015-1070-0

Onyutha, C. (2016b). Statistical analyses of potential evapotranspiration changes over the period 1930-2012 in the Nile River riparian countries. *Agricultural and Forest Meteorology*, *226–227*(C), 80–95. https://doi.org/10.1016/j.agrformet.2016.05.015

Onyutha, C. (2018). Trends and variability in African long-term precipitation. *Stochastic Environmental Research and Risk Assessment*, *32*(9), 2721–2739. https://doi.org/10.1007/s00477-018-1587-0

Onyutha, C., Acayo, G., & Nyende, J. (2020). Analyses of Precipitation and Evapotranspiration Changes across the Lake Kyoga Basin in East Africa. *Water*, *12*(4), 1134. https://doi.org/https://doi.org/10.3390/w12041134

Onyutha, C., & Willems, P. (2015). Spatial and temporal variability of rainfall in the Nile Basin. *Hydrology and Earth System Sciences*, *19*(5), 2227–2246. https://doi.org/10.5194/hess-19-2227-2015

Onyutha, C., & Willems, P. (2017). Space-time variability of extreme rainfall in the River Nile. *International Journal of Climatology*, *37*(14), 4915–4924. https://doi.org/10.1002/joc.5132

Palizdan, N., Falamarzi, Y., Huang, Y. F., Lee, T. S., Plaziden, N., Falamazir, Y., Yuk, Feng, H., & Teang, Shui, L. (2016). Precipitation trend analysis using discrete wavelet transformation at the Langat River Basin, Selangor Malaysia. *Stochastic Environmental Research and Risk Assessment*, *31*(4), 853–877. https://doi.org/10.1007/s00477-016-1261-3

Peters, E. E. (1994). *Fractal market analysis: applying chaos theory to investment and economics* (1st ed., Vol. 24).

Pettitt, A. N. (1979). A Non-Parametric Approach to the Change-Point Problem Published by : Wiley for the Royal Statistical Society A Non-parametric Approach to the Change-point Problem. *Journal of the Royal Statistical Society. Series C (Applied Statistics)*, *28*(2), 126–135. https://www.jstor.org/stable/2346729

Ponce, V., Pandey, Rajendra, P., & Ercan, S. (2000). Characterization of drought across climatic spectrum. *Journal of Hydrologic Engineering*, *5*(2), 222–224. https://doi.org/https://doi.org/10.1061/(ASCE)1084-0699(2000)5:2(222)

Rayner, N. A., Parker, D. E., Horton, E. B., Folland, C. K., Alexander, L. V., Rowell, D. P., Kent, E. C., & Kaplan, A. (2003). Global analyses of sea surface temperature, sea ice, and night marine air temperature since the late nineteenth century. *Journal of Geophysical Research: Atmospheres*, *108*(14), 1–37. https://doi.org/10.1029/2002jd002670

Ruiz-Alvarez, O., Singh, V. P., Enciso-Medina, J., Ontiveros-Capurata, R. E., & dos Santos, C. A. C. (2020). Observed trends in daily extreme precipitation indices in Aguascalientes, Mexico. *Meteorological Applications*, *27*, 1–20. https://doi.org/10.1002/met.1838

Sang, Y., Wang, Z., & Liu, C. (2013). Discrete wavelet-based trend identi fi cation in hydrologic time series. *Hydrological Processes*, *27*(2013), 2021–2031. https://doi.org/10.1002/hyp.9356

Sen, P. K. (1968). Estimates of the Regression Coefficient Based on Kendall ' s Tau Author (s): Pranab Kumar Sen Source : Journal of the American Statistical Association , Vol . 63 , No . 324 (Dec ., 1968), pp . Published by : Taylor & Francis , Ltd . on behalf of the A. *Journal of the American Statistical Association*, *63*(324), 1379–1389. https://www.jstor.org/stable/2285891

Şen, Z. (2012). Innovative trend analysis methodology. *Journal of Hydrologic Engineering*, *17*(9), 1042–1046. https://doi.org/10.1061/(ASCE)HE.1943-5584.0000556

Shamshirband, S., Hashemi, S., Salimi, H., Samadianfard, S., Asadi, E., Shadkani, S., Kargar, K., Mosavi, A., Nabipour, N., & Chau, K. W. (2020). Predicting Standardized Streamflow index for hydrological drought using machine learning models. *Engineering Applications of Computational Fluid Mechanics*, *14*(1), 339–350. https://doi.org/10.1080/19942060.2020.1715844

Sheffield, J., Gopi, G., & Wood, E. F. (2006). Development of a 50-Year High-Resolution Global Dataset of Meteorological Forcings for Land Surface Modeling. *Journal of Climate*, *19*, 3088–3111.

Sillmann, J., & Roeckner, E. (2008). Indices for extreme events in projections of anthropogenic climate change. *Climatic Change*, *86*(1–2), 83–104. https://doi.org/10.1007/s10584-007-9308-6

Tabari, H., & Aghajanloo, M. B. (2013). Temporal pattern of aridity index in Iran with considering precipitation and evapotranspiration trends. *International Journal of Climatology*, *33*(2), 396–409. https://doi.org/10.1002/joc.3432

Tadic, L., Dadic, T., & Marija, L. (2016). Variability of Hydrological Parameters and Water Balance Components in Small Catchment in Croatia. *Advances in Meteorology*, *2016*, 1–9. https://doi.org/https://doi.org/10.1155/2016/1393241

Tank, A. M. G. K., & Konnen, P. (2003). Trends in indices of daily temperature and precipitations extremes in Europe, 1946-99. *Theoretical and Applied Climatology*, *16*(22), 3665–3680. https://doi.org/https://doi.org/10.1175/1520-

0442(2003)016<3665:TIIODT>2.0.CO;2

Telesca, L., Lovallo, M., Lopez-Moreno, I., & Vicente-Serrano, S. (2012). Investigation of scaling properties in monthly streamflow and Standardized Streamflow Index (SSI) time series in the Ebro basin (Spain). *Physica A: Statistical Mechanics and Its Applications*, *391*(4), 1662–1678. https://doi.org/10.1016/j.physa.2011.10.023

Theil, H. (1950). A rank-invariant method of linear and polynomial regression analysis, Part I. In *Proceedings of the Royal Netherlands Academy of Sciences*.

Thiessen, A. H. (1911). Precipitation Averages for Large Areas. *Monthly Weather Review*, *39*(7), 1082–1084. https://doi.org/10.1175/1520-0493-38.5.786

Torrence, C., & Webster, P. J. (1999). Interdecadal changes in the ENSO-monsoon system. *Journal of Climate*, *12*(8 PART 2), 2679–2690. https://doi.org/10.1175/1520-0442(1999)012<2679:icitem>2.0.co;2

Trenberth, K. E. (1997). The Definition of El Niño. *Bulletin of the American Meteorological Society*, *78*(12), 2771–2777. https://doi.org/10.1175/1520-0477(1997)078<2771:TDOENO>2.0.CO;2

Trenbeth, K. E., Caron, J. M., Stepaniak, D. P., & Worley, S. (2002). Evolution of El Niño-Southern Oscillation and global atmospheric surface temperatures. *Journal of Geophysical Research D: Atmospheres*, *107*(7–8), 5–1. https://doi.org/10.1029/2000jd000298

Tumusiime, M. D., & Ageet, S. (2018). Assessment of Impacts of Climate Change on Hydro-meteorological Ecosystem Services and Water Stress in Lake Kyoga Catchment. *International Journal of Research and Engineering*, *5*(4), 345–354. https://doi.org/https://doi.org/10.21276/ijre.2018.5.4.2

Vicente-Serrano, S. M., López-Moreno, J. I., Beguería, S., Lorenzo-Lacruz, J., Azorin-Molina, C., & Morán-Tejeda, E. (2012). Accurate Computation of a Streamflow Drought Index. *Journal of Hydrologic Engineering*, *17*(2), 318–332. https://doi.org/10.1061/(ASCE)HE.1943-5584.0000433

Visser, A., Kroes, J., Van Vliet, M., Blenkinsop, S., & Broers, H. P. (2012). Climate change impact on the leaching of a heavy metal contamination in a small lowland catchment. *Journal of Contaminant Hydrology*, *127*(2012), 47–64.

https://doi.org/10.1016/j.jconhyd.2011.04.007

Vogel, R. M., & Wilson, I. (1996). Probability distribution of annual maximum, mean, and minimum streamflow in the United States. *Journal of Hydrologic Engineering*, *1*(2), 69–76. https://doi.org/https://doi.org/10.1061/(ASCE)1084-0699(1996)1:2(69)

Woods, R. (2005). Hydrologic Concepts of Variability and Scale. In *Encyclopedia of Hydrological Sciences* (pp. 1–18).

Xie, H., Li, D., & Xiong, L. (2014). Exploring the ability of the Pettitt method for detecting change point by Monte Carlo simulation. *Stochastic Environmental Research and Risk Assessment*, *28*(7), 1643–1655. https://doi.org/10.1007/s00477-013-0814-y

Yan, J., Chenghu, Z., & Weiming, C. (2007). Streamflow trends and hydrological response to climatic change in Tarim headwater basin. *Journal of Geographic Sciences*, *17*(1), 51–61. https://doi.org/10.1007/s11442-007-0051-8

Zhang, X., Harvey, K. D., Hogg, W. D., & Yuzyk, T. R. (2001). Trends in Canadian streamflow. *Water Resources Research*, *37*(4), 987–998. https://doi.org/https://doi.org/10.1029/2000WR900357

Zhang, Y., You, Q., Lin, H., & Chen, C. (2015). Analysis of dry/wet conditions in the Gan River Basin, China, and their association with large-scale atmospheric circulation. *Global and Planetary Change*, *133*(2015), 309–317. https://doi.org/10.1016/j.gloplacha.2015.09.005